UNIVERSIDADE ESTADUAL PAULISTA
"JÚLIO DE MESQUITA FILHO"
FACULDADE DE MEDICINA

Thania Rios Rossi Lima

Mecanismos de citotoxicidade do diuron em células uroteliais – Possível papel de lesão mitocondrial

Tese apresentada à Faculdade de Medicina, Universidade Estadual Paulista "Júlio de Mesquita Filho", Câmpus de Botucatu, para obtenção do título de Doutora em Patologia.

Orientadora: Profa. Dra. Lílian Cristina Pereira
Coorientadores: Prof. Dr. João Lauro Viana de Camargo
Profa. Dra. Carla Adriene da Silva

Thania Rios Rossi Lima

Mecanismos de citotoxicidade de diuron em células uroteliais – Possível papel de lesão mitocondrial

Tese apresentada à Faculdade de Medicina, Universidade Estadual Paulista "Júlio de Mesquita Filho", Câmpus de Botucatu, para obtenção do título de Doutora em Patologia.

Orientadora: Profa. Dra. Lílian Cristina Pereira
Coorientadores: Prof. Dr. João Lauro Viana de Camargo
Profa. Dra. Carla Adriene da Silva

Botucatu
2022

L732m

Lima, Thania Rios Rossi
Mecanismos de citotoxicidade do diuron em células uroteliais – Possível papel de lesão mitocondrial / Thania Rios Rossi Lima. -- Botucatu, 2022
120 p.

Tese (doutorado) - Universidade Estadual Paulista (Unesp), Faculdade de Medicina, Botucatu
Orientadora: Lílian Cristina Pereira
Coorientador: João Lauro Viana de Camargo

1. Diuron. 2. Herbicida. 3. Toxicidade urotelial. 4. Disfunção mitocondrial. 5. Cultura celular. I. Título.

Sistema de geração automática de fichas catalográficas da Unesp. Biblioteca da Faculdade de Medicina, Botucatu. Dados fornecidos pelo autor(a).

Essa ficha não pode ser modificada.

Dedicatória

À família

Dedico este trabalho à minha família, a qual amo muito. Sei que sempre posso contar com vocês!

Ao esposo

Dedico este trabalho também ao meu esposo, Leandro. Obrigada pelo incentivo e companheirismo, sobretudo nas horas difíceis.

Agradecimentos

Aos meus pais, Aparecido e Juliana, por terem me dado a vida e me proporcionarem inúmeras oportunidades de aprendizado. Progredir sempre, tal é a lei!

Ao meu irmão Túlio, pelo carinho e por estar sempre presente.

Aos meus avós Clarice e Luiz, e demais familiares, por me apoiarem em todos os momentos de minha vida.

Ao amor da minha vida, Leandro. Obrigada por estar presente na conclusão de mais essa etapa!

Aos queridos amigos do laboratório pelo companheirismo e por tornarem o dia-a-dia de trabalho mais leve e descontraído.

Ao Conselho Nacional de Desenvolvimento Científico e Tecnológico (CNPq), pela concessão da bolsa de doutorado (Processo nº 167774/2018-2)

À FAPESP, pelo auxílio financeiro (Processo nº 2017/25402-5).

À Coordenação de Aperfeiçoamento de Pessoal de Nível Superior (CAPES), pela concessão de bolsa durante parte do período de meu doutoramento e pela concessão da bolsa de doutorado sanduíche (CAPES-PrInt - Processo nº 88887.467311/2019-00).

Ao Núcleo de Avaliação do Impacto Ambiental sobre a Saúde Humana (TOXICAM), pelo suporte na realização deste trabalho.

Enfim, a todos que contribuíram para que este trabalho fosse concluído, meu muito obrigada!

Agradecimentos especiais

À minha orientadora, Dra. Lílian Cristina Pereira, por compartilhar seu conhecimento e por todo o suporte na realização deste trabalho. Você é exemplo de dedicação à ciência!

Ao Dr. João Lauro Viana de Camargo, o meu mais sincero agradecimento por abrir as portas do TOXICAM e me permitir fazer parte desse grupo de pesquisa de excelência.

À Dra. Carla Adriene da Silva pelo companheirismo e pelo auxílio na coorientação deste trabalho.

Vocês, queridos professores, me inspiram a aprender e ter pensamento crítico. Obrigada por acreditarem no meu potencial!

“Não há problema que não possamos resolver juntos e muito poucos os que possamos resolver sozinhos.”

Lyndon B. Johnson

Resumo

Os efeitos tóxicos de substâncias químicas sobre o sistema urinário têm sido estudados ao longo dos últimos anos, sendo que o herbicida diuron e seus metabólitos mostraram potencial cancerígeno na bexiga urinária de ratos Wistar e citotoxicidade em células uroteliais derivadas de ratos e humanos. Assim, estudos que buscam elucidar os principais eventos envolvidos na toxicidade desses compostos são essenciais para compreender o possível mecanismo de ação sobre o urotélio. Este estudo teve como objetivo investigar os mecanismos de toxicidade urotelial exercida pelo diuron e metabólitos, abordando o possível papel da disfunção mitocondrial. Após exposição aos produtos químicos, as células uroteliais humanas 1T1 apresentaram alterações relacionadas à morte e proliferação, instabilidade do ciclo celular, estresse oxidativo, e dano mitocondrial. Além disso, por meio de investigação metabolômica em mitocôndrias uroteliais isoladas de ratos Wistar foram encontradas alterações em moléculas associadas à membrana e em moléculas envolvidas no metabolismo celular. Avaliados em conjunto, tais resultados indicam potencial ação nociva do diuron e seus metabólitos sobre a função mitocondrial, o que pode ser considerado o evento iniciador de um processo sequencial que desencadeia a citotoxicidade observada neste estudo e as alterações morfológicas observadas em estudos anteriores.

Abstract

The toxic effects of chemical substances on the urinary system have been studied over the past years, being that the diuron herbicide and its metabolites showed carcinogenic potential in the urinary bladder of Wistar rats and cytotoxicity in rat and human-derived urothelial cells. Thus, studies that seek to elucidate the key-events involved in the toxicity of these compounds are essential to understand the possible mechanism of action on the urothelium. This study aimed to investigate the underlying mechanisms linked to urothelial toxicity resulting from diuron and metabolites exposure, addressing the possible role of mitochondrial dysfunction. After exposure to the chemicals, human urothelial cells 1T1 showed alterations related to death and proliferation, cell cycle instability, oxidative stress, mitochondrial and damage. Additionally, through metabolomic investigation in urothelial mitochondria isolated from Wistar rats, alterations in membrane-associated molecules and in molecules involved in cellular metabolism were found. Altogether, these results indicate potential harmful action of diuron and its metabolites on mitochondrial function, which can be considered the initiator event of a sequential process that triggers the cytotoxicity observed in this study and the morphological changes observed in previous studies.

CAPÍTULO I

CAPÍTULO II

MANUSCRITO I

MANUSCRITO II

CAPÍTULO I

CAPÍTULO II

ADME	Absorção, distribuição, metabolização e excreção
AiP	Apoptosis-induced proliferation
ATP	Adenosina-trifosfato
CCCP	Carbonyl cyanide m-chlorophenyl hydrazine
DCA	3,4-dicloroanilina
DCPMU	3-(3,4-diclorofenil)-1-metilureia
DCPU	3,4-diclorofenilureia
DMSO	Dimethyl sulfoxide
ERONs	Espécies reativas de oxigênio e nitrogênio
GHS	Globally Harmonized System
IA	Ingrediente ativo
MoA	Mode of action/Modo de ação
mtDNA	DNA mitocondrial
MTT	[3-(4,5-Dimethylthiazol-2-yl)-2,5-Diphenyltetrazolium Bromide]
PC	Phosphatidylcholine
PI	Phosphatidylinositol
PI	Propidium iodide
PS	Phosphatidylserine
PTPM	Poro de transição de permeabilidade mitocondrial
RONS	Reactive oxygen and nitrogen species
ROS	Reactive oxygen species
TIM	Translocases of the inner mitochondrial membrane
TMRM	Tetramethylrhodamine methyl ester
U.S. EPA	Agência de Proteção Ambiental norte-americana

CAPÍTULO I

CAPÍTULO II

MANUSCRITO I

Capítulo I

1. INTRODUÇÃO

1.1 Bexiga urinária como órgão-alvo de toxicidade

Quando em contato com uma substância química, inicia-se no organismo o processo de toxicocinética, pelo qual a substância é absorvida, distribuída, metabolizada e excretada (ADME) (1, 2). A absorção ocorre principalmente pelas vias dérmica, inalatória e digestiva, sendo que a resposta adversa pode iniciar logo no sítio de contato. A substância pode ser distribuída através do organismo e causar efeitos em múltiplos órgãos ou atuar em órgãos-alvo, e pode ainda sofrer biotransformação, o que favorece a excreção. No entanto, a biotransformação pode gerar metabólitos menos ou mais tóxicos, levando também a desfechos adversos. Na fase de eliminação, fezes e urina são vias primárias de grande importância (1, 2).

A urina é formada pelos néfrons nos rins e é transportada para a bexiga urinária através dos ureteres. A bexiga é uma víscera de armazenamento e sua composição microscópica é organizada em diferentes camadas: epitélio do revestimento, lâmina própria, muscularis propria e serosa. Em particular, o epitélio de revestimento da bexiga urinária, ou urotélio, é a camada mais superficial e possui em sua estrutura as células superficiais em forma de guarda-chuva (*umbrella cells*), tornando-o uma barreira protetora contra lesões nas camadas subjacentes. O urotélio também reveste a pelve renal, ureter e uretra. A bexiga possui capacidade de armazenamento de aproximadamente 500-700 mL, podendo permanecer por tempo razoável - em média 24 horas - em contato com as substâncias a serem expelidas (3, 4). Quanto mais tempo as substâncias permanecerem na bexiga, maior é a probabilidade de ação tóxica local (2).

Os efeitos da ação tóxica de substâncias químicas no sistema urinário têm sido motivo de preocupação há vários anos (5). Por exemplo, em estudo desenvolvido por Hueper, Wiley (6), foi observado que a formação de metabólitos reativos desempenha um papel fundamental no modo de ação carcinogênico das aminas aromáticas na bexiga urinária. Dentre as aminas aromáticas está o 2-acetilaminofluoreno (2-AAF), substância formulada na década de 1940 com propósito praguicida, mas que teve sua comercialização impedida após a descoberta de seu alto potencial carcinogênico para a bexiga em diferentes espécies animais (7). Dessa forma, pesquisas envolvendo o estudo da toxidade química em diferentes níveis do sistema urinário mostram-se essenciais para a compreensão do modo e mecanismos de ação subjacentes, e podem auxiliar na tomada de decisão regulatória. Nesse contexto, o cultivo de células ou tecidos em ambiente *in vitro* constitui ferramenta muito útil para a compreensão dos eventos-chave envolvidos na toxicidade de compostos químicos (8). Assim como na experimentação *in vivo*, o uso de células derivadas de seres humanos possibilita a obtenção de resultados toxicológicos representativos e que, portanto, aumentam a previsibilidade para toxicidade humana (9). Além do mais, as culturas de linhagens celulares humanas apresentam-se como uma excelente ferramenta para otimização de métodos alternativos à utilização de animais em pesquisas (10-13).

Diferentes linhagens celulares podem ser empregadas nos ensaios *in vitro* para avaliar dano causado ao urotélio, dentre elas, as células 1T1 (Figura 1). A população de células 1T1 é derivada do epitélio de ureter humano saudável e imortalizada por transfecção dos genes E6 e E7 de HPV-16 (14). O cultivo da linhagem celular 1T1 é um modelo bem caracterizado na pesquisa da biologia do

tumor de bexiga e tem sido utilizado na avaliação de citotoxicidade, além de genotoxicidade e mutagenicidade em diferentes protocolos experimentais (15-17).

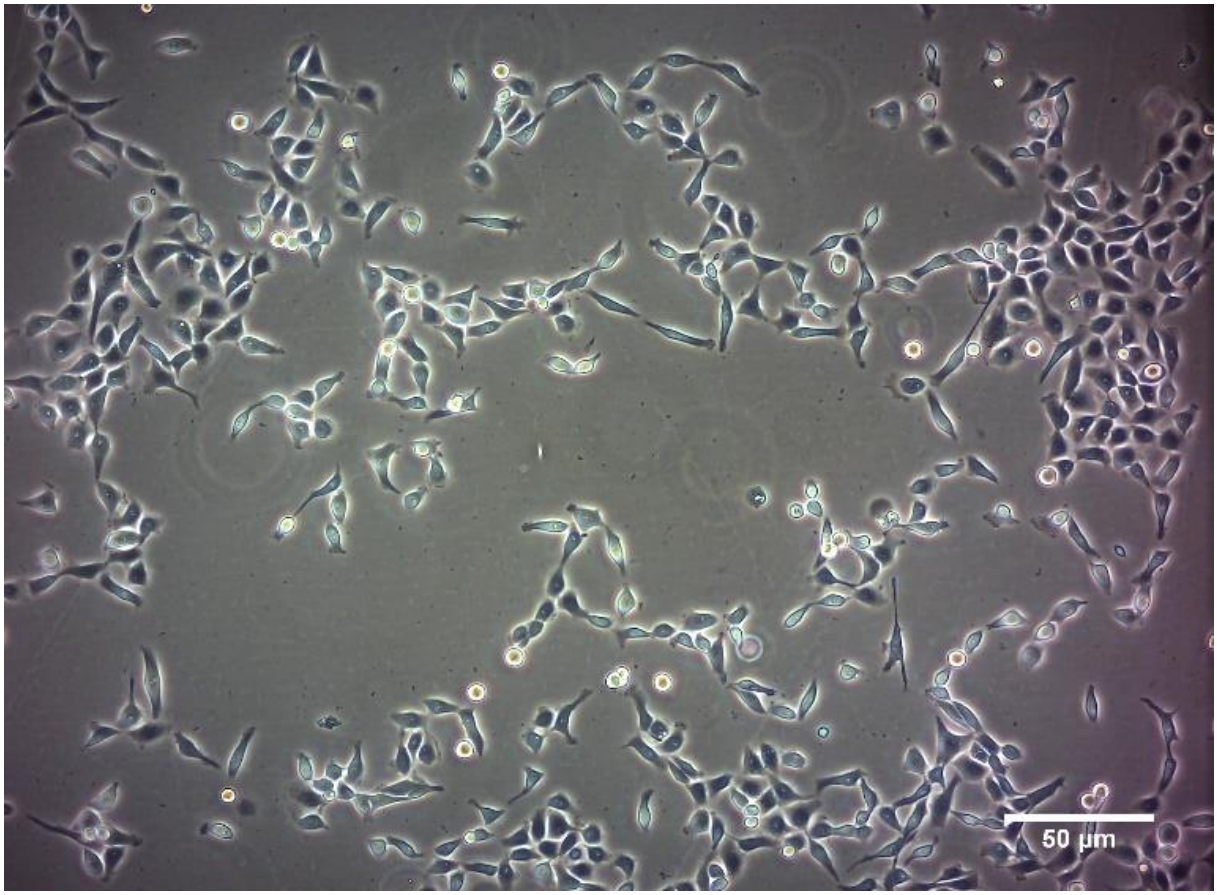

Figura 1. Cultivo de células 1T1 em monocamada. Aumento de 100x. Foto do próprio autor.

No cotidiano, o contato com substâncias potencialmente tóxicas ao organismo, incluindo o sistema urinário, muitas vezes ocorre em baixas doses, mas de forma frequente (18). Dentre essas substâncias estão os ftalatos, hidrocarbonetos policíclicos aromáticos, bem como alguns praguicidas (5, 18).

1.2 Praguicidas no Brasil

O uso de praguicidas, definidos como substâncias ou misturas de substâncias químicas responsáveis por eliminar, repelir ou controlar pragas, está

entre os principais instrumentos do atual modelo de agricultura no Brasil (19). A necessidade de aplicação dessas substâncias nas lavouras deve-se principalmente ao clima tropical, que favorece o aparecimento de pragas. Embora o Brasil seja um grande consumidor de praguicidas, também possui um extenso território de área plantada que chega a 75.866.854 hectares, ou seja, cerca de 9% do território total (20). Em 2020, as vendas internas de ingredientes ativos (IA) (Produtos Formulados) no país corresponderam a 685,745.68 mil toneladas, o que representa um aumento de 10,51% com relação ao ano anterior. Dentre as classes de praguicidas que apresentaram maior volume de vendas nesse mesmo ano, destacam-se os herbicidas, com um total de 413,833.41 toneladas de IA, sendo que somente no estado de São Paulo esse valor chegou a 47,825.02 toneladas. Do total de praguicidas comercializados em São Paulo, 47,25% pertencem a classe III de periculosidade de acordo com o Sistema Globalmente Harmonizado de Classificação (GHS, sigla em inglês) adotado pela ANVISA, na qual está inserida o herbicida diuron, que atingiu 3,723.33 toneladas em vendas no estado e 7,901.84 toneladas no Brasil (21).

1.2.1 Diuron

O diuron 3-(3,4-diclorofenil)-1,1-dimetilureia é um herbicida derivado da ureia comumente aplicado na pré- e pós-emergência de plantas infestantes em culturas de soja, abacaxi, alfafa, algodão, banana, cana-de-açúcar, cacau, café, citros, seringueira e uva (22, 23). Sua ação herbicida se dá pela inibição da reação de fotólise da água e consequente produção de espécies reativas do oxigênio e nitrogênio (ERONs) que levam à destruição peroxidativa de pigmentos como clorofila e de ácidos nucleicos, proteínas e lipídeos, inibindo a fotossíntese (24, 25). As

plantas infestantes possuem vantagem ecológica com relação à proliferação vegetativa; as sementes ou estruturas de reprodução apresentam capacidade de geminação em fases iniciais de desenvolvimento. Por outro lado, o seu ciclo de vida curto associado à área de absorção e dose aplicada as tornam mais suscetíveis à toxicidade dos herbicidas (26).

A ampla utilização do diuron na agricultura combinada à lenta degradação no solo possibilita sua dispersão para o lençol freático e contaminação aquática (27, 28). Fatores climáticos, características físicas, químicas e microbiológicas do solo e propriedades físico-químicas do herbicida influenciam a degradação no ambiente e resultam em metabólitos potencialmente tóxicos: 3-(3,4-diclorofenil)-1-metilureia (DCPMU), 3,4-diclorofenilureia (DCPU) e 3,4-dicloroanilina (DCA) (Tabela 1) (28, 29).

Tabela 1. Estrutura química do diuron e seus metabólitos.

Substância	**Estrutura química**	**Nomenclatura IUPAC***	**Referência**
Diuron	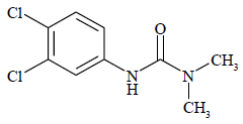	3-(3,4-diclorofenil)- 1,1-dimetilureia	(22)
DCPMU	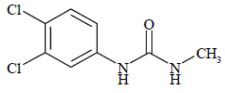	3-(3,4-diclorofenil)-1-metilureia	
DCPU	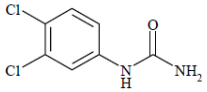	3,4-diclorofenilureia	
DCA	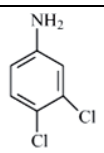	3,4-dicloroanilina	

*International Union of Pure and Applied Chemistry.

Os mesmos metabólitos são gerados durante a metabolização do herbicida em mamíferos, incluindo o homem. Neles, o diuron é absorvido pelo trato gastrointestinal e respiratório (28). A biotransformação ocorre por desmetilação, hidroxilação do anel aromático, N-oxidação, declorinação e conjugação com ácido glicurônico, sendo excretado pela urina ou, em menor quantidade, pelas fezes (23, 28). Há poucos estudos sobre o metabolismo do diuron em humanos. No entanto, em um relato isolado de intoxicação aguda, o principal metabólito encontrado na urina foi o DCPMU, seguido por pequenas quantidades de DCPU e traços de DCA (30). Em ratos, o diuron é quase que completamente absorvido e metabolizado, sendo o DCPU o principal metabólito urinário (31). Uma vez que a sua eliminação ocorre pricipalmente pela urina, o tecido urotelial é um alvo importante da toxicidade desse herbicida e/ou seus metabólitos.

1.2.2 Estudos experimentais

O diuron foi classificado pela Agência de Proteção Ambiental norte-americana (U.S. EPA) como “provável cancerígeno para a espécie humana” após estudo de carcinogenicidade de dois anos apresentar aumento das incidências de papilomas e carcinomas uroteliais na pelve renal e na bexiga de ratos Wistar de ambos os sexos expostos continuamente a 2.500 ppm via ração (25, 32). Estudos desenvolvidos em nosso laboratório - Núcleo de Avaliação do Impacto Ambiental sobre a Saúde Humana (TOXICAM) - permitiram propor o modo de ação (MoA) pelo qual o herbicida é cancerígeno para o urotélio de ratos, onde o produto parental e/ou seus metabólitos induzem sucessivamente citotoxicidade inicial, degeneração celular, esfoliação e necrose seguida de hiperplasia regenerativa contínua e potencial aparecimento de tumores. Nesses estudos *in vivo*, em que o diuron foi administrado

por via oral pela ração em concentrações de até 2.500 ppm, não foi detectado genotoxicidade em células uroteliais ou de sangue periférico pelo ensaio do cometa, nem alterações na composição urinária, como mudanças do pH ou a presença de sólidos urinários (cristais e cálculos) (31, 33-37).

Foram observadas alterações uroteliais à microscopia eletrônica de varredura (MEV) já no primeiro dia de tratamento de ratos alimentados com ração contendo 2.500 ppm de diuron, o menor período de exposição avaliado. Essas alterações consistiram em células uroteliais edemaciadas, salientes para o lúmen da bexiga, sendo denominadas "*swollen cells".* A incidência e quantidade dessas células aumentaram no 3º dia de estudo e persistiram até o 7º dia. A microscopia eletrônica de transmissão (MET) no 7º dia mostrou que essa alteração correspondia à degeneração hidrópica citoplasmática e nuclear, que resultavam no alargamento e protrusão das células uroteliais superficiais para o lúmen vesical, com ruptura da membrana celular, necrose e esfoliação (36). Uma das causas que podem levar a este quadro morfológico é a disfunção mitocondrial, fator que nos levou a aprofundar na avaliação deste parâmetro no presente trabalho.

Os estudos também mostraram aumento das incidências de necrose urotelial, hiperplasia e índice de proliferação celular em ratos Wistar machos tratados durante 15-20 semanas com 125, 500, 1.250 e 2.500 ppm de diuron na ração, sendo que resultados significativos foram observados em 2.500 ppm a partir de 7 dias de exposição (33-35, 38, 39). Esse perfil dose-resposta também foi observado quanto à expressão de genes relevantes para a carcinogênese em células uroteliais isoladas da bexiga de ratos expostos a diferentes concentrações do diuron por períodos variados. Foi possível observar, pela análise PCA (*Principal Component Analysis*) - ferramenta de resolução de dados que agrupa amostras de expressão gênica

similares em um espaço tridimensional - evidente separação entre os grupos expostos a altas concentrações (1.250 e 2.500 pm) e a baixas concentrações (60, 125 e 500 ppm) após 07 dias ou 20 semanas de exposição pela ração (39, 40).

Diferenças na resposta citotóxica aos metabólitos urinários foram demonstradas em estudos *in vitro* com células uroteliais de ratos (MYP3) e humanas (1T1). Para a linhagem MYP3, DCPMU foi o metabólito mais citotóxico, seguido por DCPU, enquanto DCA foi o metabólito mais citotóxico para as células 1T1, seguido por DCPU e DCPMU (37).

Embora o MoA citotóxico do diuron tenha sido proposto com base nesses estudos experimentais, seu mecanismo de toxicidade ainda não foi completamente estabelecido. Deste modo, ensaios utilizando métodos alternativos *in vitro* podem auxiliar no esclarecimento mecanístico dos processos bioquímicos e celulares envolvidos no dano ocasionado pela exposição ao herbicida. Esses métodos *in vitro* não só permitem a análise detalhada de efeitos subcelulares como atendem ao movimento de cuidados éticos com animais de experimentação, pela sua substituição, refinamento e redução de uso (3R's) (10).

1.3 Citotoxicidade

A proliferação celular é dependente do equilíbrio entre diferenciação e morte das células e, por isso, é uma das primeiras funções a ser afetada após exposição química (41, 42). Um agente químico tóxico pode também atuar diretamente na integridade das membranas, levando a degradação ou liberação de componentes celulares. Tais alterações da homeostasia podem desencadear diferentes tipos de morte celular (apoptose, necrose ou autofagia), o que dependerá do tipo de célula, da estrutura e função comprometidas e doses de exposição química (43).

Alterações morfológicas e bioquímicas permitem caracterizar o tipo de morte celular (Figura 2) (44). A apoptose inicia-se com indução de processos ativos, i.e, com consumo energético, dentro da própria célula, que podem envolver ativação de receptores de morte localizados na membrana celular, danos ao DNA ou eventos que levem a perda de permeabilidade da membrana mitocondrial (45, 46). Caracteristicamente, há condensação excêntrica da cromatina. Logo após, as células mortas constituem os corpos apoptóticos que são rapidamente reconhecidos e captados por células vizinhas ou macrófagos. A resposta inflamatória praticamente inexiste. A perda de assimetria de fosfolípidos de membrana e a externalização e permanência da fosfatidil serina (PS) na porção externa da membrana celular facilita o reconhecimento das células apoptóticas por macrófagos (43, 47).

Ao contrário da apoptose, a morte celular por necrose é um processo independente de energia caracterizado por alterações metabólicas que causam imediata depleção do ATP, desequilíbrio iônico e alterações morfológicas devido ao intumescimento mitocondrial e celular. O núcleo torna-se picnótico e há formação de pequenas bolhas na membrana citoplasmática. A ativação de enzimas de degradação resulta em rompimento da membrana, rápido vazamento do conteúdo celular e ativação da resposta inflamatória na região da célula morta (48, 49).

A autofagia (ou mitofagia quando relacionada com as mitocôndrias) é um processo auto-degradativo altamente dinâmico e importante para reciclagem de componentes celulares, bem como para eliminação de patógenos intracelulares. Assim como outras vias celulares, o processo autofágico pode ser modulado em várias etapas, tanto positiva quanto negativamente. De modo geral, a autofagia é considerada um mecanismo de sobrevivência, embora sua desregulação tenha sido associada à morte celular não-apoptótica (50). É caracterizada morfologicamente

por intensa vacuolização do citoplasma sem, entretanto, condensação da cromatina (43, 50, 51). Após a ativação de autofagia, a síntese de algumas proteínas como a LC3B aumenta e, por esse motivo, é utilizada como marcador desse mecanismo. Esta se associa à membrana dos autofagossomos e auxilia na sua maturação (52, 53). Os autofagossomos fagocitam os constituintes e organelas danificados, que são degradados por lisossomos (54, 55).

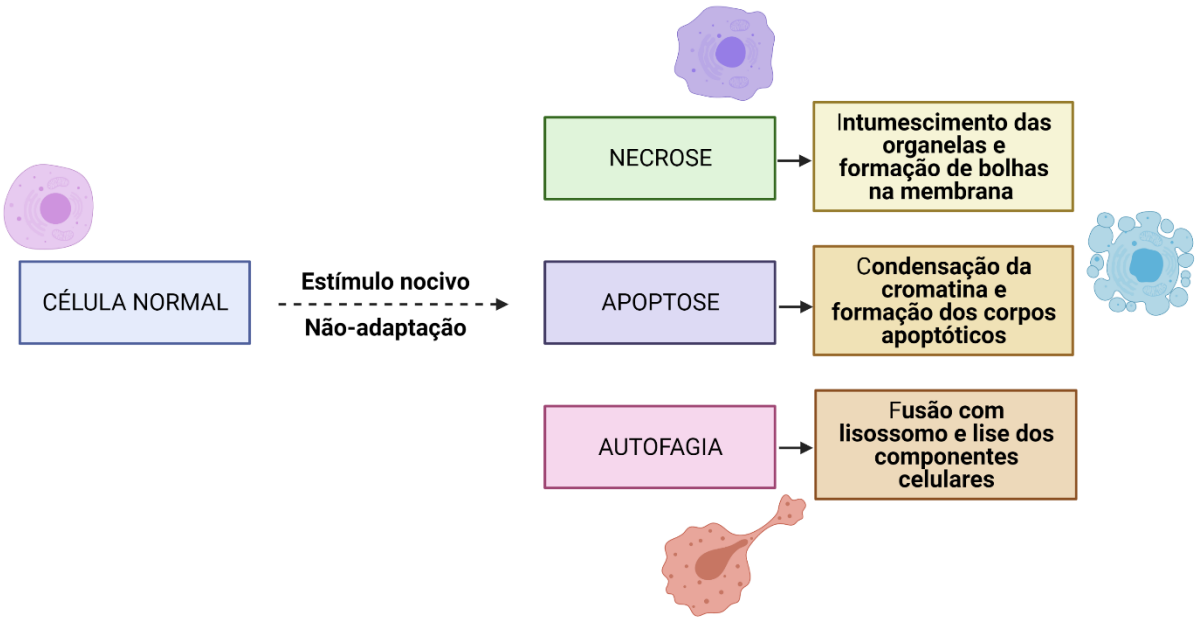

Figura 2. Caracterização morfológica dos 3 tipos mais comuns de morte celular: apoptose, necrose e autofagia. Ao entrar em apoptose a célula passa por condensação da cromatina, degradação celular e posterior fagocitose dos corpos apoptóticos. Na necrose há o inchaço das organelas, formação de bolhas na membrana com posterior ruptura celular. Já na autofagia, os componentes celulares passam por processo de autodegradação seguido da formação do autolisossomo para degradação dos resíduos celulares. *Figura criada com BioRender.com.* Fonte do próprio autor.

As vias de sinalização de morte celular podem ser ativadas em resposta a um dano no DNA. No entanto, é importante salientar que, não necessariamente ou exclusivamente, a morte das células está associada ao dano genético. Ainda, essas

sinalizações podem ser desencadeadas de forma independente ou dependente de mitocôndrias (56).

1.4 Importância da mitocôndria na toxicidade de xenobióticos

As mitocôndrias são organelas intracelulares presentes em organismos eucariontes aeróbicos e, experimentalmente, têm sido utilizadas como ferramenta para esclarecer o mecanismo de toxicidade de diferentes xenobióticos (57, 58). Sua estrutura básica é formada por uma membrana externa que é separada da membrana interna por um espaço intermembranas, e uma matriz onde estão localizados os componentes necessários à função da mitocôndria, como o DNA mitocondrial (mtDNA), proteínas e lipídios, ribossomos, RNAs, além de outras enzimas (59).

A mitocôndria é considerada a “casa de força” das células, sendo a energia produzida pela organela, a partir do ciclo de Krebs e fosforilação oxidativa, que ocorrem na matriz mitocondrial e na membrana mitocondrial interna, respectivamente, armazenada na forma de adenosina-trifosfato (ATP) (60-62). A fosforilação oxidativa compreende a última etapa do processo de respiração celular e desempenha papel crucial no metabolismo energético. Essa etapa é caracterizada pelo transporte de elétrons através de quatro grandes complexos proteicos (NADH desidrogenase; I, Succinato desidrogenase; II, Ubiquinol-citocromo c redutase; III, e Citocromo c oxidase; IV) por reações de oxido-redução, até um aceptor final, o oxigênio molecular (O_2) (Figura 3). Agentes capazes de interferir em qualquer dessas vias metabólicas, podem induzir a produção de ERONs, principalmente os radicais superóxido ($O_2^{\bullet -}$), peróxido de hidrogênio (H_2O_2) e hidroxila ($OH^{\bullet}$), que se acumulam e podem levar ao estresse oxidativo intracelular sistêmico. O estresse

oxidativo é uma condição decorrente do desequilíbrio entre a produção de ERONs e defesas antioxidantes, a favor dos oxidantes, o que pode resultar no comprometimento de componentes celulares como lipídeos, proteínas, carboidratos e DNA. Alterações na produção de ERONs podem ser causa ou consequência da disfunção mitocondrial (1, 63).

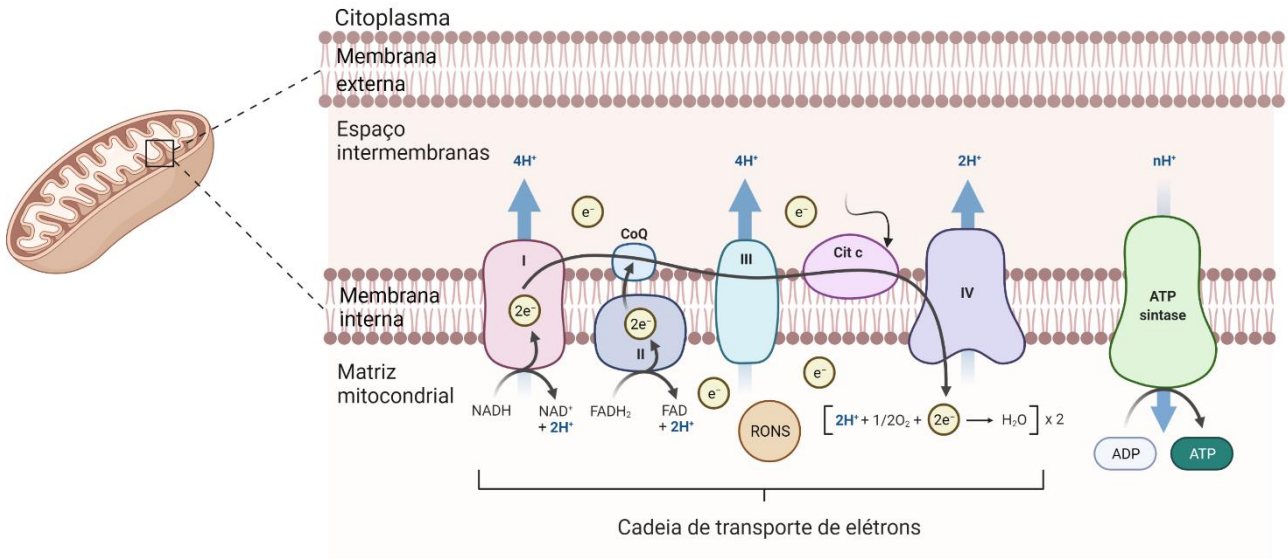

Figura 3. Etapas da fosforilação oxidativa. O transporte de elétrons através dos quatro (I, II, III, IV) complexos mitocondriais leva ao bombeamento de prótons (H^+) para o espaço intermembranas. A energia gerada pelo fluxo inverso de prótons através da ATP-sintase é utilizada para síntese de ATP. *Figura criada com BioRender.com.* Fonte do próprio autor.

Algumas características da membrana interna são de importância toxicológica como, por exemplo, o poro de transição de permeabilidade mitocondrial (PTPM) (1). O PTPM é fechado e composto por uma série de complexos proteicos que tornam a membrana impermeável à maioria dos íons e moléculas polares; entretanto, certos xenobióticos apresentam capacidade de induzir sua abertura e aumentar a permeabilidade (1, 64). Como consequência, o potencial eletroquímico da membrana entra em colapso e a fosforilação oxidativa é afetada. Ainda, a

diferença de osmolaridade entre a matriz mitocondrial e o citosol possibilita o influxo de água e causa o inchamento da organela. Vários eventos subcelulares e possivelmente reversíveis, como o edema celular, estão associados diretamente com a injúria no sistema de fosforilação oxidativa e, desta forma, caso a exposição seja de duração e intensidade (dose) suficientes para levar a célula ao ponto de não retorno, haverá a lesão irreversível e morte celular (1).

De acordo com o exposto, a função da mitocôndria é complexa, altamente regulada e essencial para a manutenção de diversos processos biológicos como sobrevivência e homeostase metabólica das células. Portanto, a interação de agentes exógenos de natureza diversa em diversos pontos deste sistema pode resultar em danos irreversíveis na estrutura e função mitocondrial (47, 65).

1.5 Metabolômica na avaliação de disfunção mitocondrial

Diferentes métodos têm sido aplicados para avaliar a ação de xenobióticos sobre a mitocôndria, que incluem técnicas citoquímicas, moleculares e bioquímicas (66). A metabolômica é uma das adições mais recentes à família "-omics", caracterizada como um método analítico de alto rendimento para medir e comparar um grande número de metabólitos (metaboloma) de baixa massa molecular (até 1.500 Daltons) presentes em amostras biológicas (67, 68).

A análise metabolômica pode ser direcionada a um grupo de pequenos metabólitos que serão quantificados e identificados, ou ser semi-direcionada à uma classe específica de metabólito (aminoácidos, ácidos orgânicos ou acirionitinas), ou ainda basear-se em uma abordagem não-alvo, na qual todos os metabólitos presentes em uma amostra serão submetidos a detecção e quantificação. A escolha

da abordagem adequada dependerá do objetivo acerca do material biológico disponível (67, 68).

Uma vez que toda atividade celular dá origem a metabólitos, a implementação desse método em um estudo tem o potencial de auxiliar no esclarecimento das alterações envolvidas nos efeitos tóxicos causados por exposição a agentes exógenos, incluindo aqueles relacionados à mitocôndria (67). Há uma série de estudos que utilizaram a análise metabolômica para avaliar danos causados por resposta a estresses ambientais ou na identificação de potenciais biomarcadores para compreensão dos mecanismos associados ao desenvolvimento de doenças. Investigação metabolômica realizada em tecido cerebral de camundongo modelo para doença de Alzheimer Familiar mostrou alterações em biomarcadores associados ao metabolismo de nucleotídeos, carboidratos, aminoácidos e de neurotransmissores, além de metabólitos associados ao ciclo de Krebs e transferência de energia, confirmando o importante papel da disfunção mitocondrial na patofisiologia da doença (69). Considerando que os metabólitos celulares são conservados em várias espécies animais, os achados de pesquisa em animais de experimentação podem ser extrapolados para humanos (67).

Outro estudo que objetivou investigar potenciais vias metabólicas envolvidas na progressão do carcinoma urotelial também mostrou desregulação de marcadores relacionados ao metabolismo de glicose, ciclo de Krebs, lipídios de membrana, aminoácido e nucleotídeos em amostras biológicas de indivíduos e linhagens celulares neoplásicas (70).

Para determinar o potencial nocivo e mecanismos de substâncias, é crucial a realização de testes utilizando sistemas diferentes do ponto de vista de complexidade biológica e de desfechos. Deste modo, os dados obtidos neste estudo

irão contribuir com os achados de testes *in vivo* já aplicados por nosso grupo de pesquisa, além de trazer novos dados associados à citotoxicidade e dano mitocondrial induzido pelo herbicida diuron e seus metabólitos, permitindo a melhor compreensão dos processos bioquímicos e celulares chaves envolvidos no seu mecanismo de ação tóxica.

REFERÊNCIAS

1. Boelsterli UA. Mechanistic toxicology: The molecular basis of how chemicals disrupt biological targets. London,2002. 312- p.

2. Lehman-McKeeman LD. Absorption, Distribution, and Excretion of Toxicants. In: Klaassen CD, III JBW, editors. Casarett and Doull´s Essentials of toxicology. 2nd ed: McGraw-Hill Publishing Company; 2010.

3. Bolla SR, Odeluga N, Jetti R. Histology, Bladder. StatPearls [Internet] Treasure Island (FL): StatPearls Publishing; 2020.

4. Guyton AC, Hall JE. Tratado de fisiologia médica. 11ª ed. Rio de Janeiro: Saunders Elsevier; 2006.

5. Lei T, Sun H, Kang Y, Zhu F, Liu H, Zhou W, et al. ADMET Evaluation in drug discovery. 18. Reliable prediction of chemical-induced urinary tract toxicity by boosting machine learning approaches. Mol Pharmaceutics. 2017;14:3935-53.

6. Hueper WC, Wiley FH, Wolfe HD. Experimental production of bladder tumors in dogs by administration of beta-naphthylamine. J Ind Hyg Toxicol. 1938;20:46-84.

7. Cohen SM. Screening for human urinary bladder carcinogens: two-year bioassay is unnecessary. Toxicology Research. 2018;7(4):565-75.

8. Kim JY, Fluri DA, Marchan R, Boonen K, Mohanty S, Singh P. 3D spherical microtissues and microfluidic technology for multi-tissue experiments and analysis. Journal of Biotechnology. 2015;205:24-35.

9. Anadón A, Martínez MA, Castellano V, Martínez-Larrañaga MR. The role of in vitro methods as alternatives to animals in toxicity testing. Expert Opin Drug Metab Toxicol. 2014;10(1):67-79.

10. Fenwick N, Griffin G, Gauthier C. The welfare of animals used in science: how the “Three Rs” ethic guides improvements. Casnadian Vetrinary Journal. 2009;50:523-30.

11. Lilienblum W, Dekan W, Foth H, Gebel T, Hengstler JG, Kahl R. Alternative methods to safety studies in experimental animals: role in the risk assessment of chemicals under the new European Chemicals Legislation (REACH). Archives of Toxicology. 2008;82:211-36.

12. Pampaloni F, Reynaud EG, Stelzer EHK. The third dimension bridges the gap between cell culture and live tissue. Nature reviews in Molecular Cell Biology. 2007;8:839-45.

13. Pampaloni F, Stelzer EHK. Three-dimensional cell cultures in toxicology. Biotechnology and Genetic Engineering Reviews. 2009;26:129-50.

14. Tamatani T, Hattori K, Nakashiro K, Hayashi Y, Wu S, Klumpp D, et al. Neoplastic conversion of human urothelial cells in vitro by overexpression of H2O2-generating peroxisomal fatty acyl CoA oxidase. International Journal of Oncology. 1999;15(4):743-52.

15. DeGraff DJ, Robinson VL, Shah JB, Brandt WD, Sonpavde G, Kang Y. Current preclinical models for the advancement of translational bladder cancer research. Mol Cancer Ther. 2013;12(2):121-30.

16. Dodmane PR, Arnold LL, Kakiuchi-Kiyota S, Qiu F, Liu X, Rennard SI. Cytotoxicity and gene expression changes induced by inorganic and organic trivalent arsenicals in human cells. Toxicology. 2013;312(1):18-29.

17. Yokohira M, Arnold LL, Lautraite S, Sheets L, Wason S, Stahl B. The effects of oral treatment with transfluthrin on the urothelium of rats and its metabolite, tetrafluorobenzoic acid on urothelial cells in vitro. Food and Chemical Toxicology. 2011;49(6):1215-23.

18. Sarwar M. Indoor risks of pesticide uses are significantly linked to hazards of the family members. Cogent Medicine. 2016;3(1):1155373.

19. MMA. Perfil nacional da gestão de substâncias químicas. Ministério do Meio Ambiente; 2003.

20. IBGE. Produção Agrícola Municipal - Tabela 1612 - Área plantada, área colhida, quantidade produzida, rendimento médio e valor da produção das lavouras temporárias 2020 [Disponível em: https://sidra.ibge.gov.br/tabela/1612].

21. IBAMA. Relatórios de comercialização de agrotóxicos 2020 [Disponível em: http://ibama.gov.br/agrotoxicos/relatorios-de-comercializacao-de-agrotoxicos].

22. USEPA. Registration eligibility decision for diuron. List A. Case 0046. Office of prevention, pesticides and toxic substances. Washington, DC: United States Environmental Protection Agency; 2003.

23. APVMA. Review of the mammalian toxicology and metabolism/toxicokinetics of diuron. Australian Pesticides and Veterinary Medicines Authority; 2011.

24. Geoffroy L, et al. Effect of oxyfluorfen and diuron alone and in mixture on antioxidative enzymes of Scenedesmusobliquus. Pestic Biochem Physiol. 2002;72(3):178-85.

25. Iyer P. Evidence on the development and reproductive toxicity of diuron: draft reproductive and cancer hazard assessment. 2002.

26. Fontes JRA, Shiratsuchi LS, Neves JL, Júlio Ld, Filho JS. Manejo integrado de plantas daninhas. Planaltina, DF: Embrapa Cerrados; 2003.

27. Field JA, et al. Diuron occurrence and distribution in soil and surface and ground water associated with grass seed production. J Environ Qual. 2003;32(1):171-9.

28. Giacomazzi S, Cochet N. Environmental impact of diuron transformation : a review. 2004;56:1021-32.

29. Gatidou G, Thomaidis NS. Evaluation of single and joint toxic effects of two antifouling biocides , their main metabolites and copper using phytoplankton bioassays. 2007;85:184-91.

30. Boven MV, Laruelle L, Daenens P. HPLC analysis of diuron and metabolites in blood and urine. J Anal Toxicol. 1990;14(4):231-4.

31. da Rocha MS, Arnold LL, Luiza M, Sartor C, Catalano SMI, Paula A, et al. Diuron-induced rat urinary bladder carcinogenesis: Mode of action and human relevance evaluations using the International Programme on Chemical Safety framework. Critical Reviews in Toxicology. 2014:1-14.

32. USEPA. Carcinogenicity peer review of diuron. Office of prevention, pesticides and toxic substances. Cincinnati: United States Environmental Protection Agency; 1997.

33. da Rocha MS, Nascimento MG, Cardoso APF, Lima LAD, Zelandi EA. Cytotoxicity and regenerative proliferation as the mode of action for Diuron-induced urothelial carcinogenesis in the rat. Toxicological sciences. 2010;113(1):37-44.

34. Fava RM, Ferragut APF, Sanches M, de Oliveira MLSC. Evaluation of early changes induced by diuron in the rat urinary bladder using different processing methods for scanning electron microscopy. Toxicology. 2015;333:100-6.

35. Nascimento MG, Luiza M, Sartor C, Lima AS, Camargo VD. Effects of Diuron [3-(3,4-dichlorophenyl)-1,1-dimethylurea] on the urinary bladder of male Wistar rats. Toxicology. 2006;224:66-73.

36. Rocha MSD, Arnold LL, Pennington KL, Muirhead D, Dodmane PR, Anwar M, et al. Diuron-induced rat bladder epithelial cytotoxicity. Toxicological sciences. 2012;130(2):281-8.

37. Rocha MSD, Arnold LL, Dodmane PR, Pennington KL, Qiu F, Lauro J, et al. Diuron metabolites and urothelial cytotoxicity: In vivo, in vitro and molecular approaches. Toxicology. 2013;314:238-46.

38. Cardoso APF, Catalano SMI, Sanches M, Garcia M, Camargo JLVD, de Oliveira MLSC. Dose–response of diuron [3-(3,4-dichlorophenyl)-1,1-dimethylurea] in the urothelial mucosa of Wistar rats. Toxicology. 2013;312:1-5.

39. Ihlaseh SM, Bailey KA, Hester SD, Jones C, Ren H, Cardoso APF, et al. Transcriptional profile of Diuron-induced toxicity on the urinary bladder of male Wistar rats to inform mode of action. Toxicological sciences. 2011;122(2):330-8.

40. Ihlaseh-catalano SM, Bailey KA, Paula A, Cardoso F, Ren H, Fry RC, et al. Dose and temporal effects on gene expression profiles of urothelial cells from rats exposed to diuron. Toxicology. 2014;325:21-30.

41. Oliveira GAR, Lapuente J, Leme DM, Ferraz ERA, Meireles G, Oliveira DP. New Paradigms for the environmental assessment: an ecotoxicological and genetic approach. New York: Nova Science Publishers; 2013.

42. Seibert H, Balls M, Fentem JH, Bianchi V, Clothier H, Dierickx PJ. Acute toxicity testing in vitro and the classification and labelling of chemicals. ATLA. 1996;24:499-510.

43. Orrenius S, Nicotera P, Zhivotovsky B. Cell death mechanisms and their implications in toxicology. 2011;119(1):3-19.

44. Grivicich I, Regner A, da Rocha AB. Morte celular por apoptose.53(3):335-43.

45. Afford S, Randhawa S. Demystified...Apoptosis. J Clin Pathol: Mol Pathol. 2000;53:55-63.

46. Haupt S, Berger M, Goldberg Z, Haupt Y. Apoptosis – the p53 network. Journal of Cell Science. 2003;116:4077-85.

47. Pereira LC, Souza AO, de Pazin M, Dorta DJ. Mitocôndria como alvo para avaliação de toxicidade de xenobiótico. Revista Brasileira de Toxicologia. 2012;25(1-2):1-14.

48. Boujrad H, Gubkina O, Robert N, Krantic S, Santos A. AIF-mediated programmed necrosis: a highly orchestrated way to die. 2007;6(21):2612-9.

49. Elmore S. Apoptosis: A review of programmed cell death. Toxicologic Pathology. 2007;35:425-516.

50. Orrenius S, Kaminskyy VO, Zhivotovsky B. Autophagy in toxicology: cause or consequence ? 2013(October 2012):1-23.

51. Shen S, Kepp O, Michaud M, Martins I, Minoux H, Metivier D. Association and dissociation of autophagy, apoptosis and necrosis by systematic chemical study. Oncogene. 2011;30(45):4544-56.

52. Lee Y-k, Lee J-a. Role of the mammalian ATG8 / LC3 family in autophagy : differential and compensatory roles in the spatiotemporal regulation of autophagy. 2016;49(8):424-30.

53. Wu J, Dang Y, Su W, Liu C, Shan Y, Pei Y, et al. Molecular cloning and characterization of rat LC3A and LC3B —Two novel markers of autophagosome. Biochemical and Biophysical Research Communications. 2006;339:437-42.

54. Amaya C, Fader CM, Colombo MI. Autophagy and proteins involved in vesicular trafficking. 2015;589:3343-53.

55. Tanida I, Ueno T, Kominami E. LC3 and Autophagy. Methods Mol Biol. 2008;445:77-88.

56. Surova O, Zhivotovsky B. Various modes of cell death induced by DNA damage. Oncogene. 2013;32:3789-97.

57. Li Y, Couch L, Higuchi M, Fang JL, L G. Mitochondrial dysfunction induced by Sertraline, an antidepressant agent. Toxicological sciences. 2012;127:589-91.

58. Stachowicz A, Suski M, Olszanecki R, Madej J, Okon K, Korbut R. Proteomic analysis of liver mitochondria of apolipoprotein E in knockout mice treated with metformin. J Proteomic. 2012;IN PRESS.

59. Fawcett DW. Mitochondria. 1981. p. 410-86.

60. Friedman JR, Nunnari J. Mitochondrial form and function. Nature. 2014;505(7483):335-43.

61. Ni H-m, Williams JA, Ding W-x. Redox biology mitochondrial dynamics and mitochondrial quality control. Redox Biology. 2015;4:6-13.

62. Roubicek DA, Souza-pinto NCD. Mitochondria and mitochondrial DNA as relevant targets for environmental contaminants. Toxicology. 2017;391:100-8.

63. Nelson DL, Cox MM. Princípios de bioquímica de Lehninger. 6ª ed. Porto Alegre: Artmed; 2014.

64. Nicholls DG, Ferguson SJ. Bioenergetics 2. London: Academic Press Inc; 1982.

65. Pereira LC, de Souza AO, Dorta DJ. Polybrominated Diphenyl Ether Congener (BDE-100) induces mitochondrial impairment. Basic & Clinical Pharmacology & Toxicology. 2013;112:18-424.

66. Connolly NMC, Theurey P, Adam-Vizi V, Bazan NG, Bernardi P, Bolaños JP, et al. Guidelines on experimental methods to assess mitochondrial dysfunction in cellular models of neurodegenerative diseases. Cell Death & Differentiation. 2017;25:542–72.

67. Esterhuizen K, Van der Westhuizen FH, Louw R. Metabolomics of mitochondrial disease. Mitochondrion. 2017;16:30145-3.

68. Braga CP, Adamec J. Metabolome Analysis. In: Shoba Ranganathan MG, Kenta Nakai, Christian Schönbach, editor. Encyclopedia of Bioinformatics and Computational Biology: Academic Press; 2019. p. 463-75.

69. Trushina E, Nemutlu E, Zhang S, Christensen T, Camp J, Mesa J, et al. Defects in mitochondrial dynamics and metabolomic signatures of evolving energetic stress in mouse models of familial Alzheimer's Disease. PLoS ONE. 2012;7(2):e32737.

70. Sahu D, Lotan Y, Wittmann B, Neri B, Hansel DE. Metabolomics analysis reveals distinct profiles of nonmuscle-invasive and muscle-invasive bladder cancer. Cancer medicine. 2017;6(9):2106–20.

2. OBJETIVOS

2.1 Geral

Este trabalho objetivou estudar os mecanismos de citotoxicidade induzidos pelo diuron e dois de seus principais metabólitos em células uroteliais, DCA e DCPMU, pela avaliação dos processos de morte celular e da função mitocondrial.

2.2 Específicos

- Caracterizar o potencial citotóxico do diuron e seus metabólitos em linhagem de células uroteliais humanas imortalizadas 1T1.
- Investigar os efeitos provocados pela exposição ao diuron e seus metabólitos na mitocôndria de células uroteliais isoladas de ratos Wistar utilizando análise metabolômica.

[1] *Capítulo II*

[1]De modo a atender às normas do Programa de Pós-Graduação em Patologia, o capítulo II desta tese é composto por dois artigos científicos: Manuscrito I a ser submetido na revista Toxicology (FI: 4.099) e Manuscrito II aceito para publicação na Toxicology Mechanisms and Methods (FI: 2.987).

MANUSCRITO I

Cytotoxic mechanism of diuron and its metabolites on urothelial cells

Thania Rios Rossi Lima[a,c], João Lauro Viana de Camargo[a,c], Carla Adriene da Silva[a,c], Lílian Cristina Pereira[b,c]

[a]São Paulo State University (Unesp), Medical School, Botucatu. [b]São Paulo State University (Unesp), School of Agriculture, Botucatu. [c]Center for Evaluation of Environmental Impact on Human Health (TOXICAM), Unesp, Medical School, Botucatu.

Address correspondence to:

Thania Rios Rossi Lima, M.Sc.

São Paulo State University (Unesp), Medical School, Botucatu - TOXICAM, UNIPEX Block 5

Botucatu - São Paulo, Brazil, 18618-970

Phone: +55 14 3880-1590, e-mail: thania.lima49@gmail.com

Abstract

Diuron, 3- (3,4-dichlorophenyl) -1,1-dimethylurea, is an herbicide used worldwide and its metabolization in the environment or in mammals gives rise to the toxic metabolites, 3- (3,4-dichlorophenyl) -1-methylurea (DCPMU) and 3,4-dichloroaniline (DCA). Previous studies indicated that the diuron herbicide induces toxicity in different tissues, especially in the urinary bladder of Wistar rats, where at high doses it may lead to the development of tumors. Our research group has established its mode of cytotoxic action (MoA) on the urinary bladder of Wistar rats, however, the associated intimate events remain unclear. The present study aimed to investigate the underlying mechanisms involved in the toxicity of those chemicals, addressing the cell death and relating with the possible role of mitochondrial dysfunction. For this purpose, human urothelial cells 1T1 were exposed to diuron, DCA and DCPMU at a six-concentration range of 0.5 to 500 µM. The tested chemicals induced alterations related to cell death and proliferation, cell cycle instability, oxidative stress and mitochondrial damage, which were more expressive for the metabolites at higher concentrations. These data corroborate with our previous study and, collectively, suggest the mitochondrial dysfunction as an initiator event triggering cellular damage.

Keywords: urothelial toxicity; mitochondrial dysfunction; herbicide exposure; cell culture.

1. Introduction

Despite policies to encourage the reduction of the pesticides usage, application of these chemicals, mainly herbicides, is still among the main models of agriculture worldwide, especially in China, United States and Brazil (Sharma 2019). Diuron (3- (3,4-dichlorophenyl) -1,1-dimethylurea) is a urea-derived herbicide of moderate organic carbon–water partition coefficient (logK_{oc}), moderate water solubility and high stability, properties that, together with soil characteristics and climatic factors, influence its dispersion in the environment (Gatidou and Thomaidis 2007; Giacomazzi and Cochet 2004). In the United States, 28 µg/L of diuron was found in surface water, while diuron and DCPMU were found in shallow ground water at concentrations of 2 and 13 µg/L, respectively. In the same study diuron and DCPMU was also detected in the soil at concentrations ranging from 0.38-0.9 mg/kg and 0.53-1.2 mg/kg, respectively (Field et al. 2003). Recently, 94 ng L^{-1} of diuron was detected in surface water in Brazil (Acayaba et al. 2020). Biodegradation and metabolization of diuron in mammals result in the toxic metabolites, 3- (3,4-dichlorophenyl) -1-methylurea (DCPMU), 3,4 -dichlorophenylurea (DCPU) and 3,4-dichloroaniline (DCA) (APVMA 2011; Giacomazzi and Cochet 2004). Since excretion in mammals occurs mainly through urine, the urothelial tissue, which lines the urinary tract from the renal pelvis and ureters to the bladder, is one important target of the toxicity of this herbicide and/or its metabolites.

Over the past years, our research group has dedicated to the study of the adverse effects of diuron and has established its mode of cytotoxic action (MoA) on the urinary bladder of Wistar rats, which involves metabolic activation leading to initial cytotoxicity followed by cell degeneration, exfoliation and necrosis, continuous regenerative hyperplasia and possible appearance of tumors after a long-term exposure (Cardoso et al. 2013; da Rocha et al. 2014; da Rocha et al. 2010; Fava et al. 2015; Ferrucio et al. 2010; Ihlaseh-

catalano et al. 2014; Ihlaseh et al. 2011; Nascimento et al. 2006; Rocha et al. 2013; Rocha et al. 2012). However, the associated subcellular and the initiating events remain unclear.

Many studies have shown that mitochondrion is a target organelle of toxicity for different xenobiotics, including pesticides (Roubicek and de Souza-Pinto 2017). Study evaluating the toxicity of diuron in two human cancer cell lines (breast adenocarcinoma: MCF-7; placental choriocarcinoma: BeWo) showed damage on cell viability and DNA induced by the herbicide, in addition to a statistically significant increase in the production of reactive oxygen and nitrogen species (RONs) in both cell lines at 200 µM (Huovinen et al. 2015). In addition, when investigating the effects of diuron on the hepatic energy metabolism using isolated perfused rat liver, Simões et al. (2017) observed decrease in the cellular ATP content leading to inhibition of the gluconeogenesis and ammonia detoxification, followed by increase in the glycolysis and fructolysis as a compensatory phenomenon. Such adverse effects are indicative of mitochondrial injury; however, similar alterations were still unexploited in the evaluation of diuron toxicity on urothelial tissue. Thereby, the present study was undertaken to elucidate the mechanism of cytotoxicity of the diuron and its metabolites on urothelial cells, addressing the cell death and relating with the possible role of mitochondrial dysfunction.

2. Material and Methods

2.1. Chemical exposure

Standard solutions of the herbicide diuron (Sigma-Aldrich Co., St Louis, MO, CAS No. 330-54-1, ≥98%) and two of its main cytotoxic metabolites for urothelial cells, DCA (Sigma-Aldrich Co., St Louis, MO, CAS No. 95-76-1, 98%) and DCPMU (Sigma-Aldrich Co., St Louis, MO, CAS No. 3567-62-2, ≤100%) were dissolved in 0.05 % DMSO + Tween 20. Solvents were tested in the 1T1 cells and no toxicity was observed at this concentration. Chemical exposure

was carried out using a concentration range between 0.5 to 500 µM, which comprises concentrations found in the environment and used in previous experimental studies, remaining below the dietary carcinogenic dose for Wistar rats (2,500 part per million - ppm): 500 µM diuron, DCA and DCPMU equals to 116.5 ppm, 81.0 ppm and 109.5 ppm, respectively (Field et al. 2003; Rocha et al. 2013). These concentrations were used in all cytotoxicity assays, in addition to the negative (0.05 % DMSO + Tween 20) and positive controls that include carbonyl cyanide m-chlorophenyl hydrazone (CCCP; Sigma-Aldrich Co., St Louis, MO, CAS No. 555-60-2), terc-butyl hydroperoxide (TBOOH; Merckmillipore, Darmstadt, BRD, CAS No. 75-91-2), cisplatin (Sigma-Aldrich Co., St Louis, MO, CAS No. 15663-27-1) and starvation medium (Hank's Balanced Salt Solution supplemented with 10 mM Hepes, pH 7.4) applied according to the requirement of each assay.

2.2. Cytotoxicity analysis

2.2.1. Cellular culture

Population of 1T1 immortalized urothelial cells derived from a normal human ureter epithelium was provided by Prof. Dr. Samuel Cohen, University of Nebraska Medical Center, USA. Cells were grown in Keratinocyte-SFM medium (1x), supplemented with bovine pituitary extract (minimum 25 mg) and recombinant human EGF (minimum 2.5 µg) (Gibco-BRL, Grand Island, NY, Cat No. 17005-042), at 37 °C in a 5% CO_2 atmosphere. After cultivation, the cells were incubated with diuron or with each of its metabolites for 24 and 48 hours. Experiments were performed in triplicate and repeated three times.

2.2.2. Kinetic study - Cell growth curve

Two different passages of 1T1 cells (1^{st} and 28^{th}) were chosen for this kinetic analysis. A total of 10^4 cells/mL were cultured in 24-well plates and, during seven days, three replicates/day were trypsinized and the number of cells was determined by counting in the

Neubauer chamber. From the cell growth curves, it was possible to determine the cell growth phases, as well as the growth rate (α), duplication time (h) and latency time (h) (Freshney, 2010; Iloki Assanga et al. 2013).

2.2.3. Cellular metabolic capacity - MTT

Approximately $5x10^4$ cells/mL were cultured in 24-well plates. After 24 and 48 hours of exposure to chemicals, incubation with [3-(4,5-Dimethylthiazol-2-yl)-2,5-Diphenyltetrazolium Bromide] (MTT) (Sigma-Aldrich Co., St Louis, MO, CAS No. 298-93-1) was carried out for 3 hours at 37 °C in a 5% CO_2 atmosphere. The Formazan salt generated from the metabolism of the dye MTT by the cells was solubilized in DMSO/Glycine solution. The absorbance was measured at 570 nm, using a spectrophotometer (Synergy™ HTX, BioTek) (Denizot et al. 1986).

2.2.4. Cell proliferation

Cell proliferation was assessed using sulforhodamine B (Sigma-Aldrich Co., St Louis, MO, CAS No. 3520-42-1), according to Skehan et al. (1990). Approximately $5x10^4$ cells/mL were incubated in 24-well plates. After incubation, the culture medium was removed and the cells washed with buffered saline. The adhered cells were fixed with methanol for two hours, washed and stained with sulforhodamine B 0.5%. The absorbance of the solubilized dye was measured at 540 nm, using a spectrophotometer (Synergy™ HTX, BioTek).

2.2.5. Cell cycle analysis

Approximately 10^5 cells/mL were exposed to chemical compounds. After 24 and 48 hours of treatment, the cells were washed with cold PBS, trypsinized, centrifuged and subsequently incubated on ice and protect from light for 30 minutes with 164 µL of hypotonic fluorescent solution (HFS) containing sodium citrate 0.1%, triton 0.1% and PI 5 µg/mL. Cell populations at Sub-G0, G0/G1, S, and G2/M phases were detected in a flow

cytometer (Guava® EasyCyte 8, Merckmillipore) immediately after incubation (de Camargo, 2015).

2.2.6. Live/Dead assay

To simultaneously evaluate cell function based on its cytoplasmic metabolism and cell viability based on integrity maintenance of the cell membrane. After exposure, approximately 10^5 cells/mL were incubated for 30 minutes with phosphate buffered saline (PBS) containing calcein-AM and ethidium homodimer (Invitrogen, Eugene, OR, Cat. No. L3224) at final concentration of 1 µM and 4 µM, respectively. Then, the number of viable cells (stained green by calcein) and non-viable cells (stained red by ethidium) were determined in a flow cytometer (Guava® EasyCyte 8, Merckmillipore).

2.2.7. Annexin V/PI assay

After incubating 10^5 cells/mL with diuron and metabolites, the cells were incubated for 15 minutes, at 37 °C, with 100 µl of solution containing binding buffer (Hepes 100 mmol/L, NaCl 1.5 mol/L, KCl 50 mmol/L, $MgCl_2$ 10 mmol/L, $CaCl_2$ 25 mmol/L, pH 7.4) and FITC Annexin V (BD Pharmingen™, Cat. No. 556419). The samples were kept in ice and, at the moment of reading, 100 µl of solution containing 5 µg/mL of propidium iodide (PI) was added in binding buffer. Exposure of phosphatidyl serine residues on the cell surface and damage to the cell membrane were detected by fluorescent labeling with annexin V and/or PI, respectively, by flow cytometry (Guava® EasyCyte 8, Merckmillipore) (Zhivotovsky et al. 1999).

2.2.8. Nuclear abnormalities

Cells (10^5 cells/mL) were cultured in 24-well plates on sterile coverslips and, after chemical exposure for 24 and 48 hours, they were fixed using absolute methanol for 2 hours at -20 °C and stained with Hoechst 33342 (1 µM). Coverslips with the cell monolayer adhered to their surface were transferred to a glass slide, over a drop of Slowfade® Gold Antifade

Reagent Slide Mounting Solution (Life Technologies Co., CA, USA, Cat No. S36963). Apoptotic cells were detected by nuclear morphological changes (nuclei with visible signs of condensation and fragmentation) with the aid of a fluorescence microscope at 40X magnification and the number of cells showing nuclear abnormalities was expressed as a percentage of the total number of cells. Cisplatin (1 mg/mL) was used as a positive control (adapted from Crowley et al. 2016).

2.2.9. Lysosome accumulation

After exposure of the cells (10^5 cells/mL) to the test chemicals for 24 and 48 hours, they were carefully washed with PBS and incubated with 100 nM of LysoTracker Red DND-99 (Molecular Probes, ThermoFhisher Scientific, Cat No. L7528) and 1 µM of Hoechst 33342 (Sigma-Aldrich Co., St Louis, MO, CAS no. 875756-97-1) for 30 minutes under constant agitation. The fluorescent dye LysoTracker was used in order to monitor the distribution of lysosomes in cells after exposure to diuron, DCA and DCPMU, since it has an affinity for acidic organelles, and for marking lysosomes it has been widely used for the evaluation of the autophagy process (Chikte et al. 2014; Rodriguez-Enriquez et al. 2006). The cells were then evaluated and photographed with the aid of a fluorescence microscope. As a positive control for autophagy induction, the nutrient-deficient medium, also known as starvation medium was used.

2.2.10. LC3B accumulation

Manufacturer protocol of the LC3B Antibody Kit for Autophagy (Molecular Probes, ThermoFisher Scientific, Cat No. L10382) was adapted for 1T1 cells and performed as follows: after the period of exposure to the compounds, the culture medium was discarded, the cells were then washed with PBS and fixed with 3.7% formaldehyde for 15 minutes at

room temperature and incubated with blocking solution containing BSA 1% (w/v) and Triton x-100 0.01% (v/v) diluted in PBS for 1 hour under gentle and constant agitation, to permeabilize the cells and block possible nonspecific binding sites. The cells were then incubated with anti-LC3 antibody 0.25 µg/mL overnight at 4 °C. The next day, the antibody was discarded, cells were carefully washed with PBS and incubated with secondary antibody conjugated with Alexa Fluor® 594 (Molecular Probes, ThermoFisher Scientific, Cat No. A-21207) at a 1:2000 dilution for 3 hours at room temperature under gentle and constant agitation. In order to show the cell nuclei and to detect the mitophagy process, 1 µM Hoechst 33342 and 20 nM MitoTracker (Molecular Probes, ThermoFisher Scientific, Cat No. M7514) was used, respectively. Cells were photographed under fluorescence microscope and analyzed using ImageJ software (version 1.53K) by counting the number of puncta labeling pattern for the LC3 protein/nucleus. Three independent experiments were also carried out using 50 nM Chloroquine for 16 hours, a classic inhibitor of the autophagy signaling pathway.

2.2.11. Mitochondrial membrane potential

After exposure to the chemicals, approximately 10^5 cells/mL were incubated with tetramethylrhodamine methyl ester (TMRM) (Invitrogen, Eugene, OR, Cat No. T668) 6.6 µmol/L, at 37 °C for 30 minutes. The samples were centrifuged and the pellet resuspended in 200 µL of PBS solution. The fluorescence of TMRM captured and retained by viable mitochondria was determined by flow cytometry (Guava® EasyCyte 8, Merckmillipore).

In addition, the same marker was also evaluated by fluorescence microscopy. For this, 10^5 cells/mL were plated on sterile coverslips, exposed to chemical compounds, and incubated with TMRM under the same conditions mentioned above. Then, the coverslips

were removed from each culture well and placed in an inverted position so that the cells are positioned between the coverslip and the slide (Imberti et al. 1993).

2.2.12. Accumulation of Reactive Oxygen and Nitrogen Species (RONS)

Formation and accumulation of RONS were measured by incubating 10^4 cells/mL in PBS solution containing 5 µM of 5-(6)-chloromethyl-2',7'-dichlorodihy-drofluorescein diacetate, acetyl ester (CM-H_2DCFDA) (Invitrogen, Eugene, OR, Cat No. C6827) for 30 minutes at 37 °C; the fluorescence was analyzed in spectrophotometer (Synergy™ HTX, BioTek) at 503 and 528 nm for excitation and emission, respectively (Lebel et al. 1992). Fluorescence values were normalized by the amount of cellular protein obtained for each corresponding well, using Bradford reagent (Sigma-Aldrich Co., St Louis, MO, Cat No. B6916).

3. Statistical analysis

The results of the cytotoxicity tests with 1T1 cells were evaluated by Analysis of Variance (ANOVA), followed by the Dunnett`s post-hoc test to compare the different groups treated in relation to their respective negative controls using the GraphPrism program (San Diego, USA, version 8.0.2 for Windows).

4. Results

4.1. Cytotoxicity assays

4.1.1. Kinetic study - Cell growth curve

The 1T1 cells appeared in increasing numbers as the experiment lasted longer (Figure 1A). From the analysis of cell growth curves, it was possible to identify the latency and exponential phases (Figure 1B). When the experiment was carried out using cells at first-passage, the latency phase ended on the 2nd cultivation day, from which the exponential phase began. When twenty eighth-passage was used, the cell growth rate showed stability from the first to the second day of culture and later recovery. Thus, the increase in the

growth rate was considered as a second exponential phase. Although the plateau and decline phases are not represented on the curves, it can be said that these events started on the 8th day, since the cells had already reached 100% confluence on the last evaluation day (7th day).

In addition, it was possible to determine some parameters such as growth rate (α), doubling time (h) and latency time (h). It has been estimated that first-passage 1T1 cells take 33.4 hours to adapt (latency time) and, since then, have shown a growth rate of 0.20, taking about 35.6 hours to duplicate. For the twenty eight-passage, was estimated a latency time of 20.9 hours. Those cells presented a growth rate of 0.34 and 0.19, taking about 21.2 and 36.2 hours to duplicate in the exponential phase I and II, respectively (Figure 1C).

4.1.2. MTT reduction rate

A propensity to increase the MTT reduction rate was observed at the lowest concentration (0.5 µM) and intermediate concentrations up to 10 µM after 24 hours of exposure, consolidated at 48 hours. However, at the higher concentrations (100 µM and 500 µM) a significant decrease in this rate was found for all chemicals (diuron, DCA and DCPMU) compared to the negative control; with 24 hours of exposure, the decrease was 48.6% and 38.6% - 81.2% respectively for DCA 500 µM and DCPMU 100 µM - 500 µM, while after 48 hours this decrease at higher concentrations was more expressive (25.9% - 37.43% for diuron 100 µM - 500 µM; 57,8% - 78.6% for DCA 100 µM - 500 µM and 95.2% for DCPMU 500 µM) (Figure 2).

4.1.3. Cell proliferation

Increased cell proliferation was observed for all chemicals. For diuron, significant increases were observed at 24 and 48 hours in the lowest (0.5 µM) and intermediate concentrations up to 10 µM, but a significant decrease in 500 µM 24 hours. When cells were

exposed for 24h and 48h to DCA, they showed significant increases in proliferation from 0.5 to 10 µM. The DCPMU metabolite also induced an increase in cell proliferation in both exposure times, at concentrations of 0.5 - 10 µM (Figure 3 and 4).

4.1.4. Cell cycle alterations

As there were changes in cell content at concentrations in which there was no indication of cell death, the influence of chemical compounds on the functioning of the cell cycle was evaluated. For this purpose, propidium iodide was used as a marker, which has the ability to intercalate with the DNA molecule and emit fluorescence.

After 24 hours, a statistically significant decrease in the number of cells in the S phase of the cell cycle was observed in diuron and DCA 500 µM. After 48 hours, the number of cells in the S phase also decreased significantly from 0.5 up to 10 µM, and at 500 µM in DCPMU; DCA showed a significant decrease in 0.5 and 1 µM in the same phase. Additionally, an increase in the number of cells in the Sub-G0 phase was seen in diuron at 10 µM, as well as in DCA at 5 µM. Decrease in the G1/G0 phase was only observed in diuron 10 µM (Figure 5A and B).

4.1.5. Live/Dead

Progressive increase in non-viable cells was observed for all chemicals and at both exposure times. Exposure to DCA and DCPMU showed a significant increase in the percentage of non-viable cells followed by reduction in viable cells at highest concentration (500 µM), especially in DCPMU at 48 hours (Figure 6).

4.1.6. Annexin V/PI

After 24 and 48 hours, most of the cells were in the process of late apoptosis (or necrosis) (PI+/An+) being this result more remarkable for the metabolites at higher concentrations tested. For DCA at both times of exposure, most of the cells were not viable

(PI+/An-) at 500 µM. Significative increase in late apoptosis was seen for DCPMU 48 horas at intermediate concentrations (5 and 10 µM) (Figure 7).

4.1.7. Nuclear abnormalities

In order to confirm the results indicative of activation of the apoptotic pathway observed with Annexin V/PI, an assay was carried out to assess the induction of nuclear condensation and fragmentation in 1T1 cells. It was possible to see that diuron and DCA presented statistically significant results at the tested concentrations of 0.5 to 500 µM after 24 hours of exposure, while for DCPMU the same occurred only at higher concentrations. After 48 hours, the chemical compounds showed more pronounced significant results at 100 and 500 µM. Fluorescence microscopy micrographs show an increase in the number of cells with condensation and nuclear fragmentation at these concentrations (Figures 8 and 9).

4.1.8. Autophagy - Accumulation of lysosomes and LC3B

Based on previous data, which demonstrate cytotoxicity resulting from exposure to diuron and metabolites, we decided to verify the presence of autophagy after exposure of 1T1 cells to the compounds. Under conditions in which the autophagic process is activated, the labeling of lysosomes with the LysoTracker Red DND-99 probe appears clustered or dotted. As can be seen in Figures 10 and 11, there was no significant increase in LysoTracker labeling, except at the lowest concentrations for diuron and DCPMU within 24 hours.

We also verified the autophagy by the LC3B protein labeling profile using fluorescence microscopy. Our results showed a significant increase in LC3B accumulation at the highest concentrations only for DCA (Figures 12 and 13A and B). The MitoTracker accumulation could be seen in green in the cytoplasm of some cells. As autophagy is highly dynamic, Chloroquine, an inhibitor of the autophagic process, was added to the culture medium for 16 hours in three independent experiments to assess whether the LC3B labeling

pattern would be altered if the autophagic process was inhibited before the end of the 24-hour and 48-hour incubation. Pre-incubation with Chloroquine induced a clear increase in protein accumulation in all compounds and both exposure times, being significant mainly at 48 hours in higher concentrations (100 and 500 µM) for DCA and DCPMU (Figures 12 e 13C and D). As can be seen in the micrographs, MitoTracker accumulation was more evident and occurred concomitant with the accumulation of LC3B, generating a yellowish color in the overlapping images.

4.1.9. Mitochondrial membrane potential

All chemicals - parental and metabolites - were able to alter the mitochondrial membrane potential (ΔΨm), in both exposure times. There was a tendency to decrease the ΔΨm at all concentrations, being that metabolites induced significant reduction at 100 and 500 µM after 24 and 48 hours. At 48 hours, concentrations of diuron from 10 µM up to 500 µM also significantly reduced the mitochondrial membrane potential (Figures 14 and 15).

4.1.10. RONS production by 1T1 cells

RONS production was observed in diuron, DCA and DCPMU after both times of exposure – 24 and 48 hours. Significative alterations occurred specially in diuron exposure and was dose-response (Figure 16).

5. Discussion and Conclusions

Although diuron, DCA and DCPMU are easily eliminated by the organism considering its octanol-water partition coefficient (logK_{ow}) 2.68, 2.90 and 2.94, respectively, the time length that chemicals are stored in the bladder before excretion can lead to direct and sufficient impact to induce damage on urothelial cells. In order to elucidate the events involved in the diuron and metabolites cytotoxicity on the human 1T1 urothelial cells, assays were performed addressing different endpoints. First, is important to note that the kinetic

study of the cell growth curves showed that 1T1 cells follow the growth pattern of monolayer cultures (Iloki Assanga et al. 2013). This type of analysis is crucial to understand the cellular behavior and support discussion of results, besides assisting in the planning of experiments. There were variations between the two cell passages used regarding the analyzed parameters, and the fact that there are two growth peaks when the older passage was used suggests cell death followed by an adaptation of the cell culture to the environment. Considering the results, it is suggested that for carrying out experiments with 1T1 cells, an intermediate passage to those shown is adequate. Furthermore, it demonstrates that the exposure time of 24 and 48 hours are sufficient to cover a complete life cycle of 1T1 cells exposed to the compound.

For all chemicals and at both exposure times, an increase in the ability to reduce MTT dye was observed at the lowest concentration (0.5 µM) and at intermediate concentrations up to 10 µM, while at the highest concentrations (100 and 500 µM) this rate was lower when compared to the negative control. Likewise, there was an increase in cell proliferation for all chemicals and at both exposure times. As the duplication time for 1T1 cells is 21.9 hours (Figure 1), it can be affirmed that the increased reduction rate of MTT observed in diuron and its metabolites is due to the greater number of cells converting the dye into formazan crystals. These results corroborate with the findings of our previous study with male Wistar rats exposed to 2,500 ppm of diuron in the diet: there was a dose-dependent increase, after 15 weeks of exposure, of hyperplasia and the urothelial cell proliferation index (Rocha et al. 2010). It is well-known that cell proliferation can be initiated as a form of compensatory mechanism, referred to as apoptosis-induced proliferation (AiP). This process is triggered particularly by the effector enzymes caspase-3 and -7, critical mediators of mitochondrial events of apoptosis, which induce activation of signaling cascades and growth factors and,

consequently, stimulate the mitotic division of neighboring cells. Mitogen activation includes signaling supported by extracellular ROS production and ROS-mediated recruitment of immune cells (Fogarty and Bergmann 2017; Lakhani et al. 2006). This caspase-driven AiP mechanism appears to occur in cells exposed to the lower up to intermediate concentrations in the present study, but fails when the cells are exposed to higher concentrations.

Deregulation of the cell proliferation is associated with alterations in the cell cycle (Gérard and Goldbeter 2014). Rocha et al. (2013) reported cytotoxicity induced by DCA and DCPMU in MYP3 rat urothelial cell line and human 1T1 cells, being that both metabolites were associated with changes in oxidative stress genes, metabolism of amino acids and lipids, inflammation, besides genes involved in the cell cycle and DNA replication and repair. Herein, we observed significant decrease in the number of cells was mainly seen in the S phase at 24 and 48 hours, being that after 48 hours of exposure, we also observed alterations in the number of cells in sub-G0 and G1/G0 phases. This reduction in S-phase can be attributed to the checkpoint role of G1 and G2 phases along the cell cycle, which prevents damaged cells to replicate (S phase) or divide (M phase) (Barnum and O'Connell 2014; Yan Li et al. 2015). In addition, increase of cell population with fragmented genetic material (Sub-G0 phase) suggests apoptosis (Zak et al. 2010). Together, these findings reflect cell cycle instability after exposure to diuron and metabolites.

From the live/dead and annexin V/PI assays it was possible to observe that cell death occurs at different levels after exposure to the chemical compounds, with a more marked increase in the rate of cells in late apoptosis, especially for the diuron metabolites at higher concentrations. Such induction of apoptosis was confirmed by the increase in nuclear condensation and fragmentation at these concentrations. In an experimental Swiss mouse model of urinary bladder carcinogenesis, exposure to 1,250 or 2,500 ppm of dietary diuron

was found to increase the urothelial hyperplasia but did not alter the apoptotic index (de Moura et al. 2010). In turn, male Wistar rats exposed to 2,500 ppm of diuron presented in the microarray analysis significant increase in differentially expressed genes related to different biological functions, including to cell death (Ihlaseh-catalano et al. 2014).

In addition to apoptosis, exposure to contaminants in many cases is also related to the induction of the autophagy process. (Orrenius et al. 2013). Autophagy is a cellular process that sometimes protects the cell from cell death, but in other cases is considered to induce cell death. (Vinod et al. 2014). In the present study, we demonstrated for the first time in the literature that the tested compounds act as autophagic modulators in 1T1 cells, possibly in an attempt to protect the cell from diuron and metabolites toxicity. However, when autophagy fails in its role of cellular recycling after chemical stress, cells undergo apoptosis. Furthermore, the results suggest that the autophagic process is activated in the mitochondria (mitophagy) as co-localization of labels with MitoTracker and LC3B was observed. Such alteration in the homeostasis of this organelle is commonly related to dissipation of mitochondrial membrane potential and RONS accumulation, which in turn may be precursors of apoptotic events via the mitochondrial pathway (Pereira et al. 2012).

It is currently well established that RONS overproduction generates oxidative stress, a harmful condition to the cell. On the other hand, low levels of RONS can also activate various signaling pathways to stimulate cell proliferation and survival (Roubicek and de Souza-Pinto 2017). In a previous study, alterations were identified in genes related to oxidative stress after exposure to diuron and metabolites (Rocha et al. 2013) and, likewise, significant production of RONS was found in this study for the same compounds when compared to the negative control. Although oxidative stress is known to cause mitochondrial impairment, it may have arisen as a consequence of damage to this organelle in urothelial

cells. Wistar rats exposed to 2,500 ppm of diuron presented urothelial changes on scanning electron microscopy (SEM) that consisted of urothelial protruding cells into the bladder lumen, being called *swollen* cells (Rocha et al. 2012). This morphological scenario can be generated by mitochondrial dysfunction (Pereira et al. 2012; Rose et al. 2017). In the present study, a decrease in the mitochondrial membrane potential (ΔΨm) was observed, mainly at the metabolites higher concentrations. The ΔΨm is generated by proton pumps (H+) across the inner mitochondrial membrane which is harnessed to make ATP. Long-lasting drop or rise of ΔΨm normal levels may induce unwanted loss of cell viability and be a cause of various adverse effects (Zorova et al. 2018). Instabilities of ΔΨm have been associated to the oscillations of the mitochondrial permeability transition (MPT). In this context, mitochondrion can release or accumulate unwanted substances, including cations. Ca^{2+} is a well-recognized regulator of mitochondrial respiration and intermediary metabolism. However, Ca^{2+} and also K^{+} play a critical role in mitochondrial swelling since influx or efflux of these ions enhances osmotic pressure favoring the high-water accumulation in the matrix, which will impair mitochondrial integrity leading to cell death (Javadov et al. 2018).

The presented results corroborate the hypothesis that hepatic metabolism of diuron in mammals generates compounds with greater potential for cytotoxicity and that cellular changes can be triggered by mitochondrial dysfunction, as described in the most recent mechanistic framework proposed by our research group (Souza et al. 2020). On 1T1 urothelial cells, it can be seen that the metabolites DCA and DCPMU induce cell death and mitochondrial damage mainly at high concentrations, but some toxic effects could also be observed at the low and intermediate concentrations used here. In summary, this difference in the toxic action profile between concentrations is valuable in understanding the behavior of the evaluated compounds in different exposure scenarios. In addition, understanding the

mechanisms involved in the toxicity of those products is important for the establishment of treatment and prevention strategies, in addition to aid in the regulatory aspects of this herbicide.

6. Acknowledgments

The authors are grateful to Vickeline Namba and Ana Paula Doria for assistance in the implementation of the cellular culture model. Paulo Roberto Cardoso provided technical assistance.

7. Conflict of interest statement

This study is associated to the Botucatu Medical School, UNESP, SP, Brazil. After its completion, TRRL assumed job position in a private company. The authors have no conflicts of interest to declare.

8. Funding

This work was supported by the São Paulo Research Foundation (FAPESP) [Grant No. 2017/25402-5]; the National Council for Scientific and Technological Development (CNPq) [Grant No. 167774/2018-2]; and by the Center for Evaluation of Environmental Impact on Human Health (TOXICAM), UNESP, Brazil.

References

Acayaba, R.D., de Albuquerque, A.F., Ribessi, R.L., Umbuzeiro, G.A., Aragão, G. and Montagner, C.C. 2020. Occurrence of pesticides in waters from the largest sugar cane plantation region in the world. Environ Sci Pollut Res.

APVMA. 2011. Review of the mammalian toxicology and metabolism/toxicokinetics of diuron. Australian Pesticides and Veterinary Medicines Authority.

Barnum, K.J. and O'Connell, M.J. 2014. Cell cycle regulation by checkpoints. Methods in molecular biology 1170, 29-40.

Cardoso, A.P.F., Catalano, S.M.I., Sanches, M., Garcia, M., Camargo, J.L.V.D. and de Oliveira, M.L.S.C. 2013. Dose–response of diuron [3-(3,4-dichlorophenyl)-1,1-dimethylurea] in the urothelial mucosa of Wistar rats. Toxicology 312, 1-5.

Chikte, S., Panchal, N. and Warnes, G. 2014. Use of LysoTracker Dyes: A flow cytometric study of autophagy. Cytometry Part A 85, 169-178.

Crowley,L.C, Marfell, B.J and Waterhouse, N.J. 2016. Analyzing Cell Death by Nuclear Staining with Hoechst 33342. Cold Spring Harb Protoc; doi:10.1101/pdb.prot087205.

da Rocha, M.S., Arnold, L.L., Luiza, M., Sartor, C., Catalano, S.M.I., Paula, A., Cardoso, F., Pontes, M.G.N., Ferrucio, B., Dodmane, P.R. and Cohen, S.M. 2014. Diuron-induced rat urinary bladder carcinogenesis: Mode of action and human relevance evaluations using the International Programme on Chemical Safety framework. Critical Reviews in Toxicology, 1-14.

da Rocha, M.S., Nascimento, M.G., Cardoso, A.P.F., Lima, L.A.D. and Zelandi, E.A. 2010. Cytotoxicity and regenerative proliferation as the mode of action for Diuron-induced urothelial carcinogenesis in the rat. Toxicological sciences 113, 37-44.

de Moura, N.A., Grassi, T.F., Rodrigues, M.A.M. and Barbisan, L.F. 2010. Potential eVects of the herbicide Diuron on mammary and urinary bladder two-stage carcinogenesis in a female Swiss mouse model. Arch Toxicol 84, 165-173.

Fava, R.M., Ferragut, A.P.F., Sanches, M. and de Oliveira, M.L.S.C. 2015. Evaluation of early changes induced by diuron in the rat urinary bladder using different processing methods for scanning electron microscopy. Toxicology 333, 100-106.

Ferrucio, B., Franchi, C.A.d.S., Boldrin, N.F., de Oliveira, M.L.C.S. and de Camargo, J.L.V. 2010. Evaluation of Diuron (3- [3 , 4-dichlorophenyl] -1 , 1-dimethyl urea) in a two-stage mouse skin carcinogenesis assay. Toxicologic Pathology 38, 756-764.

Field, J.A., Reed, R.L., Sawyer, T.E., Griffith, S.M. and P. J. Wigington, J. 2003. Diuron occurrence and distribution in soil and surface and ground water associated with grass seed production. Journal of environmental quality 32, 171-179.

Fogarty, C.E. and Bergmann, A. 2017. Killers creating new life: caspases drive apoptos isinduced proliferation in tissue repair and disease. Cell Death and Differentiation 24, 1390–1400.

Freshney, R.I. 2010. Culture of animal cells: A manual of basic technique. 6th Edition, Wiley, New York.

Gatidou, G. and Thomaidis, N.S. 2007. Evaluation of single and joint toxic effects of two antifouling biocides , their main metabolites and copper using phytoplankton bioassays. 85, 184-191.

Gérard C. and Goldbeter A. 2014. The balance between cell cycle arrest and cell proliferation: control by the extracellular matrix and by contact inhibition. Interface Focus 6;4(3):20130075.

Giacomazzi, S. and Cochet, N. 2004. Environmental impact of diuron transformation : a review. 56, 1021-1032.

Huovinen, M., Loikkanen, J., Naarala, J. and Vähäkangas, K. 2015. Toxicity of diuron in human cancer cells. Toxicology in vitro 29, 1577–1586.

Ihlaseh-catalano, S.M., Bailey, K.A., Paula, A., Cardoso, F., Ren, H., Fry, R.C., Lauro, J., Camargo, V.D. and Wolf, D.C. 2014. Dose and temporal effects on gene expression profiles of urothelial cells from rats exposed to diuron. Toxicology 325, 21-30.

Ihlaseh, S.M., Bailey, K.A., Hester, S.D., Jones, C., Ren, H., Cardoso, A.P.F., Oliveira, M.L.C.S., Wolf, D.C. and Camargo, L.V.D. 2011. Transcriptional profile of Diuron-induced toxicity on the urinary bladder of male Wistar rats to inform mode of action. Toxicological sciences 122, 330-338.

Iloki Assanga, S.B., Gil-Salido, A.A., Lewis Luján, L.M., Rosas-Durazo, A., Acosta-Silva, A.L., Rivera-Castañeda, E.G. and Rubio-Pino, J.L. 2013. Cell growth curves for different cell lines and their relationship with biological activities. International Journal for Biotechnology and Molecular Biology Research 4, 60-70.

Javadov, S., Chapa-Dubocq, X. and Makarov, V. 2018. Different approaches to modeling analysis of mitochondrial swelling. Mitochondrion 38, 58-70.

Lakhani, S.A., Masud, A., Kuida, K., Jr., G.A.P., Booth, C.J., Mehal, W.Z., Inayat, I. and Flavell, R.A. 2006. Caspases 3 and 7: Key mediators of mitochondrial events of apoptosis. Science 311, 847–851.

Nascimento, M.G., Luiza, M., Sartor, C., Lima, A.S. and Camargo, V.D. 2006. Effects of Diuron [3-(3,4-dichlorophenyl)-1,1-dimethylurea] on the urinary bladder of male Wistar rats. Toxicology 224, 66-73.

Orrenius, S., Kaminskyy, V.O. and Zhivotovsky, B. 2013. Autophagy in toxicology: cause or consequence ? , 1-23.

Pereira, L., Souza, A.O.d., Pazin, M. and Dorta, D.J. 2012. Mitocôndria como alvo para avaliação de toxicidade de xenobiótico. Revista Brasileira de Toxicologia 25, 1-14.

Rocha, M.S.D., Arnold, L.L., Dodmane, P.R., Pennington, K.L., Qiu, F., Lauro, J., Camargo, V.D. and Cohen, S.M. 2013. Diuron metabolites and urothelial cytotoxicity: In vivo, in vitro and molecular approaches. Toxicology 314, 238-246.

Rocha, M.S.D., Arnold, L.L., Pennington, K.L., Muirhead, D., Dodmane, P.R., Anwar, M., Battalora, M., Camargo, J.L.V.D. and Cohen, S.M. 2012. Diuron-induced rat bladder epithelial cytotoxicity. Toxicological sciences 130, 281-288.

Rocha, M.S.d., Nascimento, M.G., Cardoso, A.P.F., Lima, P.L.A.d., Edneia A. Zelandi, Camargo, J.o.L.V.d. and Oliveira, M.L.C.S.d. 2010. Cytotoxicity and regenerative proliferation as the Mode of Action for diuron-induced urothelial carcinogenesis in the rat. Toxicological sciences 113, 37-44.

Rodriguez-Enriquez, S., Kim, I., Currin, R.T. and Lemasters, J.J. 2006. Tracker dyes to probe mitochondrial autophagy (mitophagy) in rat hepatocytes. Autophagy 2, 39-47.

Rose, J., Brian, C., Woods, J., Pappa, A., Panayiotidis, M.I., Powers, R. and Franco, R. 2017. Mitochondrial dysfunction in glial cells: Implications for neuronal homeostasis and survival. Toxicology 391, 109-115.

Roubicek, D.A. and de Souza-Pinto, N.C. 2017. Mitochondria and mitochondrial DNA as relevant targets for environmental contaminants. Toxicology.

Sharma, A., Kumar, V., Shahzad, B. et al. 2019. Worldwide pesticide usage and its impacts on ecosystem. SN Applied Sciences 1, 1446.

Simões, M.d.S., Bracht, L., Parizotto, A.V., Comar, J.F., Peralta, R.M. and Bracht, A. 2017. The metabolic effects of diuron in the rat liver. Environmental toxicology and pharmacology 54, 53-61.

Skehan, P., Storeng, R., Scudiero, D., Monks, A., McMahon, J., Vistica, D., Warren, J.T., Bokesch, H., Kenney, S. and Boyd, M.R. 1990. New colorimetric cytotoxicity assay for anticancer-drug screening. JNCI: Journal of the National Cancer Institute 82, 1107–1112.

Vinod, V., Padmakrishnan, C.J., Vijayan, B. and Gopala, S. 2014. How can I halt thee? The puzzles involved in autophagic inhibition. Pharmacological Research 82, 1-8.

Yan Li, Olena Barbash and Diehl, J.A. 2015. Regulation of the cell cycle. Cancer biology, pp. 165-179.

Zhivotovsky, B., Samali, A., Gahm, A. and Orrenius, S. 1999. Caspases: Their intracellular localization and translocation during apoptosis. Cell death and differentiation, 644–651.

Zorova, L.D., Popkova, V.A., Plotnikova, E.Y., Silacheva, D.N., Pevznera, I.B., Jankauskasa, S.S., Babenkoa, V.A., Zorovc, S.D., Balakirevad, A.V., Juhaszovae, M., Sollotte, S.J. and Zorov, D.B. 2018. Mitochondrial membrane potential. Anal Biochem 552, 50-59.

Figures

Figure 1.

(A)

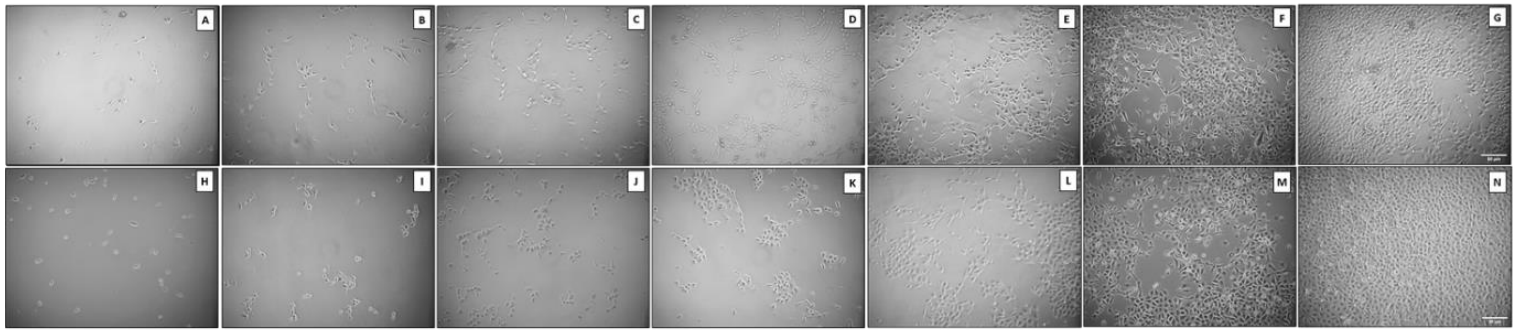

(B)

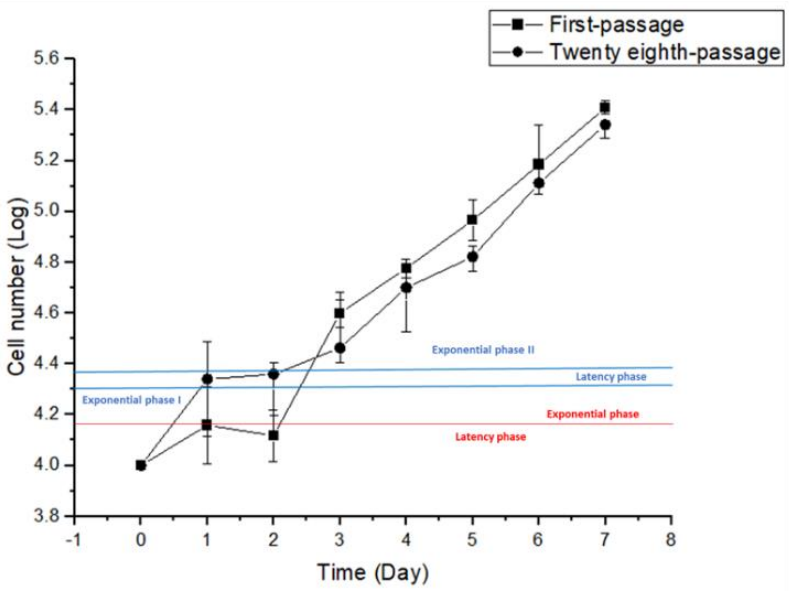

(C)

	1T1		
	First-passage	Twenty eighth-passage	
Parameter	Exponential phase	Exponential phase I	Exponential phase II
Growth rate (α)	0.20	0.34	0.19
Duplication time (h)	35.6	21.2	36.2
Latency time (h)	33.4	20.9	

Figure 2.

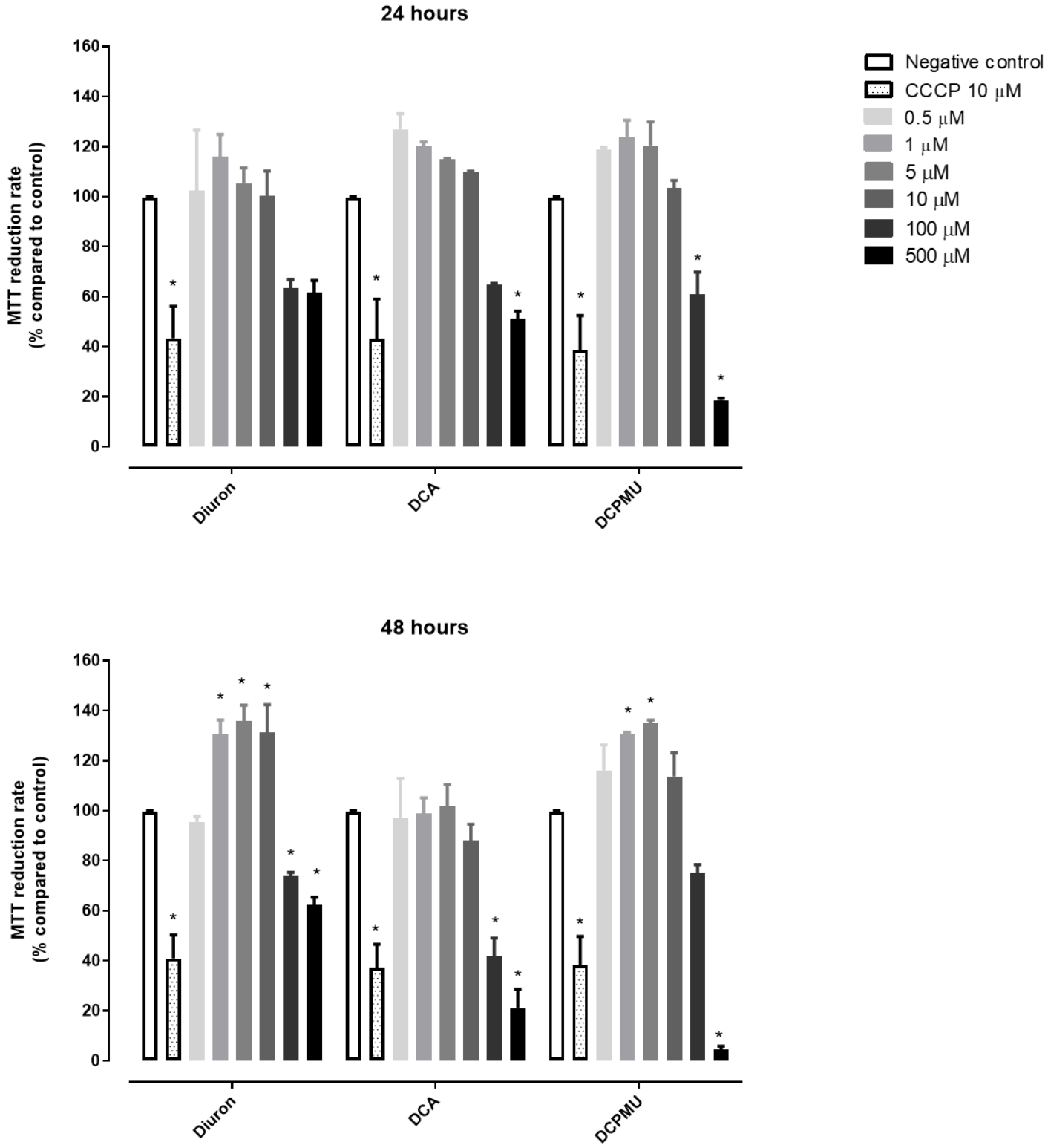
24 hours
MTT reduction rate
(% compared to control)
160
140
120
100
80
60
40
20
0
Diuron
DCA
DCPMU
Negative control
CCCP 10 μM
0.5 μM
1 μM
5 μM
10 μM
100 μM
500 μM
48 hours
MTT reduction rate
(% compared to control)
160
140
120
100
80
60
40
20
0
Diuron
DCA
DCPMU

Figure 3.

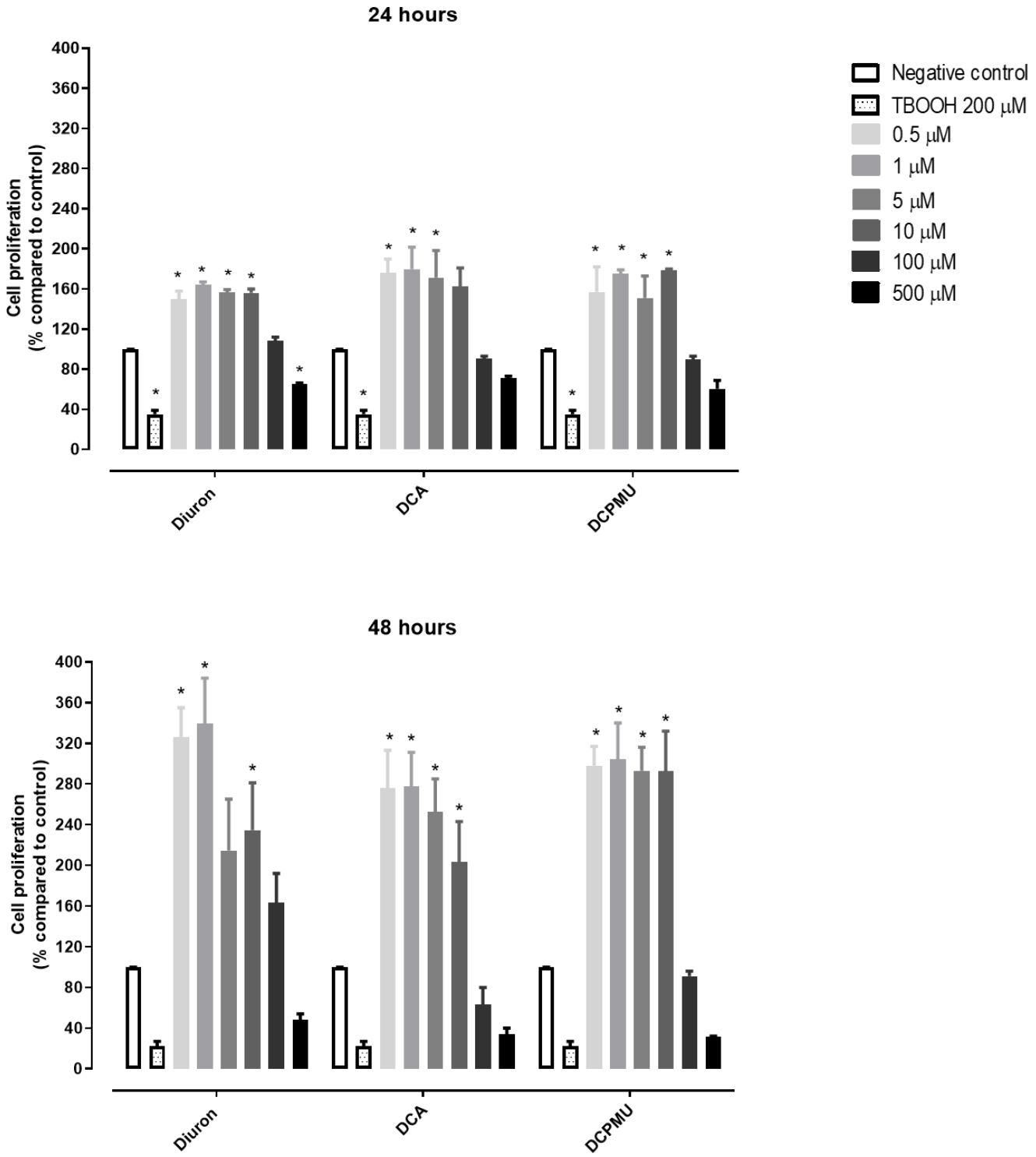
24 hours
Cell proliferation (% compared to control)
400
360
320
280
240
200
160
120
80
40
0
Diuron
DCA
DCPMU
Negative control
TBOOH 200 μM
0.5 μM
1 μM
5 μM
10 μM
100 μM
500 μM
48 hours
Cell proliferation (% compared to control)
400
360
320
280
240
200
160
120
80
40
0
Diuron
DCA
DCPMU

Figure 4.

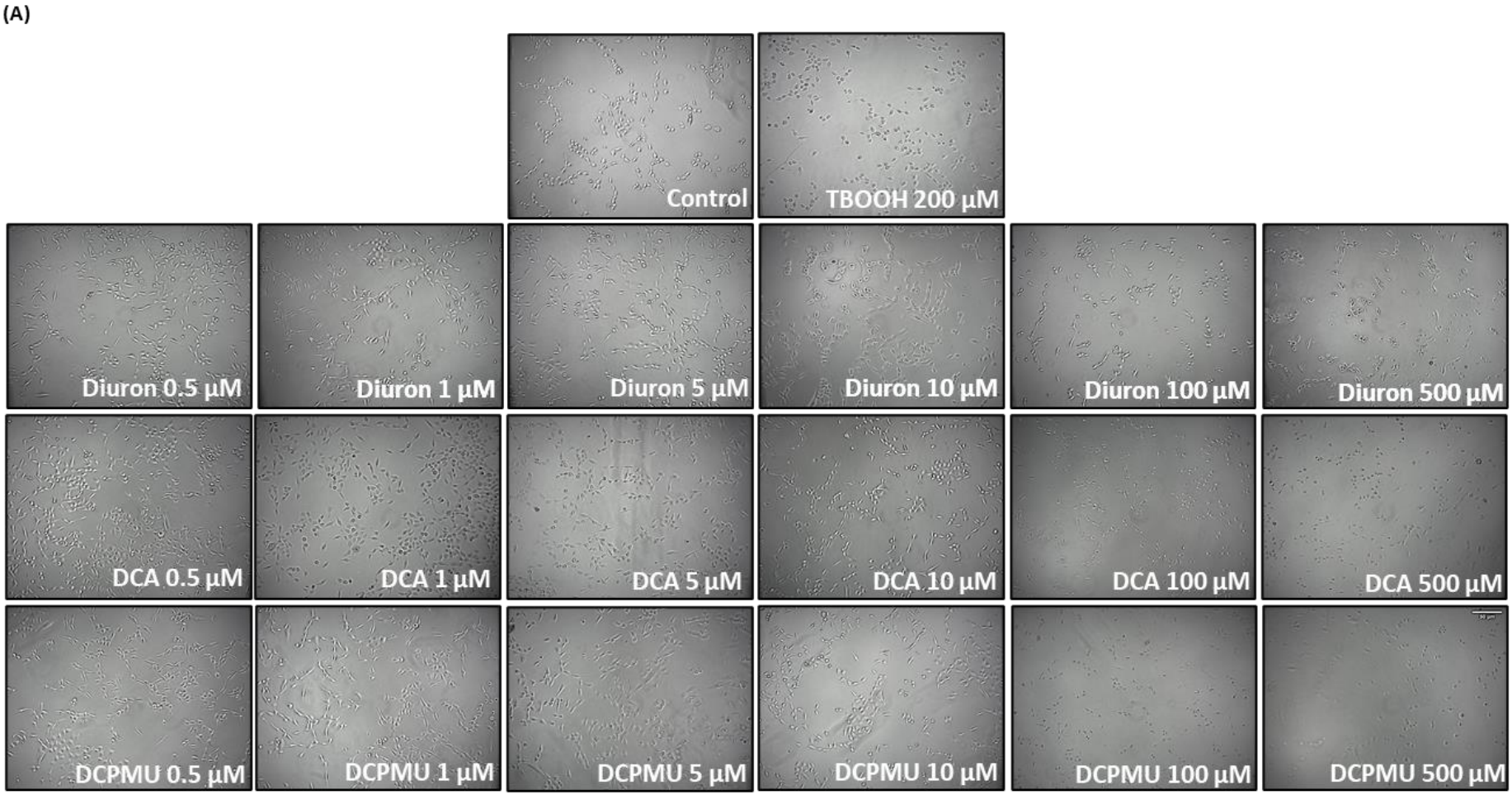
(A)
Control
TBOOH 200 µM
Diuron 0.5 µM
Diuron 1 µM
Diuron 5 µM
Diuron 10 µM
Diuron 100 µM
Diuron 500 µM
DCA 0.5 µM
DCA 1 µM
DCA 5 µM
DCA 10 µM
DCA 100 µM
DCA 500 µM
DCPMU 0.5 µM
DCPMU 1 µM
DCPMU 5 µM
DCPMU 10 µM
DCPMU 100 µM
DCPMU 500 µM

(B)

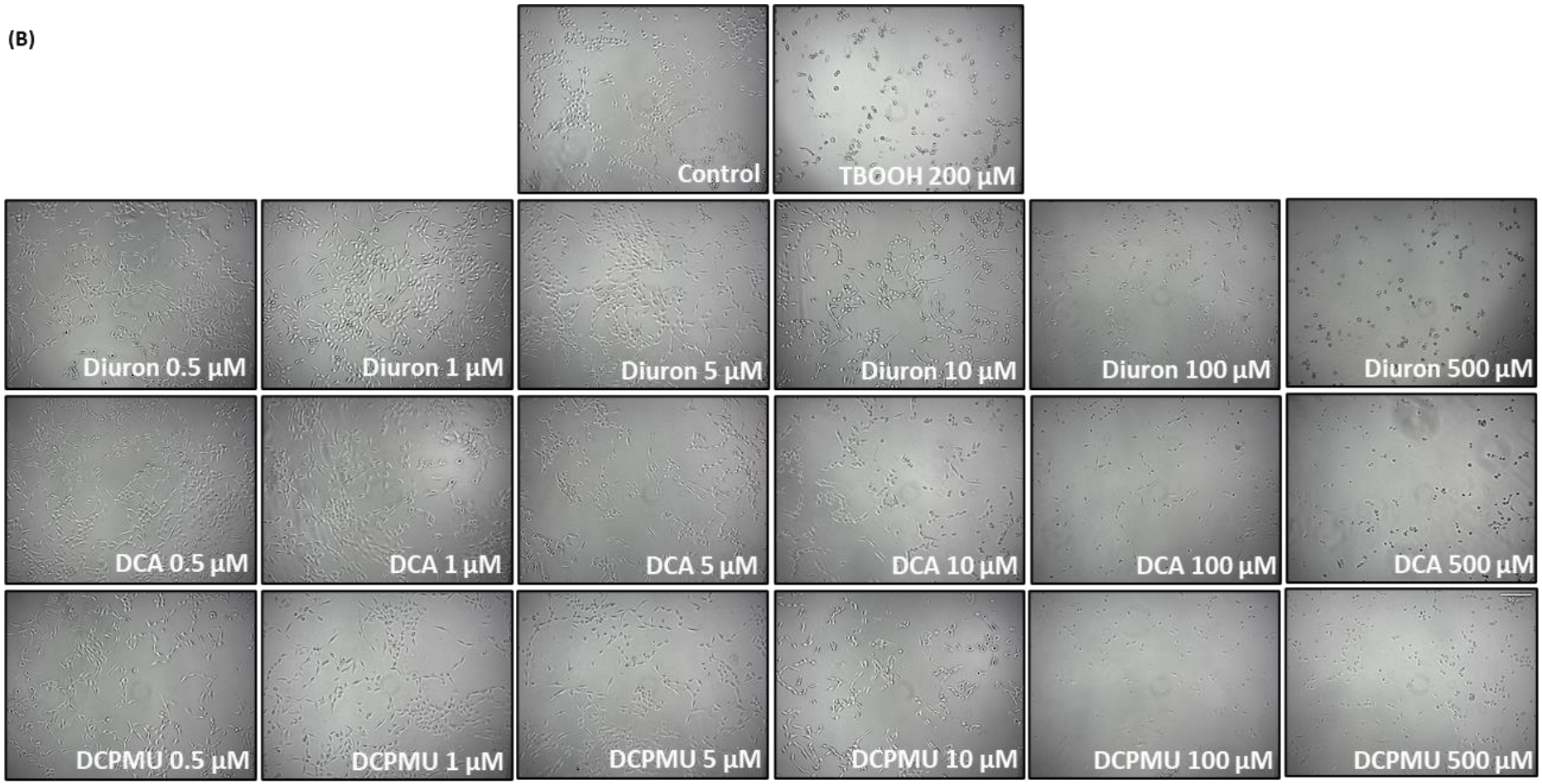
Control
TBOOH 200 µM
Diuron 0.5 µM
Diuron 1 µM
Diuron 5 µM
Diuron 10 µM
Diuron 100 µM
Diuron 500 µM
DCA 0.5 µM
DCA 1 µM
DCA 5 µM
DCA 10 µM
DCA 100 µM
DCA 500 µM
DCPMU 0.5 µM
DCPMU 1 µM
DCPMU 5 µM
DCPMU 10 µM
DCPMU 100 µM
DCPMU 500 µM

Figure 5.

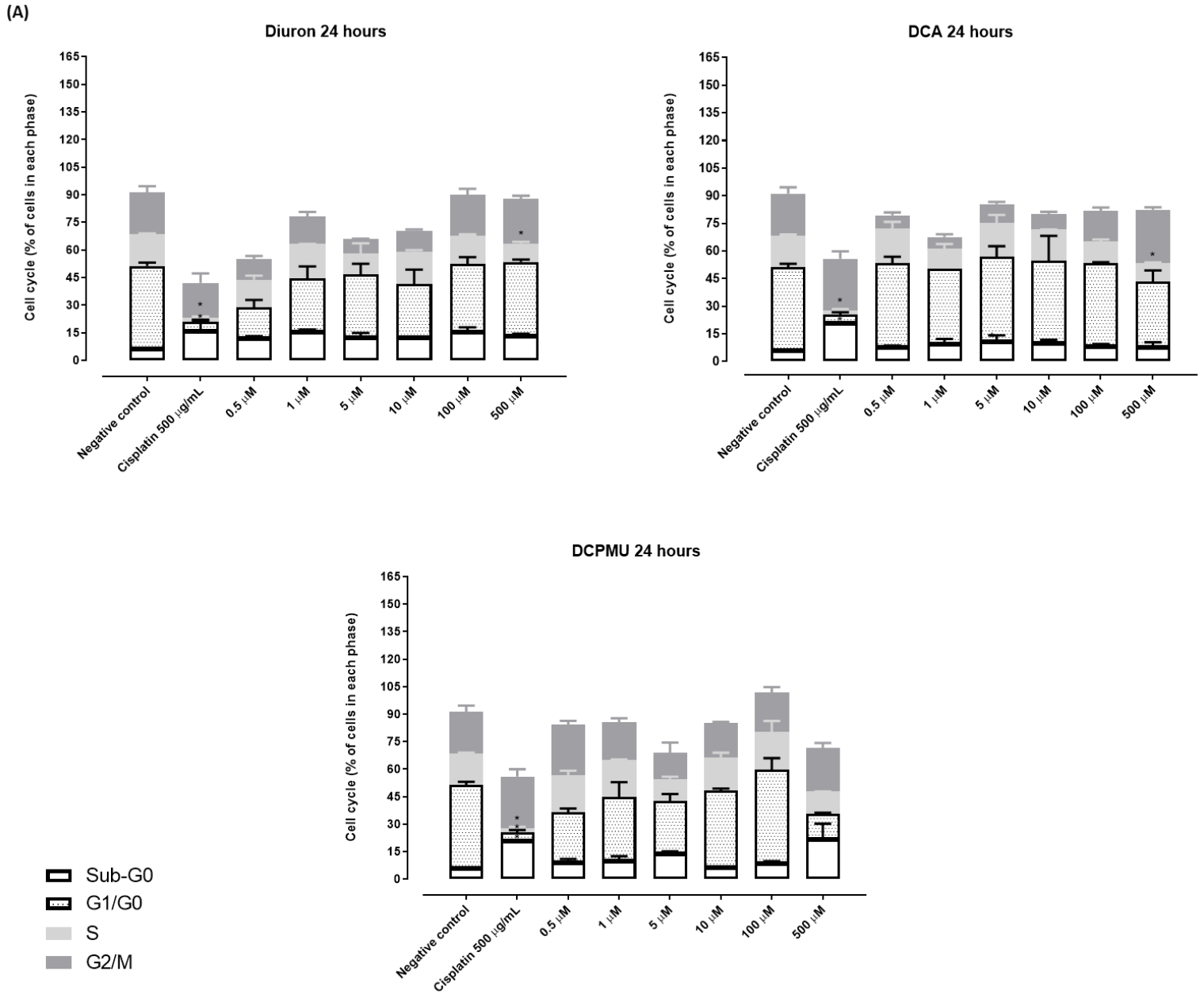
(A)
Diuron 24 hours
DCA 24 hours
DCPMU 24 hours
Cell cycle (% of cells in each phase)
Negative control
Cisplatin 500 µg/mL
0.5 µM
1 µM
5 µM
10 µM
100 µM
500 µM
Sub-G0
G1/G0
S
G2/M

(B)

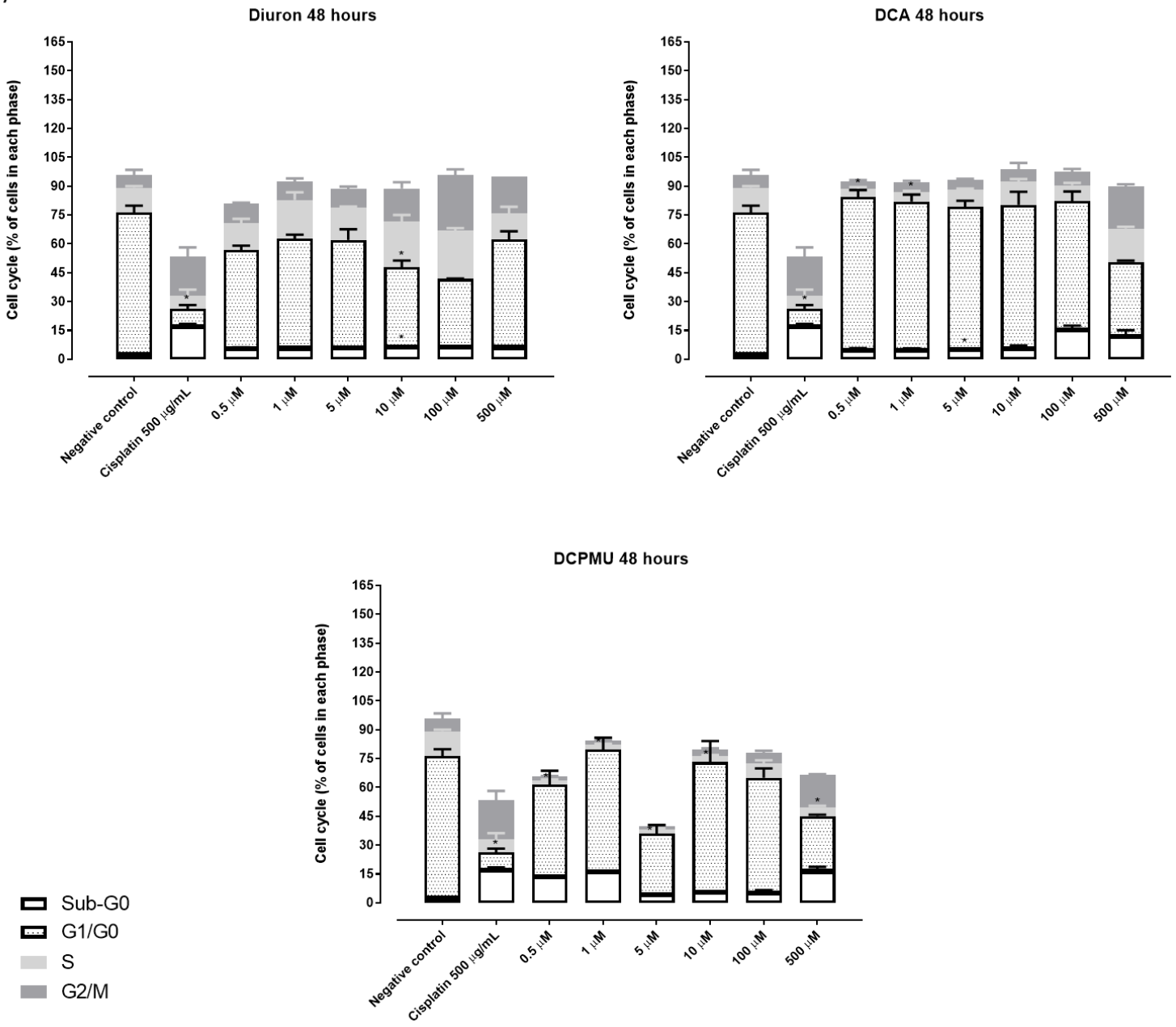
Diuron 48 hours
DCA 48 hours
DCPMU 48 hours
Cell cycle (% of cells in each phase)
165
150
135
120
105
90
75
60
45
30
15
0
Negative control
Cisplatin 500 µg/mL
0.5 µM
1 µM
5 µM
10 µM
100 µM
500 µM
Sub-G0
G1/G0
S
G2/M

Figure 6.

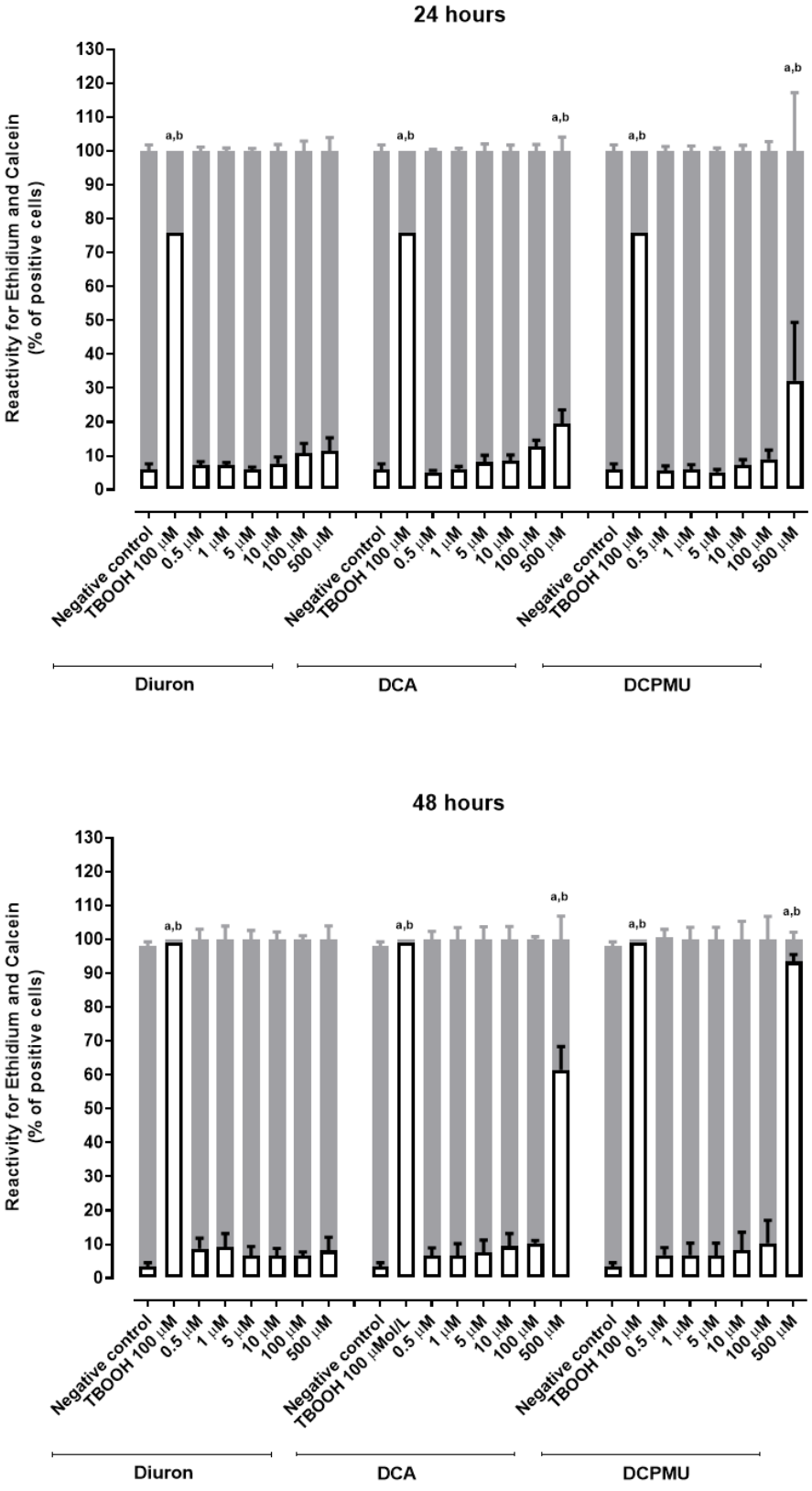
24 hours
Reactivity for Ethidium and Calcein (% of positive cells)
a,b
Negative control
TBOOH 100 µM
0.5 µM
1 µM
5 µM
10 µM
100 µM
500 µM
Diuron
DCA
DCPMU
48 hours
Reactivity for Ethidium and Calcein (% of positive cells)
a,b
Negative control
TBOOH 100 µMol/L
0.5 µM
1 µM
5 µM
10 µM
100 µM
500 µM
Diuron
DCA
DCPMU

Figure 7.

(A)

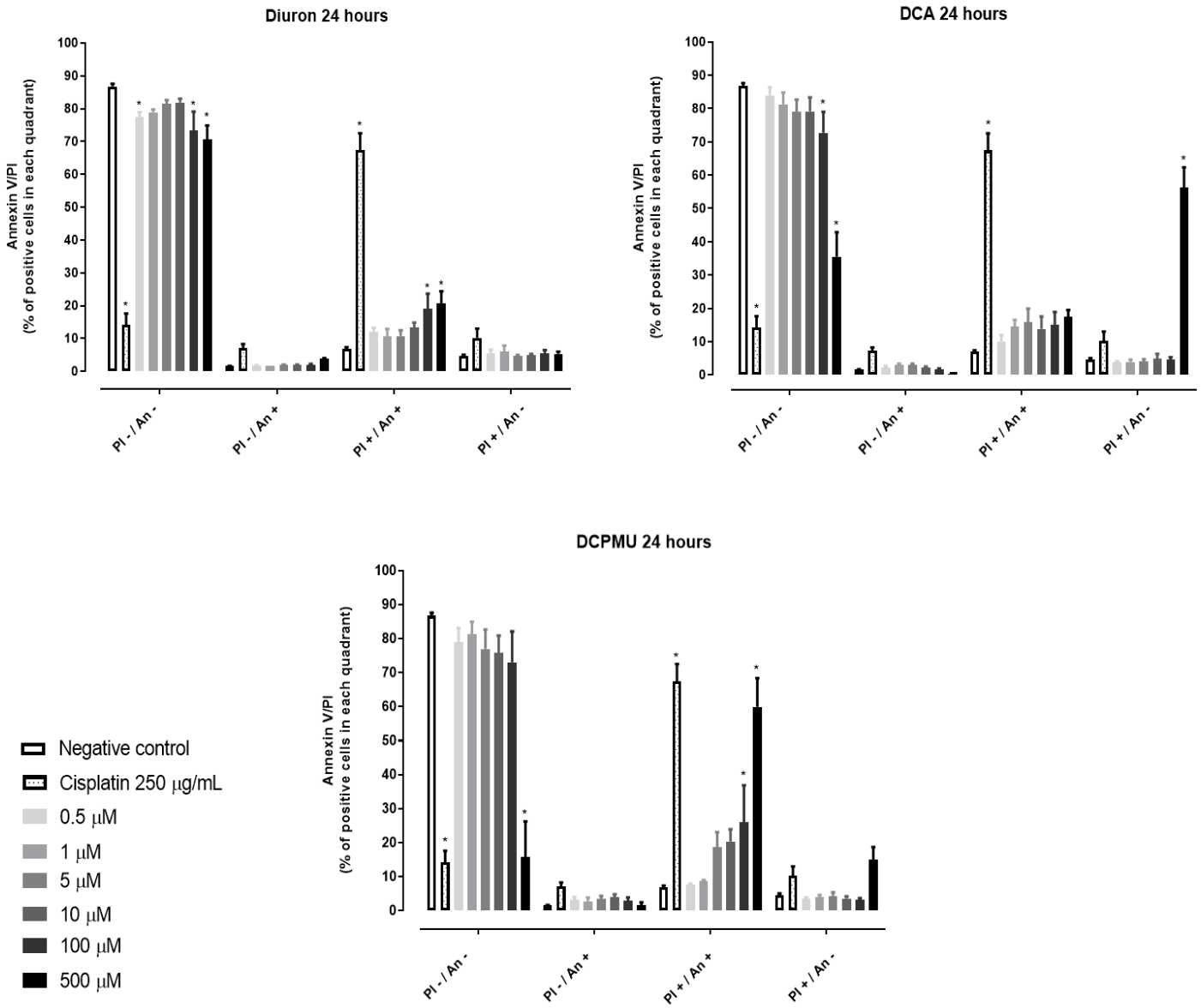
Diuron 24 hours
DCA 24 hours
DCPMU 24 hours
Annexin V/PI
(% of positive cells in each quadrant)
PI - / An -
PI - / An +
PI + / An +
PI + / An -
Negative control
Cisplatin 250 µg/mL
0.5 µM
1 µM
5 µM
10 µM
100 µM
500 µM

(B)

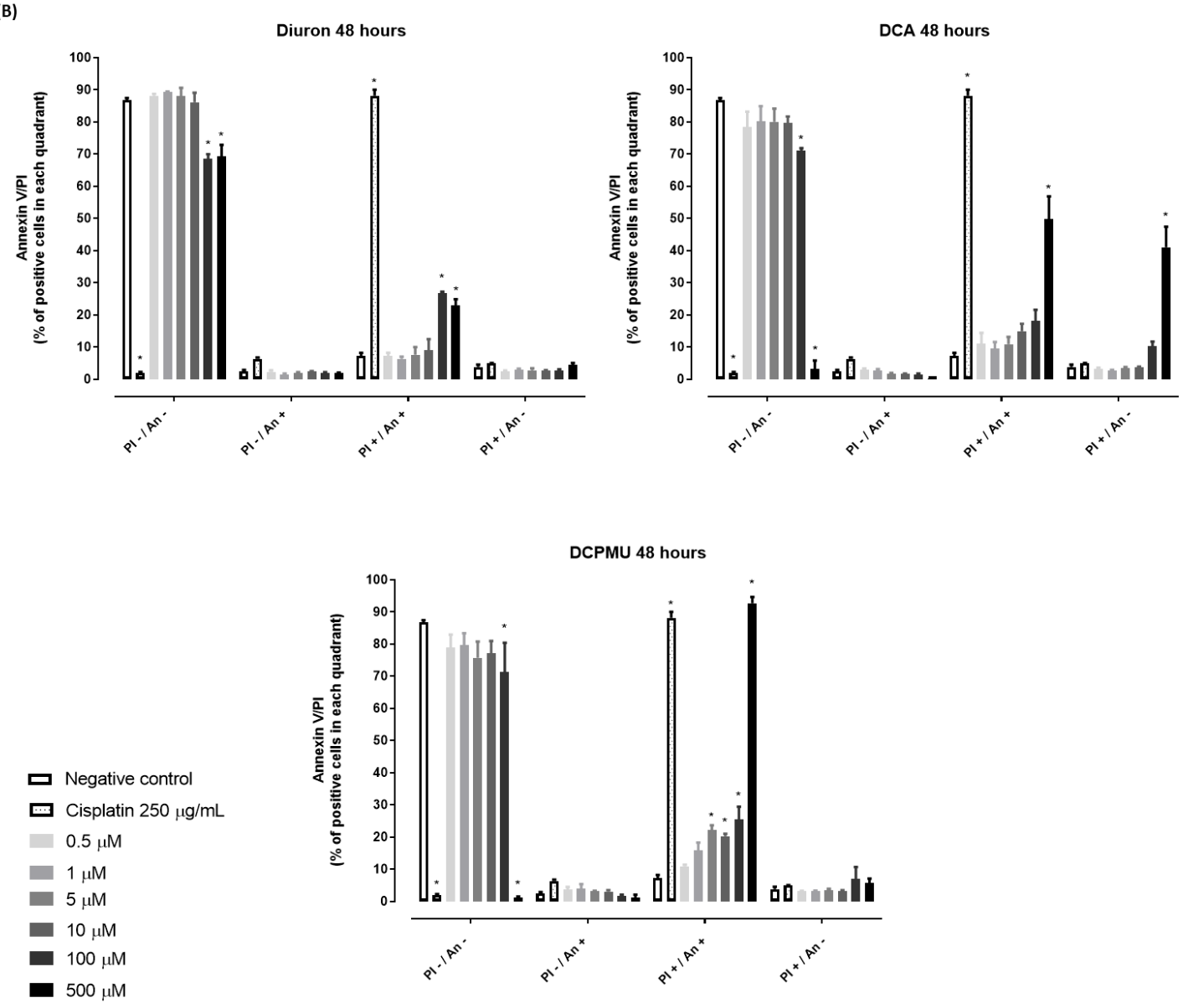
Diuron 48 hours
DCA 48 hours
DCPMU 48 hours
Annexin V/PI
(% of positive cells in each quadrant)
PI - / An -
PI - / An +
PI + / An +
PI + / An -
Negative control
Cisplatin 250 µg/mL
0.5 µM
1 µM
5 µM
10 µM
100 µM
500 µM

Figure 8.

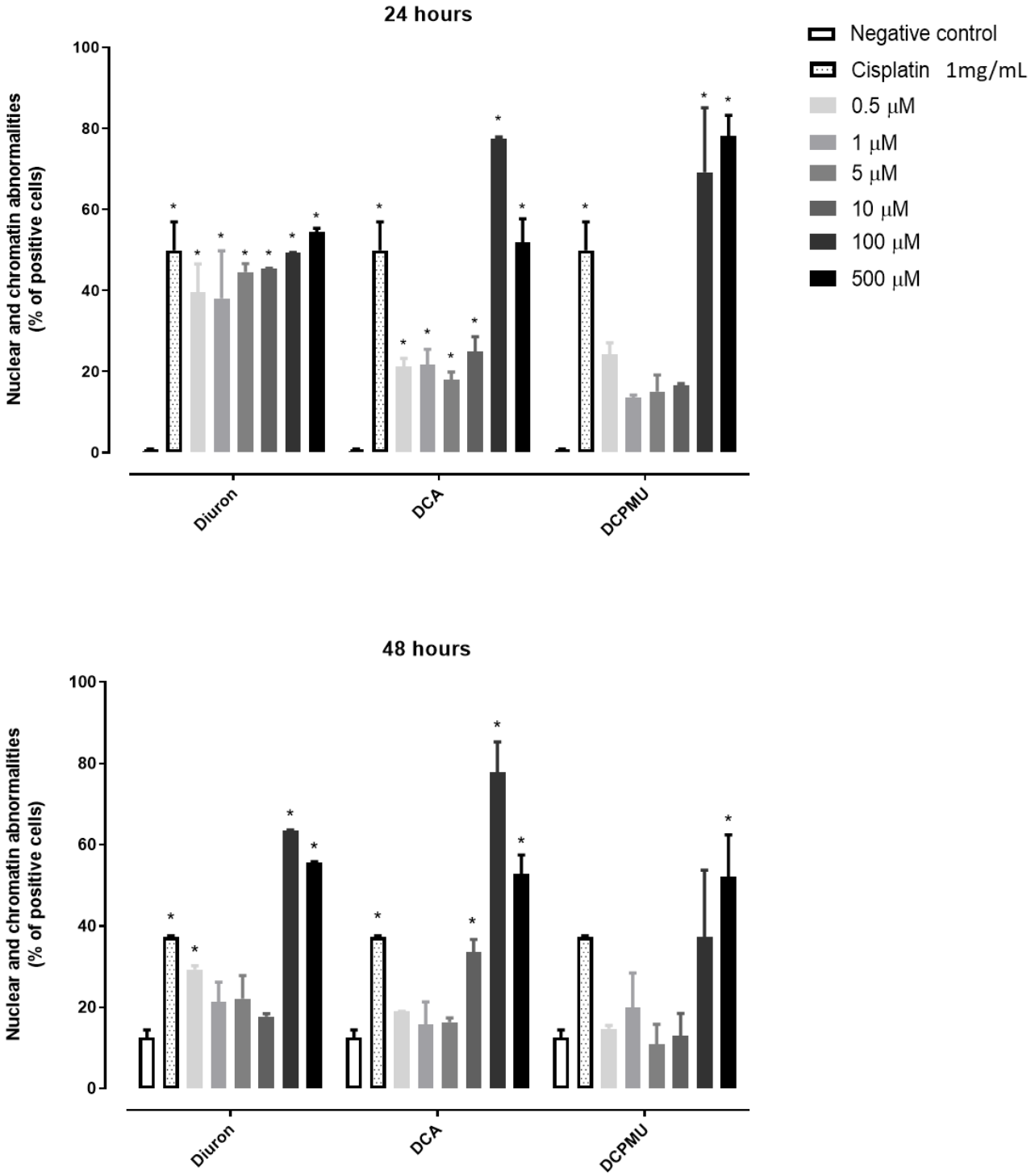
24 hours
Nuclear and chromatin abnormalities (% of positive cells)
100
80
60
40
20
0
Diuron
DCA
DCPMU
Negative control
Cisplatin 1mg/mL
0.5 μM
1 μM
5 μM
10 μM
100 μM
500 μM
48 hours
Nuclear and chromatin abnormalities (% of positive cells)
100
80
60
40
20
0
Diuron
DCA
DCPMU

Figure 9.

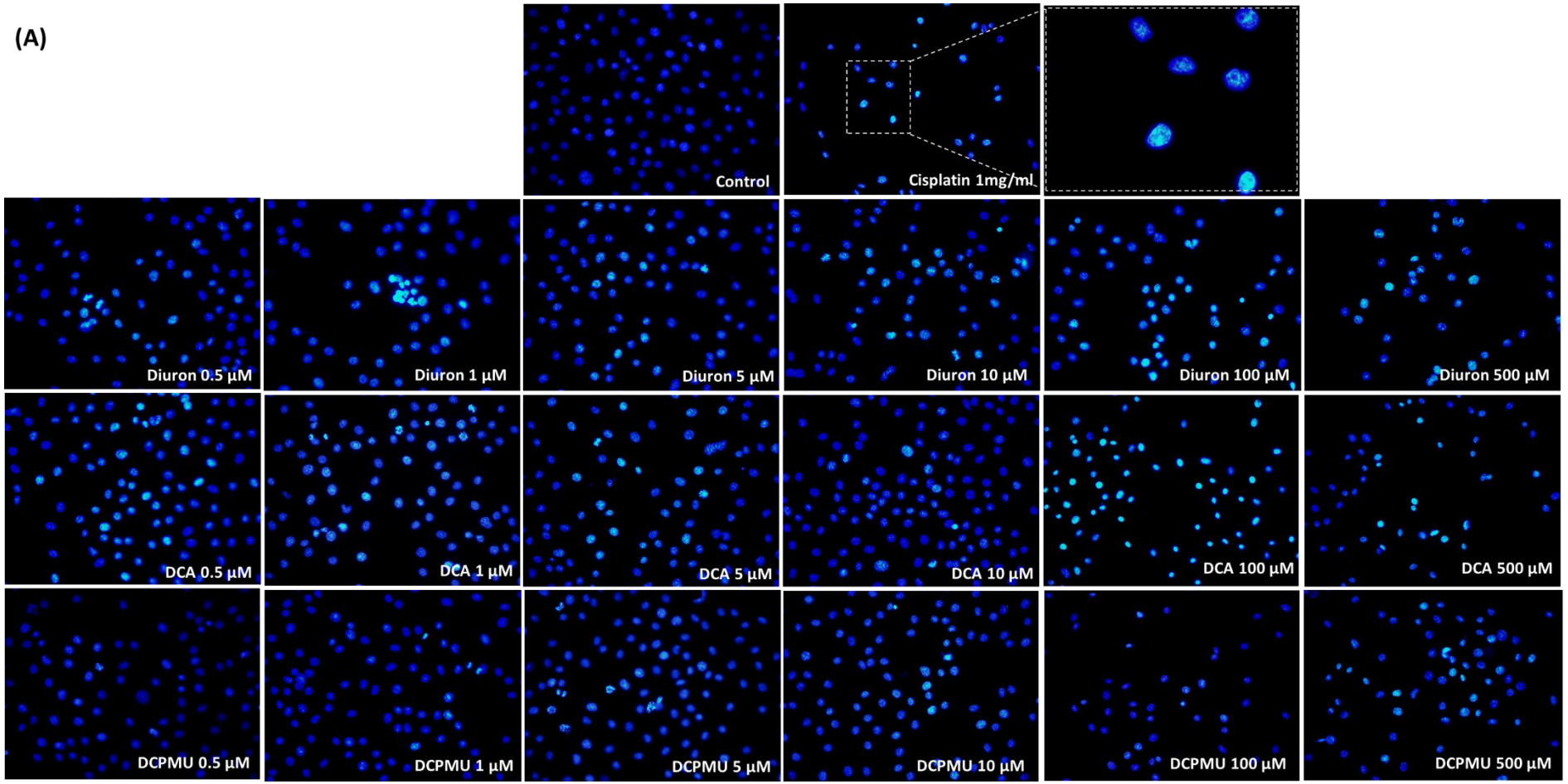
(A)
Control
Cisplatin 1mg/ml
Diuron 0.5 µM
Diuron 1 µM
Diuron 5 µM
Diuron 10 µM
Diuron 100 µM
Diuron 500 µM
DCA 0.5 µM
DCA 1 µM
DCA 5 µM
DCA 10 µM
DCA 100 µM
DCA 500 µM
DCPMU 0.5 µM
DCPMU 1 µM
DCPMU 5 µM
DCPMU 10 µM
DCPMU 100 µM
DCPMU 500 µM

(B)

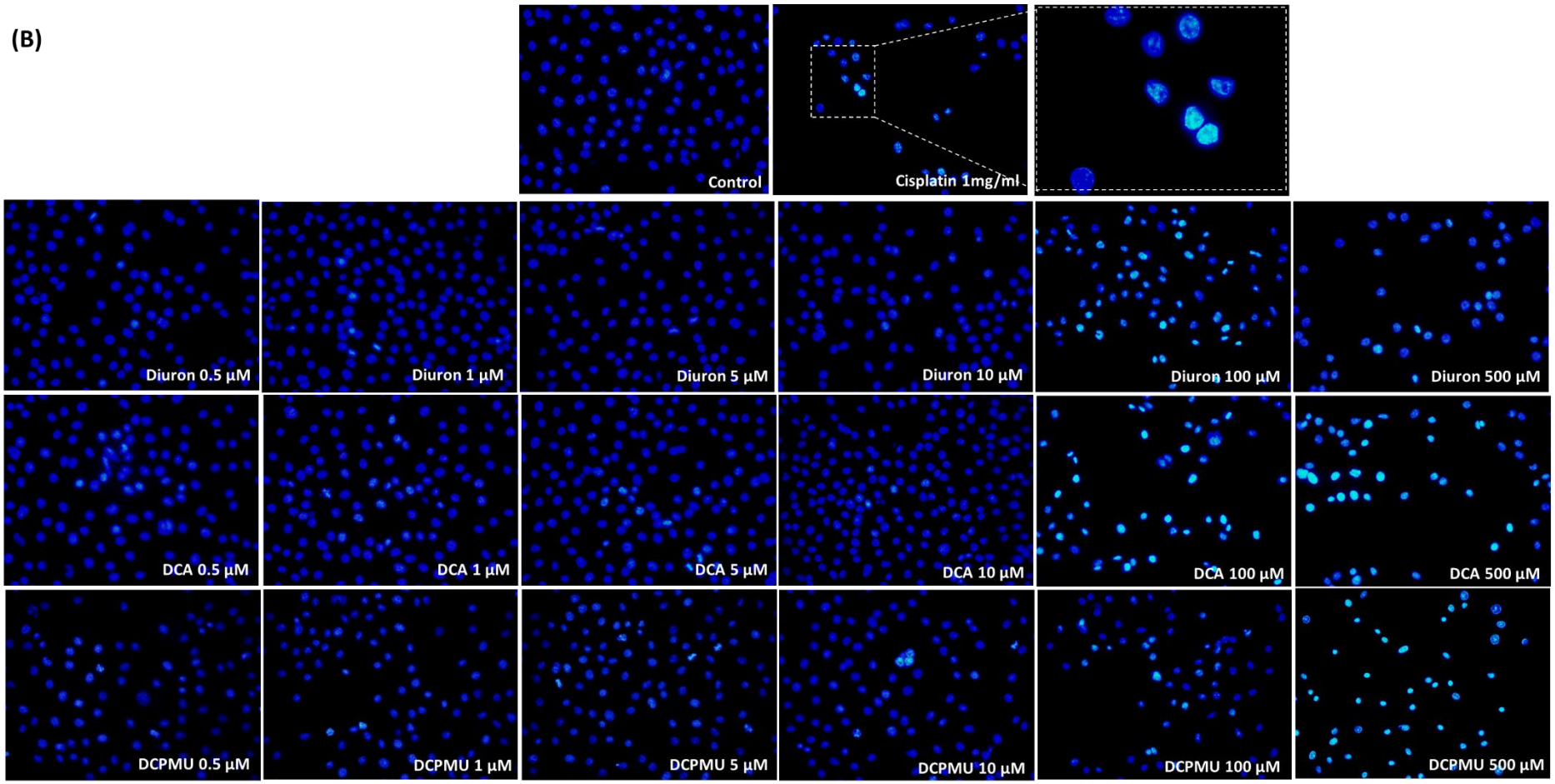
Control
Cisplatin 1mg/ml
Diuron 0.5 µM
Diuron 1 µM
Diuron 5 µM
Diuron 10 µM
Diuron 100 µM
Diuron 500 µM
DCA 0.5 µM
DCA 1 µM
DCA 5 µM
DCA 10 µM
DCA 100 µM
DCA 500 µM
DCPMU 0.5 µM
DCPMU 1 µM
DCPMU 5 µM
DCPMU 10 µM
DCPMU 100 µM
DCPMU 500 µM

Figure 10.

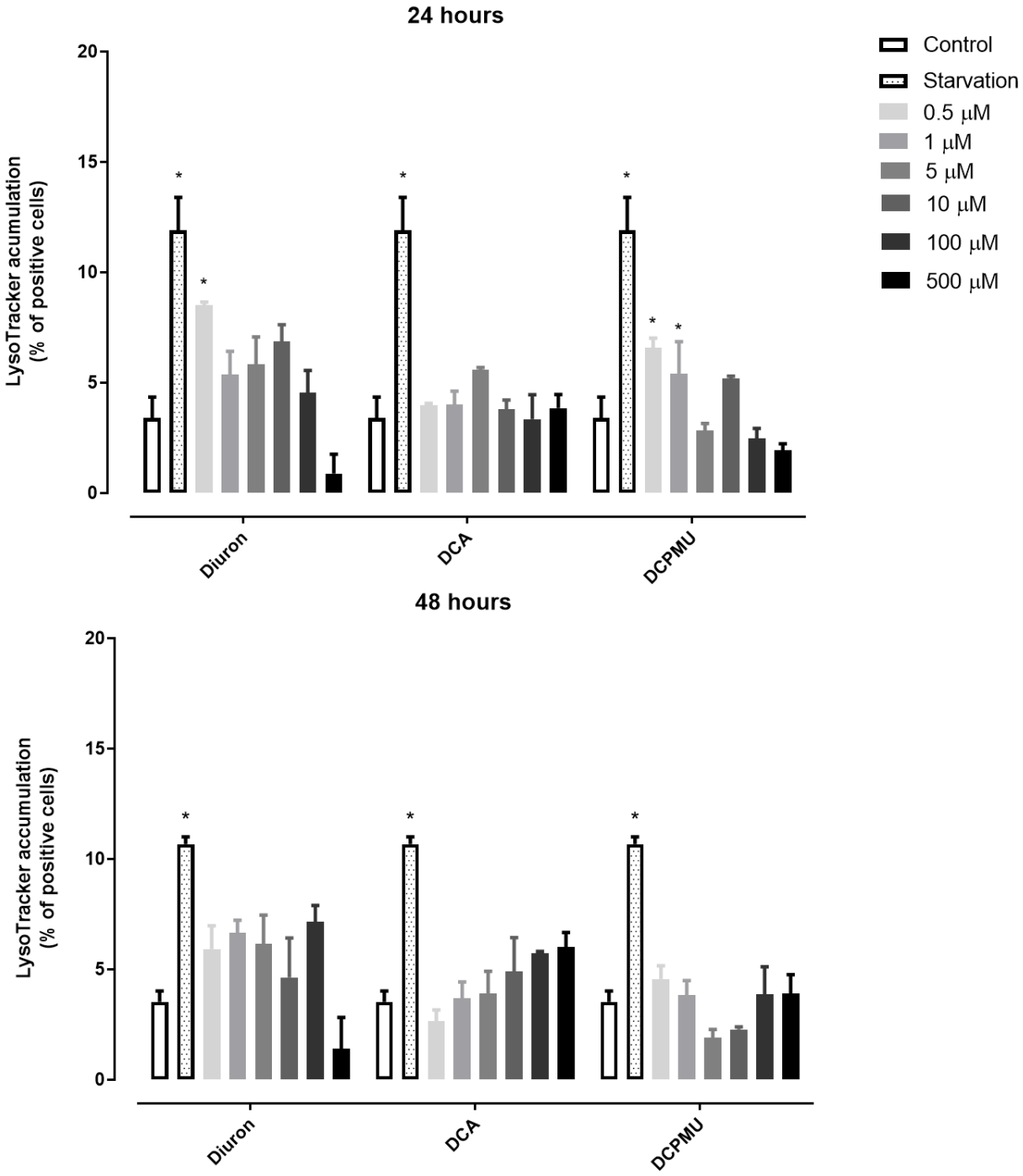
24 hours
LysoTracker acumulation (% of positive cells)
20
15
10
5
0
Diuron
DCA
DCPMU
Control
Starvation
0.5 μM
1 μM
5 μM
10 μM
100 μM
500 μM
48 hours
LysoTracker accumulation (% of positive cells)
20
15
10
5
0
Diuron
DCA
DCPMU

Figure 11.

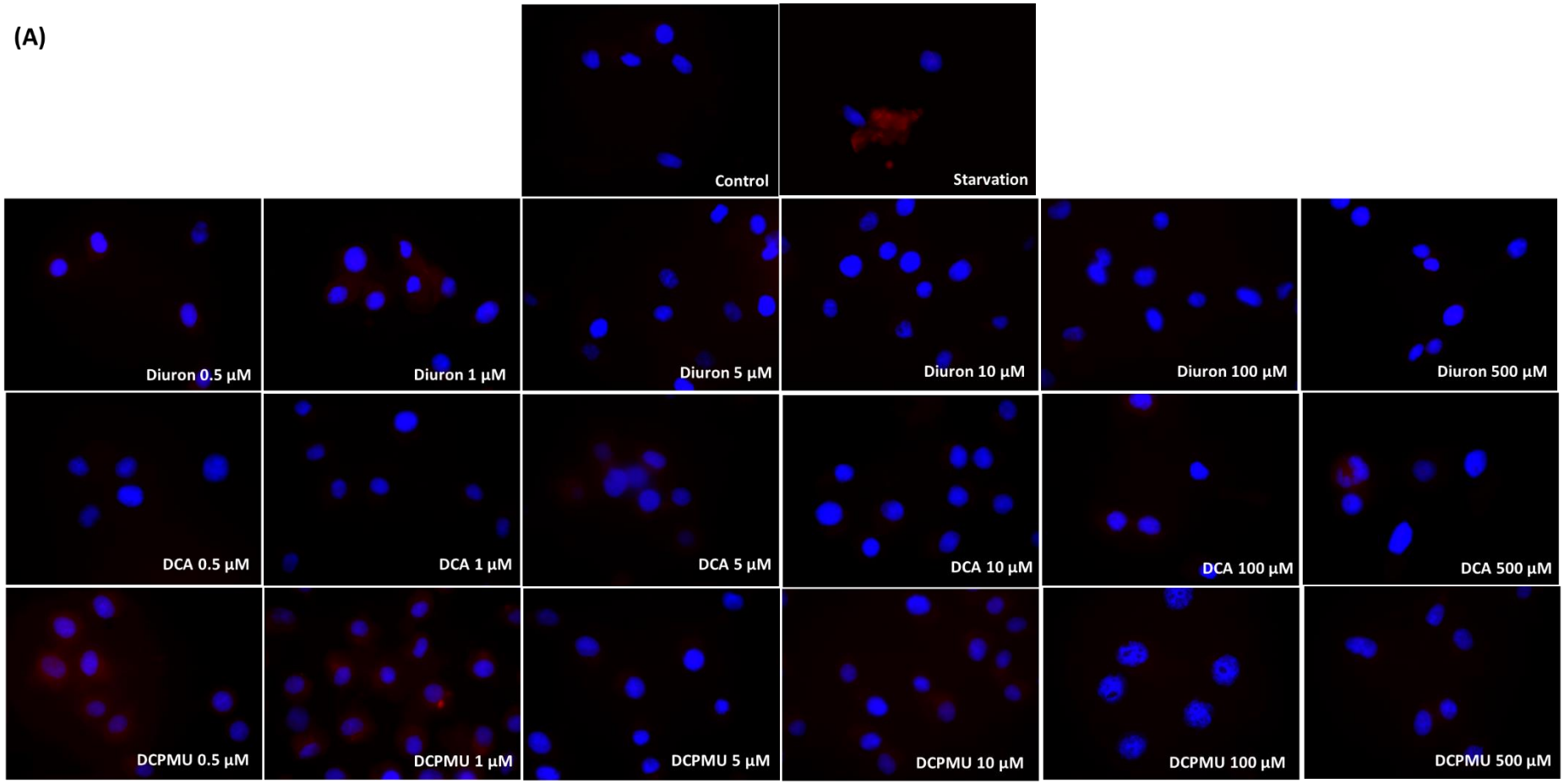
(A)
Control
Starvation
Diuron 0.5 µM
Diuron 1 µM
Diuron 5 µM
Diuron 10 µM
Diuron 100 µM
Diuron 500 µM
DCA 0.5 µM
DCA 1 µM
DCA 5 µM
DCA 10 µM
DCA 100 µM
DCA 500 µM
DCPMU 0.5 µM
DCPMU 1 µM
DCPMU 5 µM
DCPMU 10 µM
DCPMU 100 µM
DCPMU 500 µM

(B)

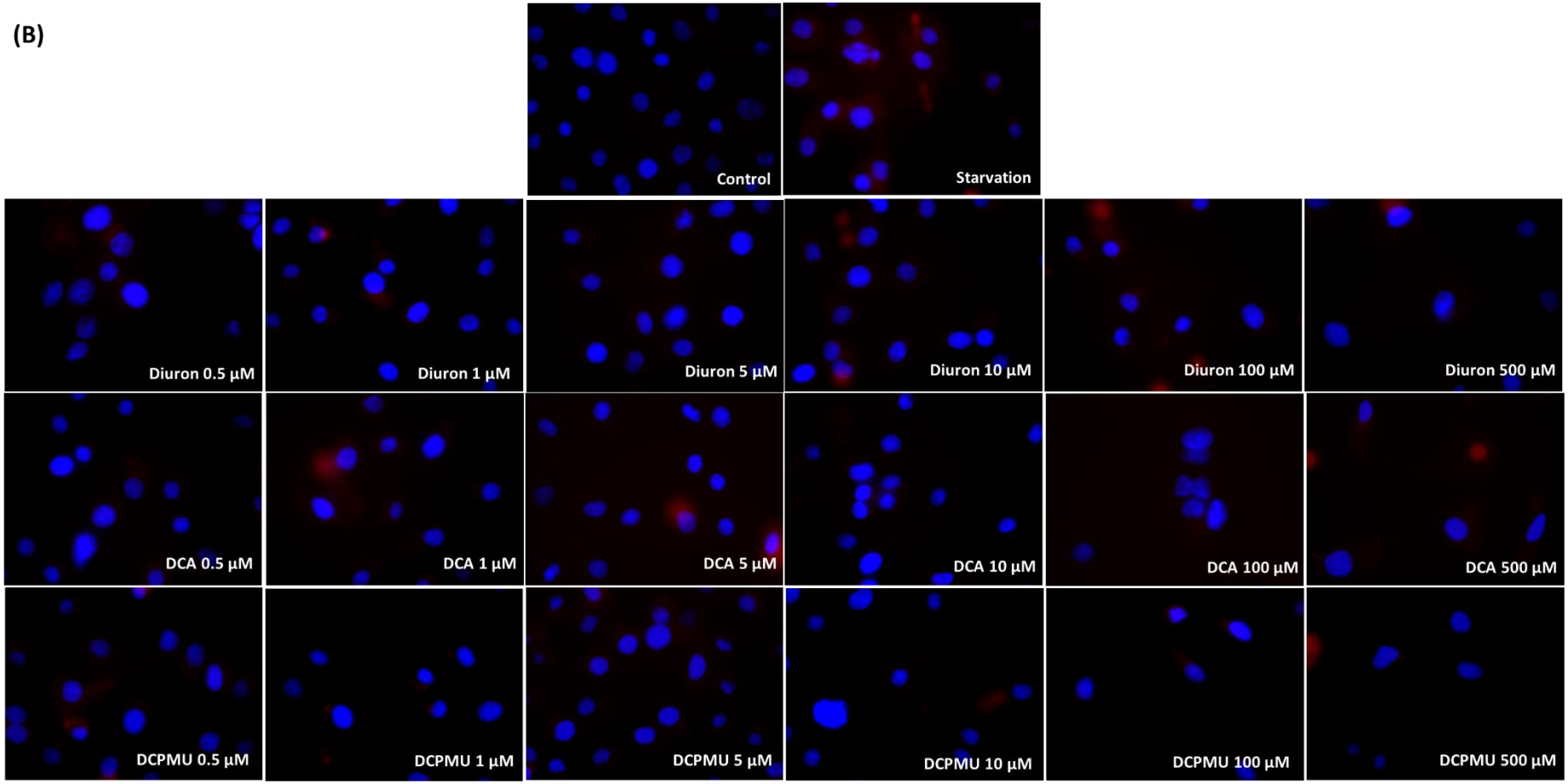
Control
Starvation
Diuron 0.5 µM
Diuron 1 µM
Diuron 5 µM
Diuron 10 µM
Diuron 100 µM
Diuron 500 µM
DCA 0.5 µM
DCA 1 µM
DCA 5 µM
DCA 10 µM
DCA 100 µM
DCA 500 µM
DCPMU 0.5 µM
DCPMU 1 µM
DCPMU 5 µM
DCPMU 10 µM
DCPMU 100 µM
DCPMU 500 µM

Figure 12.

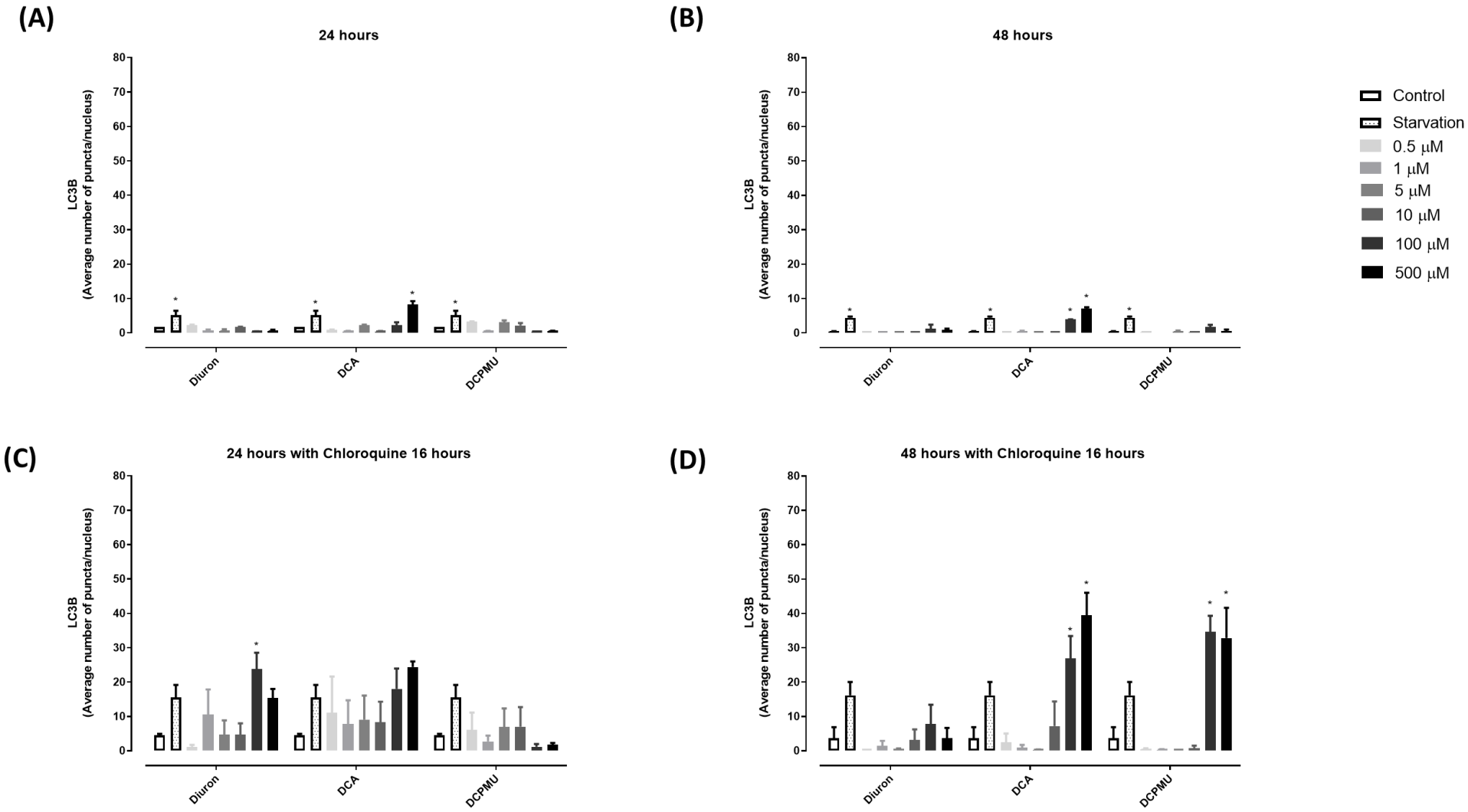
(A)
24 hours
(B)
48 hours
(C)
24 hours with Chloroquine 16 hours
(D)
48 hours with Chloroquine 16 hours
LC3B
(Average number of puncta/nucleus)
0
10
20
30
40
50
60
70
80
Diuron
DCA
DCPMU
Control
Starvation
0.5 μM
1 μM
5 μM
10 μM
100 μM
500 μM

Figure 13.

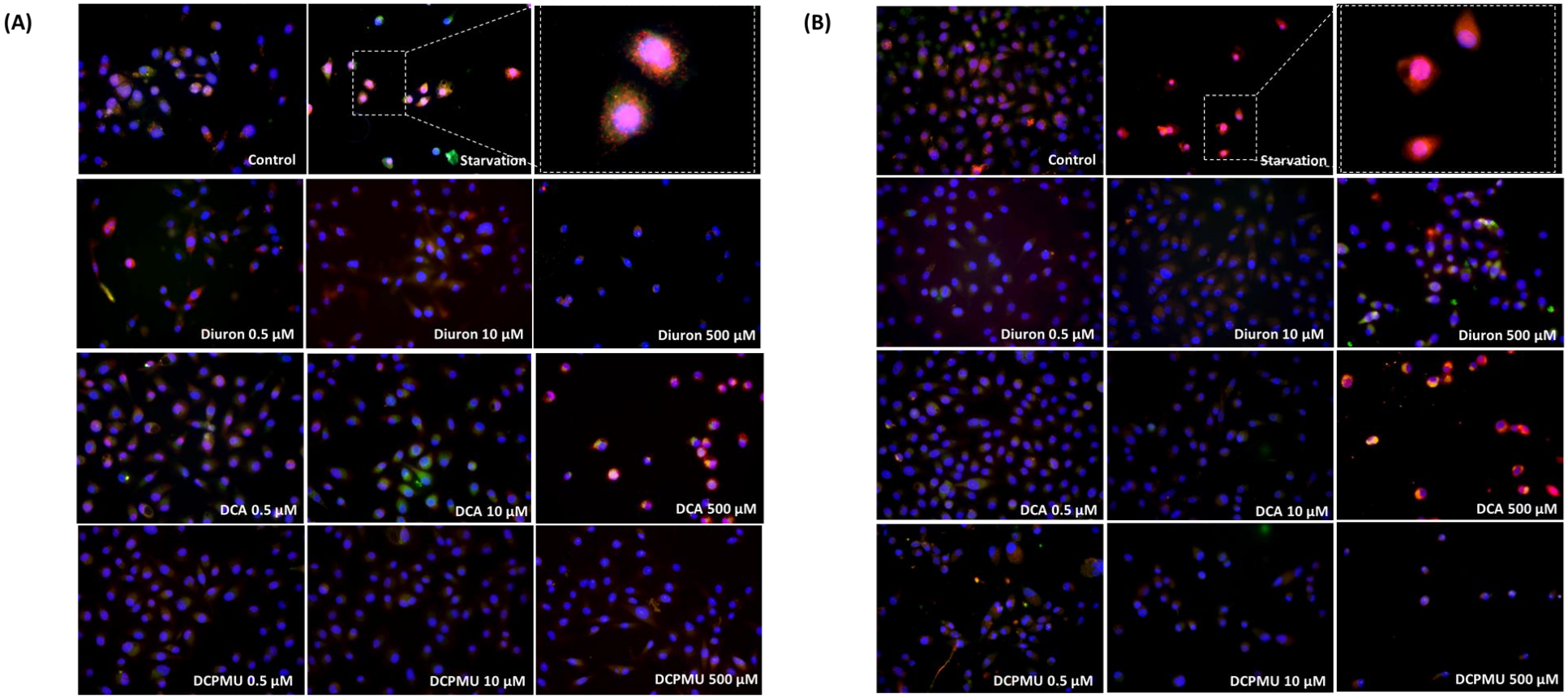
(A)
Control
Starvation
Diuron 0.5 µM
Diuron 10 µM
Diuron 500 µM
DCA 0.5 µM
DCA 10 µM
DCA 500 µM
DCPMU 0.5 µM
DCPMU 10 µM
DCPMU 500 µM
(B)
Control
Starvation
Diuron 0.5 µM
Diuron 10 µM
Diuron 500 µM
DCA 0.5 µM
DCA 10 µM
DCA 500 µM
DCPMU 0.5 µM
DCPMU 10 µM
DCPMU 500 µM

(C)

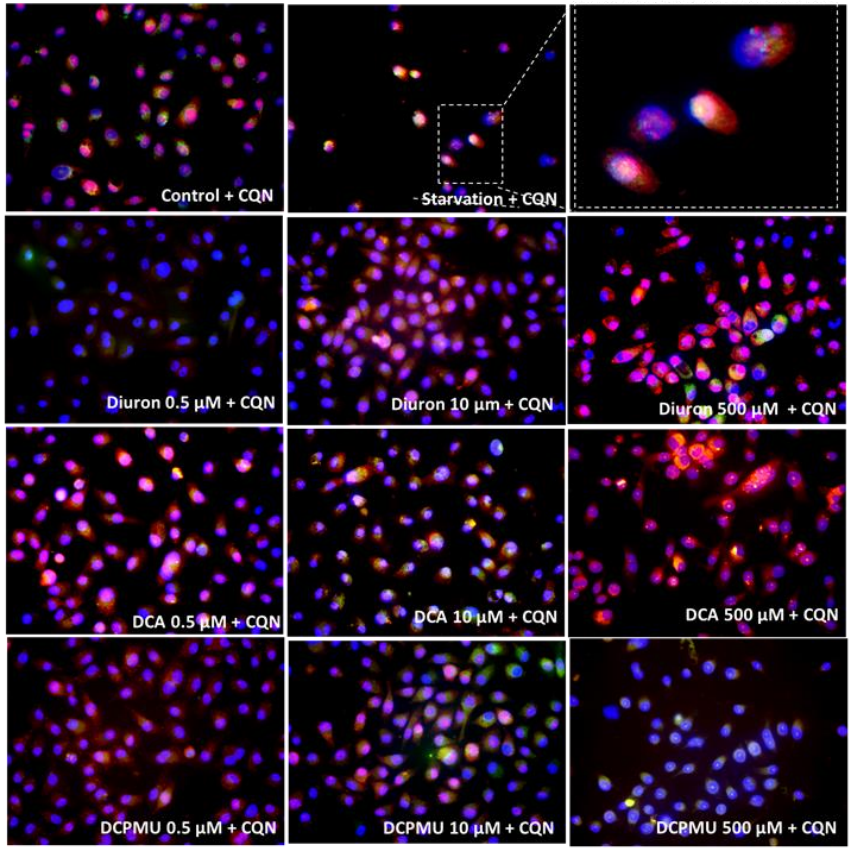
Control + CQN
Starvation + CQN
Diuron 0.5 µM + CQN
Diuron 10 µm + CQN
Diuron 500 µM + CQN
DCA 0.5 µM + CQN
DCA 10 µM + CQN
DCA 500 µM + CQN
DCPMU 0.5 µM + CQN
DCPMU 10 µM + CQN
DCPMU 500 µM + CQN

(D)

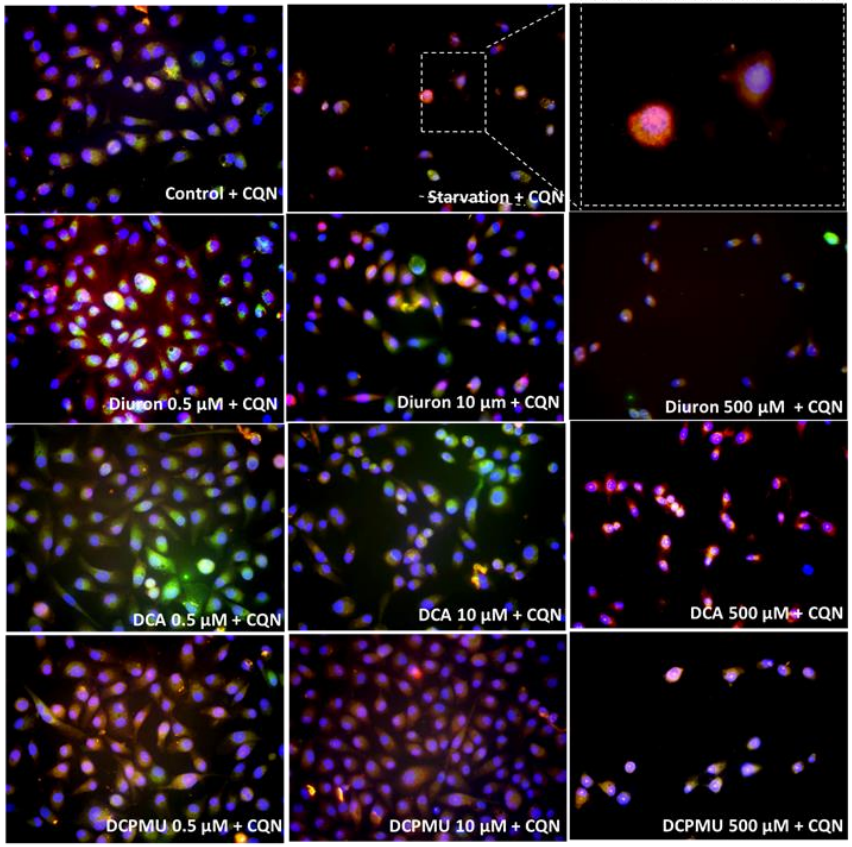
Control + CQN
Starvation + CQN
Diuron 0.5 µM + CQN
Diuron 10 µm + CQN
Diuron 500 µM + CQN
DCA 0.5 µM + CQN
DCA 10 µM + CQN
DCA 500 µM + CQN
DCPMU 0.5 µM + CQN
DCPMU 10 µM + CQN
DCPMU 500 µM + CQN

Figure 14.

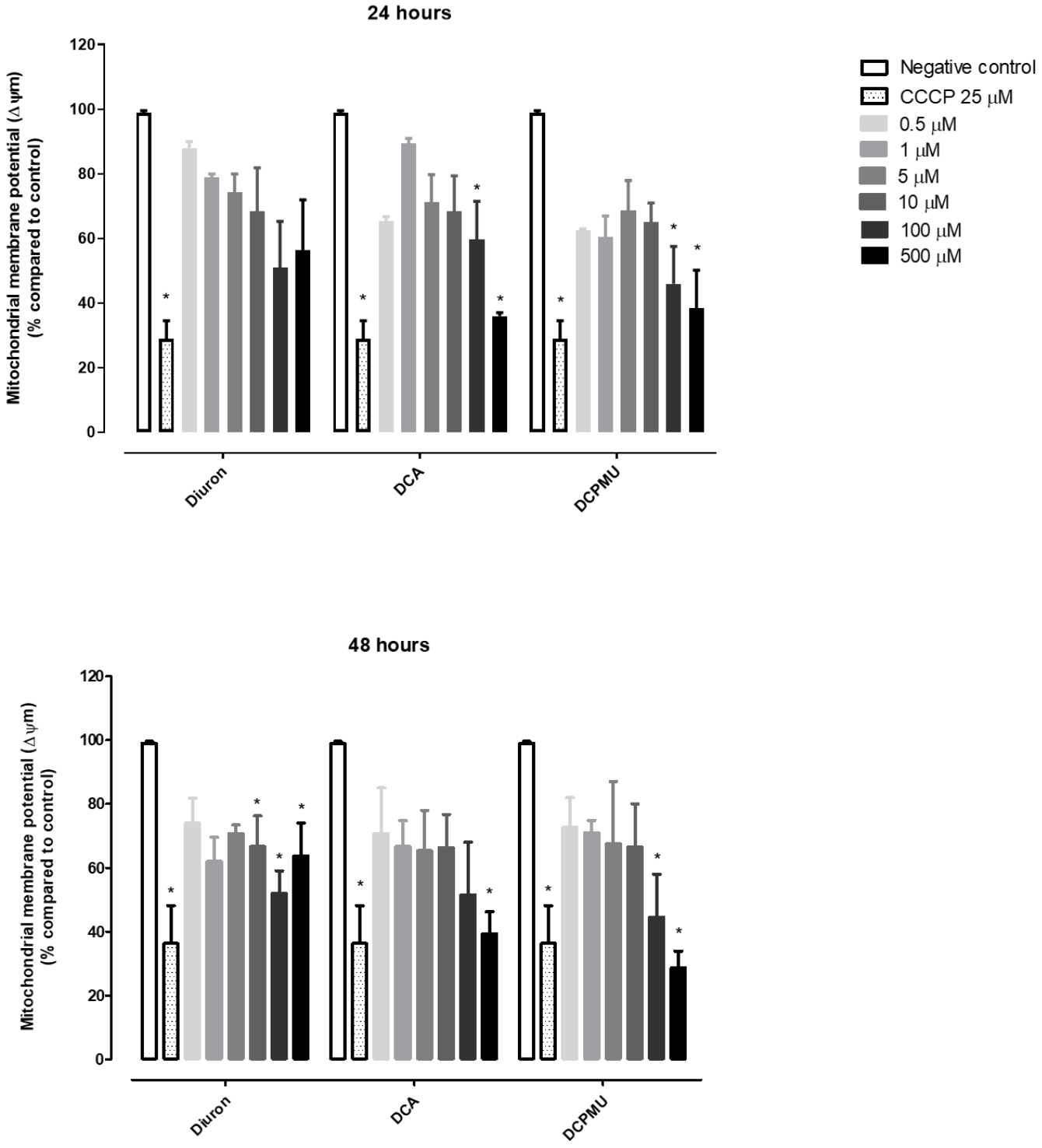
24 hours
Mitochondrial membrane potential (Δψm)
(% compared to control)
120
100
80
60
40
20
0
Diuron
DCA
DCPMU
Negative control
CCCP 25 μM
0.5 μM
1 μM
5 μM
10 μM
100 μM
500 μM
48 hours
Mitochondrial membrane potential (Δψm)
(% compared to control)
120
100
80
60
40
20
0
Diuron
DCA
DCPMU

Figure 15.

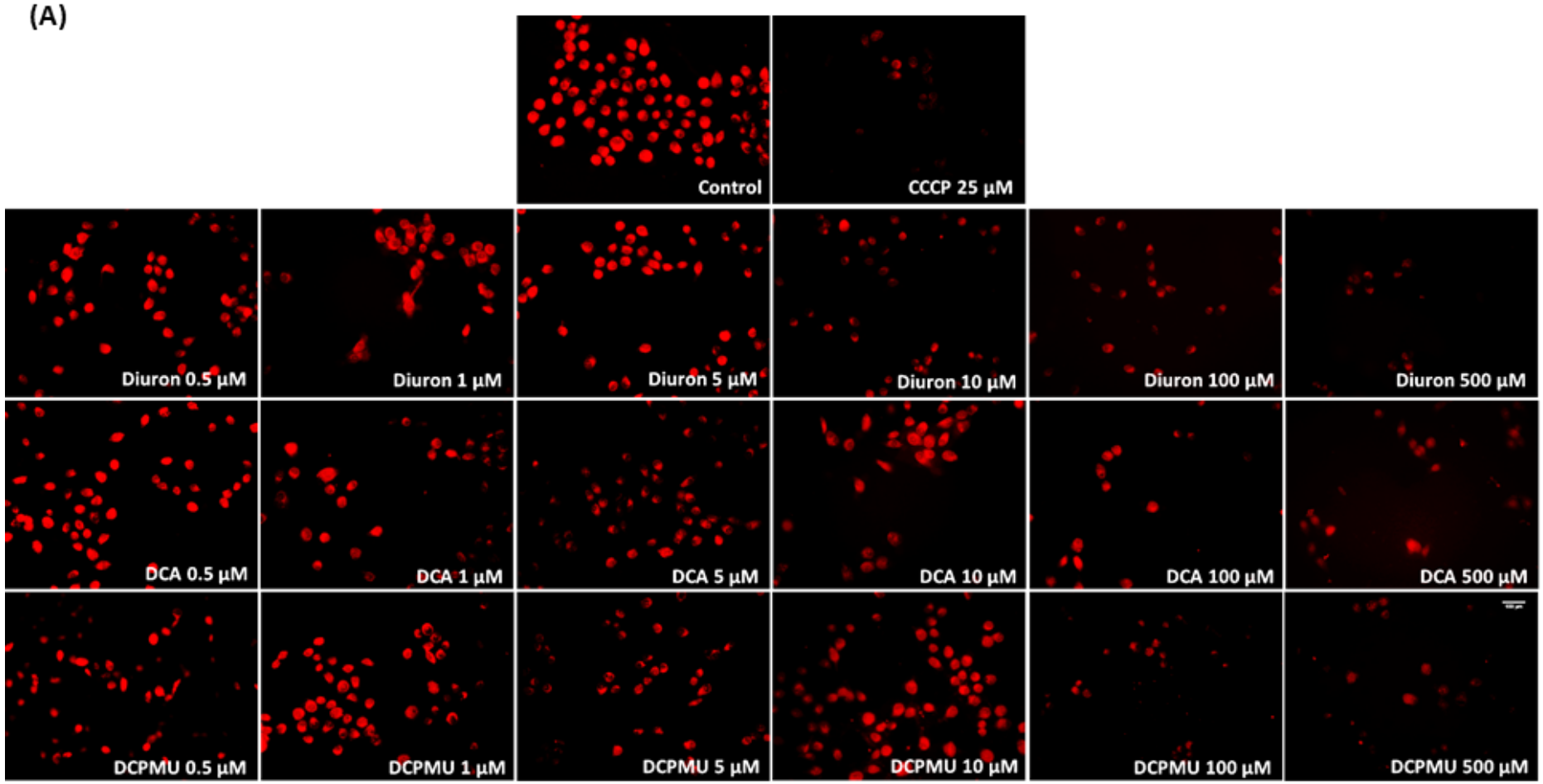
(A)
Control
CCCP 25 µM
Diuron 0.5 µM
Diuron 1 µM
Diuron 5 µM
Diuron 10 µM
Diuron 100 µM
Diuron 500 µM
DCA 0.5 µM
DCA 1 µM
DCA 5 µM
DCA 10 µM
DCA 100 µM
DCA 500 µM
DCPMU 0.5 µM
DCPMU 1 µM
DCPMU 5 µM
DCPMU 10 µM
DCPMU 100 µM
DCPMU 500 µM

(B)

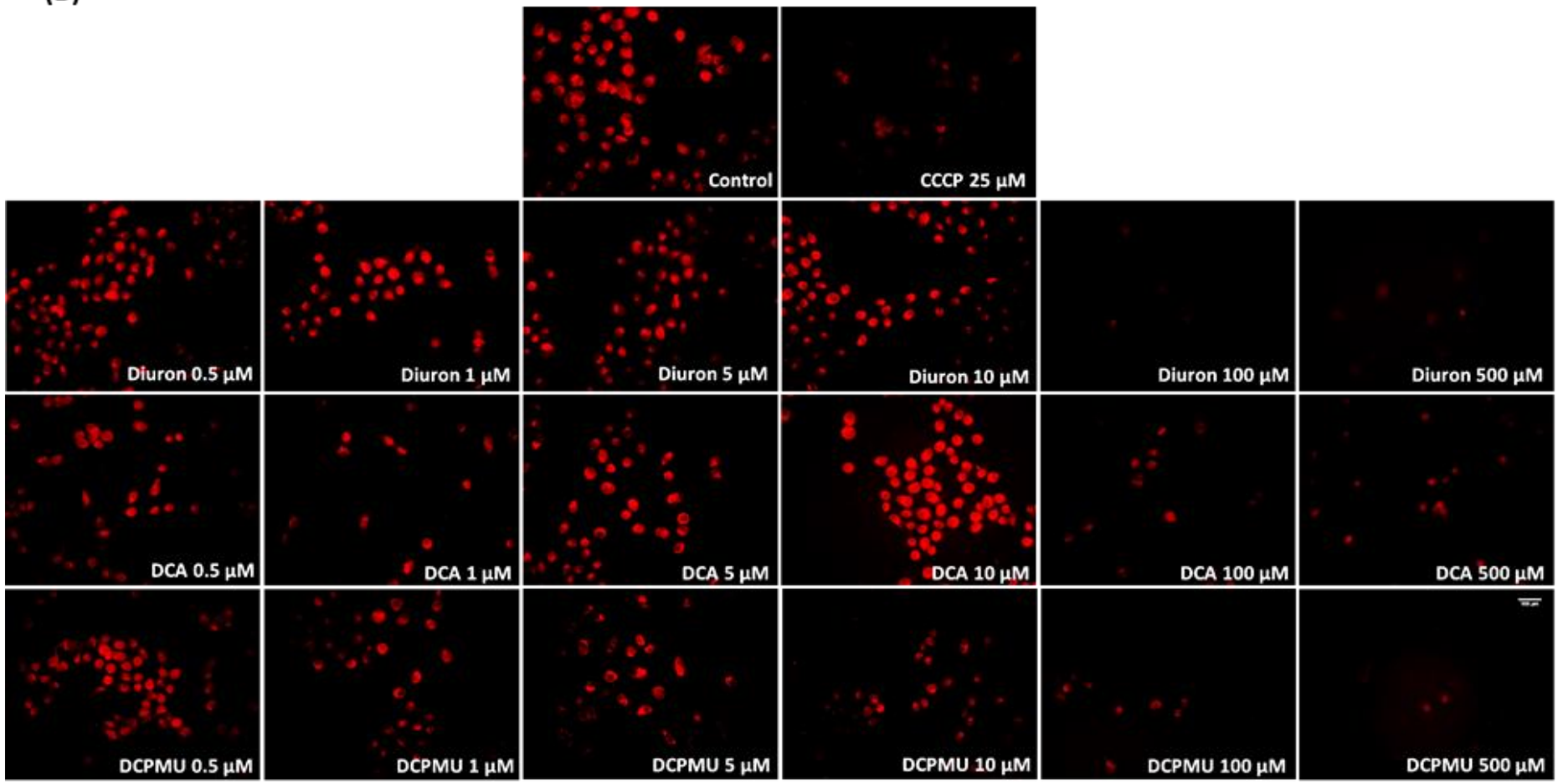
Control
CCCP 25 µM
Diuron 0.5 µM
Diuron 1 µM
Diuron 5 µM
Diuron 10 µM
Diuron 100 µM
Diuron 500 µM
DCA 0.5 µM
DCA 1 µM
DCA 5 µM
DCA 10 µM
DCA 100 µM
DCA 500 µM
DCPMU 0.5 µM
DCPMU 1 µM
DCPMU 5 µM
DCPMU 10 µM
DCPMU 100 µM
DCPMU 500 µM

Figure 16.

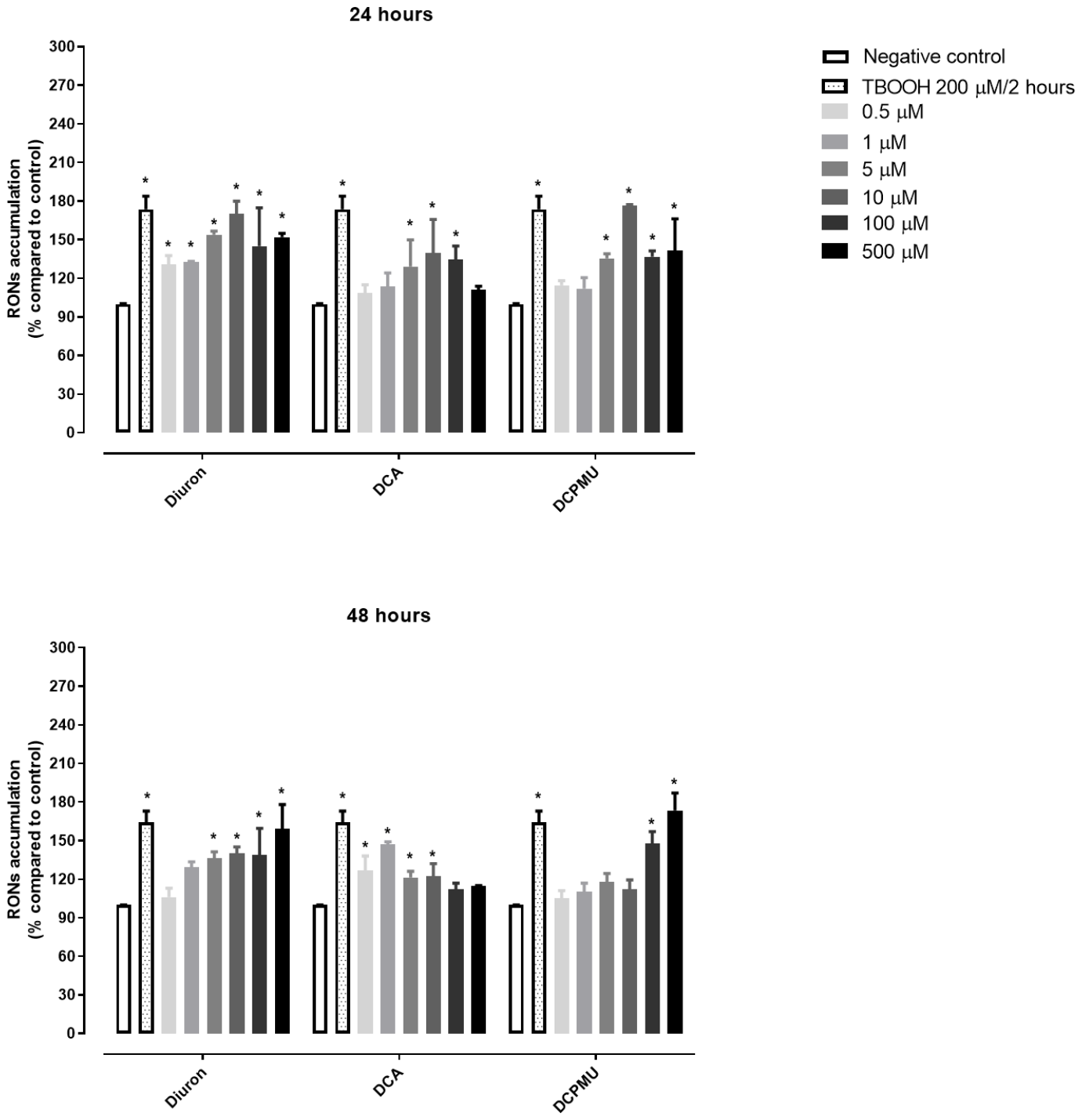
24 hours
RONs accumulation (% compared to control)
300
270
240
210
180
150
120
90
60
30
0
Diuron
DCA
DCPMU
Negative control
TBOOH 200 µM/2 hours
0.5 µM
1 µM
5 µM
10 µM
100 µM
500 µM
48 hours
RONs accumulation (% compared to control)
Diuron
DCA
DCPMU

Figure captions

Figure 1. Kinetic study of the cell growth. (A) Images of 1T1 cells at first (A - G) and twenty eighth-passage (H – N) captured under optical microscope (100x magnification) during 7 days. (B) Growth curve of 1T1 cells represented by the log of the number of cells counted from 1st to 7th day of cultivation. (C) Parameters obtained from the growth curve of 1T1 cells in monolayer.

Figure 2. MTT reduction rate (%). Exposure to chemicals up to 24h or 48h. Negative Control: DMSO/Tween 20; Positive Control: Carbonyl cyanide m-chlorophenyl hydrazone (CCCP). One-way ANOVA followed by Dunnett`s test. Data are expressed as Mean ± SEM. *Significant difference when $p < 0.05$.

Figure 3. Cell proliferation (%). Exposure to chemicals up to 24h or 48h. Negative Control: DMSO/Tween 20; Positive Control: TBOOH - Terc-butyl hydroperoxide. One-way ANOVA followed by Dunnett`s test. Data are expressed as Mean ± SEM. *Significant difference when $p < 0.05$.

Figure 4. Micrographs in 100X magnification showing the proliferation of the 1T1 cells after exposure to the chemicals for 24 (A) and 48 (B) hours. The images are representative of three independent experiments. 50 µm scale bar.

Figure 5. Cell cycle; % of cells in each phase. Exposure to chemicals up to (A) 24h or (B) 48h. Negative Control: DMSO/Tween 20; Positive Control: Cisplatin 500 µg/mL. Two-way ANOVA followed by Dunnett`s test. Data are expressed as Mean ± SEM. *Difference considered significant when $p<0.05$.

Figure 6. Percentage (%) of live and dead cells. Exposure to chemicals up to 24h or 48h. Negative Control: DMSO/Tween 20; Positive Control: TBOOH - Terc-butyl hydroperoxide. One-way ANOVA followed by Dunnett`s test. Data are expressed as Mean ± SEM. [a]Difference between control and calcein assumed when $p < 0.05$, [b]difference between control and ethidium assumed when $p < 0.05$.

Figure 7. Percentage (%) of positive cells for Annexin V/PI. Exposure to chemicals up to 24h or 48h. Negative Control: DMSO/Tween 20; Positive Control: Cisplatin 250 µg/mL. Two-way ANOVA followed by Dunnett`s test. Data are expressed as Mean ± SEM. *Significant difference assumed when $p < 0.05$.

Figure 8. Percentage (%) of cells positive for nuclear condensation and fragmentation. Exposure to chemical products for up to 24h or 48h. Negative Control: DMSO/Tween 20; Positive Control: Cisplatin 1 mg/mL. One-way ANOVA followed by Dunnett's test. Data are expressed as Mean ± SEM ($p < 0.05$).

Figure 9. Micrographs for nuclear condensation and fragmentation of 1T1 cells incubated after exposure to the chemicals for 24 (A) and 48 (B) hours and stained with Hoechst 33342. 400X magnification; 100 µm.

Figure 10. Monitoring of the location of lysosomes in the cytosol of 1T1 cells using the LysoTracker probe. Negative Control: DMSO/Tween 20; Positive Control: Starvation. One-way ANOVA followed by Dunnett's test. Data are expressed as Mean ± SEM ($p < 0.05$).

Figure 11. Micrographs at 1000X magnification showing the accumulation of the LysoTracker probe in a clustered/dotted pattern after exposure to the chemicals for 24 (A) and 48 (B) hours. Nuclei are stained with Hoechst 33342.

Figure 12. Effect of diuron and metabolites on protein conversion from LC3 to LC3B in 1T1 cells exposed for 24 and 48 hours. Negative Control: DMSO/Tween 20; Positive Control: Starvation medium. One-way ANOVA followed by Dunnett's test. Data are expressed as Mean ± SEM ($p < 0.05$).

Figure 13. Micrographs showing cell nuclei labeled in blue, the LC3B protein in red, and the MitoTracker probe in green. Co-location of the MitoTracker probe and LC3B is shown with yellowish placement. Figures A and B: without addition of Chloroquine. Figures C and D: with addition of 50 nM Chloroquine for 16 hours. 400X magnification; 100 µm.

Figure 14. Mitochondrial membrane potential (ΔΨm). Exposure to chemicals up to 24h or 48h. Negative Control: DMSO/Tween 20; Positive Control: Carbonyl cyanide m-chlorophenyl hydrazone (CCCP). One-way ANOVA followed by Dunnett`s test. Data are expressed as Mean ± SEM. *Significant difference when $p <0.05$.

Figure 15. Micrographs in 400X magnification showing the accumulation of the TMRM probe in 1T1 cells intact mitochondria after exposure to the chemicals for 24 (A) and 48 (B) hours. The images are representative of three independent experiments. 100 µm scale bar.

Figure 16. Production of RONS (%). Exposure to chemicals up to 24h or 48h. Negative Control: DMSO/Tween 20; Positive Control: TBOOH - Terc-butyl hydroperoxide. One-way ANOVA followed by Dunnett`s test. Data are expressed as Mean ± SEM. *Difference considered significant when $p <0.05$.

MANUSCRITO II

Molecular signatures associated with diuron exposure on rat urothelial mitochondria

Thania Rios Rossi Lima[a,c] (https://orcid.org/0000-0003-1798-8708)

Estela de Oliveira Lima[a] (https://orcid.org/0000-0003-0479-0364)

Jeany Delafiori[d] (https://orcid.org/0000-0003-2481-0465)

Rodrigo Ramos Catharino[d] (https://orcid.org/0000-0001-7219-2644)

João Lauro Viana de Camargo[a,c] (https://orcid.org/0000-0003-3833-4172)

Lílian Cristina Pereira[a,b,c] (https://orcid.org/0000-0003-0024-7655)

[a]São Paulo State University (Unesp), Medical School, Botucatu. [b]São Paulo State University (Unesp), School of Agriculture, Botucatu. [c]Center for Evaluation of Environmental Impact on Human Health (TOXICAM), Unesp, Medical School, Botucatu. [d]Innovare Biomarkers Laboratory, School of Pharmaceutical Sciences, University of Campinas (UNICAMP), Campinas.

Address correspondence to:

Thania Rios Rossi Lima, M.Sc.

São Paulo State University (Unesp), Medical School - TOXICAM, UNIPEX - Block 5

Botucatu - São Paulo, Brazil, 18618-970

Phone: +55 14 3880-1590, e-mail: thania.lima49@gmail.com

Abstract

Diuron, 3- (3,4-dichlorophenyl)-1,1-dimethylurea, is a worldwide used herbicide whose biotransformation gives rise to the metabolites, 3-(3,4-dichlorophenyl)-1-methylurea (DCPMU) and 3,4-dichloroaniline (DCA). Previous studies indicate that diuron and/or its metabolites are toxic to the bladder urothelium of the Wistar rats where, under certain conditions of exposure, they may induce successively urothelial cell degeneration, necrosis, hyperplasia and eventually tumors. The hypothesis was raised that the molecular initiating event (MIE) of this Adverse Outcome Pathway (AOP) is the mitochondrial toxicity of those compounds. Therefore, this study aimed to investigate *in vitro* the metabolic alterations resulting from urothelial mitochondria isolated from male Wistar rats exposure to diuron, DCPMU and DCA at 10 and 100 µM. A non-targeted metabolomic analysis using mass spectrometry showed discriminative clustering among groups and alterations in the intensity abundance of membrane-associated molecules phosphatidylcholine (PC), phosphatidylinositol (PI) and phosphatidylserine (PS), in addition to methylhexanoyl-CoA and, particularly for diuron 100 µM, dehydro-L-gulonate, all of them involved in critical mitochondrial metabolism. Collectively, these data indicate the mitochondrial dysfunction as a MIE that triggers cellular damage and death observed in previous studies.

Keywords: Herbicide; DCA; DCPMU; mitochondrial dysfunction; diuron toxicity.

Introduction

Numerous studies used metabolomics to assess damage caused by environmental stresses or to identify potential biomarkers to understand the mechanisms of disease development (Houten et al. 2016; Walker et al. 2016; Surowiec et al. 2019). Metabolomics is one of the most recent additions to the "-omics" family, characterized as a high-throughput analytical method for measuring and comparing a large number of low molecular mass (up to 1500 Daltons) metabolites (metabolome) present in biological samples (Braga and Adamec 2019; Wishart 2019). Since the metabolome is at the endpoint of all cellular activity, the implementation of its analysis may contribute to clarify subcellular alterations involved in the toxic effects caused by xenobiotics, including environmental contaminants such as pesticides (Braga and Adamec 2019; Wishart 2019). Considering that most of cellular metabolites are conserved in several animal species, research findings in experimental animals can be extrapolated to humans (Wishart 2019), in order to elucidate the mode of action (MoA) and mechanisms of action of toxic chemicals.

Diuron, 3-(3,4-dichlorophenyl) 1,1-dimethylurea, is a worldwide used herbicide whose biodegradation in the environment or metabolization in mammals results in the metabolites 3- (3,4-dichlorophenyl)-1-methylurea (DCPMU), 3,4 -dichlorophenylurea (DCPU) and 3,4-dichloroaniline (DCA) (Giacomazzi and Cochet 2004; APVMA 2011). Since in mammals the excretion of these compounds occurs mainly through urine, the urothelial tissue which lines the urinary tract from the renal pelvis and ureters to the bladder, is one of the most affected by their potential toxicity. Previous studies with diuron demonstrated that its MoA on the urinary bladder of Wistar rats involves chemical metabolic activation leading to initial cytotoxicity followed by cell degeneration, exfoliation and necrosis, continuous regenerative hyperplasia and eventual tumors after a long-term exposure (Nascimento et al. 2006; da Rocha et al. 2010; Ferrucio et al. 2010; Ihlaseh et al. 2011; da Rocha et al. 2012;

Cardoso et al. 2013; da Rocha et al. 2013; da Rocha et al. 2014; Ihlaseh et al. 2014; Fava et al. 2015). Recently, the hypothesis was put forward that this sequence of successive events induced by diuron and/or its metabolites could comprise an Adverse Outcome Pathway (AOP) in which the mitochondrial toxic damage represents the initiating molecular event (MIE) (Souza et al. 2020).

Recently, metabolomics has been increasingly applied in the mitochondrial-related disease research and diagnosis (Esterhuizen et al. 2017). However, up to date, there are no studies available in the literature addressing mitochondrial metabolomic changes of urothelial cells resulting from exposure to the herbicide diuron and/or its metabolites, as proposed here. Bearing this in mind, the present study aimed to investigate the effects of urothelial mitochondria exposure to diuron and two of its main toxic metabolites, DCPMU and DCA using a non-targeted metabolomics approach. The present results may contribute to understand the findings of *in vivo* and *in vitro* studies already developed by our research group (Nascimento et al. 2006; da Rocha et al. 2010; Ferrucio et al. 2010; Ihlaseh et al. 2011; da Rocha et al. 2012; Cardoso et al. 2013; da Rocha et al. 2013; da Rocha et al. 2014; Ihlaseh et al. 2014; Fava et al. 2015) through a better comprehension of key biochemical and cellular events involved in the urothelial toxicity of those compounds.

Material and Methods

Experimental animals

Four-weeks old male Wistar rats (n=3) obtained from the Multidisciplinary Center of Biological Investigations (CEMIB UNICAMP, Campinas, SP, Brazil) were kept under controlled conditions at the bioterium of the Department of Pathology, Botucatu Medical School (UNESP, SP, Brazil) such as temperature at 21 ± 3°C, relative humidity at 50 ± 20%,

four cycles of daily air exhaustion, and a 12/12-hour light/dark period with basal food and water provided *ad libitum*. The animals were sacrificed by decapitation when they weighed approximately 180g. The present study was approved by the local Committee for Ethics in Animal Experimentation (Protocol No. 1253/2017).

Mitochondrial isolation

After euthanasia, the bladder was immediately removed and inflated with 0.9% NaCl solution. With the aid of a glass microcapillary, the bladder was inverted to expose the urothelial epithelium. The urothelial cells were gently removed by scraping and immersed in approximately 5 mL of 0.9% NaCl solution (Cohen et al. 2007). Shortly afterwards, the bladder mitochondria were isolated by differential centrifugation. First, the suspension was centrifuged at 770 *g*, 4 °C, for 5 minutes; then, the resulting supernatant was centrifuged at 9800 *g*, 4 °C, for 10 minutes and, finally, the pellet was centrifuged at 4500 *g*, 4 °C, for 15 minutes. The sediment containing the fraction rich in mitochondria was carefully resuspended with 1 mL of 0.9% NaCl solution and mitochondrial proteins were determined by the biuret reaction (Pedersen et al. 1978).

Chemical exposure assay

In order to evaluate the metabolic alterations triggered in isolated urothelial mitochondria exposed to diuron or its metabolites (Diuron CAS no. 330-54-1; DCA CAS no. 95-76-1; DCPMU CAS no. 3567-62-2, Sigma-Aldrich Co., St Louis, MO), we selected 10 µM and 100 µM concentrations based on previous cytotoxicity results of our research group (da Rocha et al. 2013). The compounds were dissolved in 0.05 % DMSO + Tween 20, which was also used as negative control (NC); 2 µM carbonyl cyanide m-chlorophenyl hydrazone (CCCP; Sigma-Aldrich Co., St Louis, MO, CAS no. 555-60-2) was used as positive control.

Mitochondrial samples (1 µg/mL) were then exposed *in vitro* to each of the chemical compounds during 30 minutes at room temperature and stored in a freezer at -80 °C until the moment of mass spectrometry analysis.

Mass spectrometry analysis

To assess the metabolic profile, three analytical replicates of each sample condition were prepared. Briefly, 40-µL aliquots of each sample were added to a plastic conical tube containing 200 µL of tetrahydrofuran and vortexed for 30 seconds at room temperature. After agitation, the content was diluted with methanol (1000 µL q.s.), homogenized and centrifuged at 1228 *g* for 5 minutes at 4 °C for protein precipitation. Subsequently, 100 µL of each supernatant was diluted to 500 µL with methanol. After preparation, the samples were positively ionized with 0.1% formic acid and direct infused in a ESI-LTQ-XL Discovery mass spectrometer (Thermo Scientific, Bremen, Germany). Fifteen acquisitions were made for each replicate in the mass range of 50–1400 *m/z* using the positive ion mode and 50 scans per acquisitions. Instrument parameters were defined as follow: flow rate of 10 $\mu L.mL^{-1}$, capillary temperature at 275°C, spray voltage of 5 kV, and sheath gas at 5 arbitrary units. All spectra were analyzed and visualized using the XCalibur software (v. 2.4, Thermo Scientific, San Jose, Ca). This protocol was carried out at Innovare Biomarkers Laboratory, School of Pharmaceutical Sciences, University of Campinas (UNICAMP), Campinas, SP, Brazil (Melo et al. 2017).

Statistical analysis and markers annotation

The acquired mass spectra data were into binary datasets for the comparison of exposed samples (CCCP, diuron 10, diuron 100, DCPMU 10, DCPMU 100, DCA 10 e DCA 100) individually with negative controls (NC). Each dataset was filtered with interquartile

range, normalized with quantile normalization and auto-scaled before supervised multivariate analysis using Partial Least Squares Discriminant Analysis (PLS-DA) for sample clustering provided by MetaboAnalyst (www.metaboanalyst.ca) (Chong et al. 2018). From PLS-DA analysis, discriminant *m/z* were selected considering a Variable Importance in Projection score (VIP score) over 1.5. The annotation of biomarkers was initially performed based on the comparison between theoretical and experimental masses by consulting the online database METLIN (Scripps Center for Metabolomics, La Jolla, CA, USA). Then, the chemical structure of the selected biomarkers was elucidated according to the ion fragmentation profile through *in tandem* mass spectrometry (MS/MS), and their comparison with theoretical mass fragmentation using the Mass Frontier software (v. 6.0, Thermo Scientific, San Jose, CA). A heat map with Euclidean distance measure and Ward clustering method was used to illustrate markers distribution among samples. Significance of the markers were evaluated through t-test (significant with p- value < 0.05 FDR-adjusted) and groups separation using Principal Component Analysis (PCA).

Results

In the PLS-DA analysis, separation was found between the selected groups of isolated mitochondria exposed to negative control (0.05% DMSO + Tween 20) and those exposed to each one of the chemical compounds (Figure 1). This difference was also seen when comparing the negative control with the positive CCCP control, a well-known mitochondrial uncoupler. Interestingly, a clustering of the data generated by the positive control and diuron together was observed when compared to the negative control, suggesting that both chemicals, diuron and CCCP, may be able to alter similar biochemical routes, by modifying the abundance of common metabolites (Figure 1A).

[Figure 1 near here]

Based on VIP score values greater than 1.5, *m/z* features that metabolically discriminated the experimental groups were selected. Some identified molecules are crucial components of biological membranes - phosphatidylcholine (PC), phosphatidylinositol (PI) and phosphatidylserine (PS) -, in addition to methylhexanoyl-CoA and dehydro-L-gulonate, molecules directly or indirectly linked to mitochondrial metabolism. A heat map analysis of each group averages provided the abundance distribution of such relevant markers (Figure 2). The consistency of enhanced levels of the 4 common markers with CCCP reinforces their correlation with mitochondrial impairment. In general, markers' intensities are dose dependent; however, dehydro-L-gulonate is only enhanced due to diuron 100 µM exposure. Structural characteristics of annotated molecules are described in Table 1. The metabolites successfully discriminated negative controls from exposed conditions as demonstrated by validation approaches using PCA (see Supplementary File Figure S1), and their significances displayed in Table S1 (Supplementary File).

[Figure 2 near here]

[Table 1 near here]

Discussion and Conclusion

Since mitochondria play a crucial role in different biological processes within the cell, including energy generation, regulation of apoptosis and redox balance, the integrity of this organelle is imperative to ensure an adequate cellular response to chemical aggression (Meyer et al. 2018; Dreier et al. 2019; Pascual 2021). Impairment of mitochondrial structure and function can be caused by xenobiotics through direct or indirect interaction with mitochondrial proteins, lipids, and ribonucleic acids, which can trigger other cellular

damages (Roubicek and de Souza-Pinto 2017; Burgos-Aceves et al. 2018).

In the present metabolomics analysis of isolated urothelial mitochondria exposed to diuron and its metabolites, the intensities of the molecules PC, PI and PS were increased compared to the negative control. These phospholipids are abundant in the eukaryotic membranes that compose the physical and functional barrier between cells and the surrounding environment, acting as signaling mediators and providing the permeability required for the mitochondrial biochemical processes, such as the cellular respiration (Ball et al. 2018). In the mitochondria, PS serves as substrate to produce phosphatidylethanolamine (PE) through decarboxylation by PS decarboxylase (PSD) (Figure 3). In turn, PE methylation leads to production of PC (Van der Veen et al. 2017), i.e., increases in PC levels occurs at the expense of PE levels. Mitochondrial abnormally high or low PE/PC molar ratio can affect energy metabolism and impact other cellular activities, since PC is involved in the maintenance of the membrane fluidity and release of cytochrome c into the cytosol, while PE has been proposed to participate in different biological functions, such as in autophagosome synthesis during the autophagic process (Mejia and Hatch 2016; Van der Veen et al. 2017). In fact, plasma concentration of fragmented PC was elevated in Wistar rats following induction of oxidative stress by vitamin E deficiency and high oxygen concentration (Frey et al. 2000). In addition, increased PC/lysophosphatidylcholine (LPC) ratios were found in plasma lipid extracts of individuals with Parkinson's disease, condition with pathophysiology known to be associated with mitochondrial dysfunction (Vukajlović et al. 2020). Conversely, inhibition of the PSD gene (~85%) in Chinese Hamster Ovary (CHO) cells was associated to decreased PE, which severely impaired cell survival, growth, respiratory capacity, mitochondrial ultrastructure and ATP production (Tasseva et al. 2013; Mejia and Hatch 2016). Experimental evidences suggest that increased levels of some membrane phospholipids prevent cells from demanding microenvironmental conditions and may be considered as a tumor biomarker

(Szlasa et al. 2020). Phosphatidylinositol accumulation generally occurs when PI specific phospholipase C (PI PLC) remains inactive or mutated (Szlasa et al. 2020). Study using C6 glioma cell line demonstrated an association between increased phosphatidylinositol 3-kinase signaling with increased invasiveness and matrix metalloproteinases activity in malignant gliomas (Kubiatowski et al. 2001). Mitochondrial DNA mutations play an important role in glioblastoma pathogenesis, favoring abnormal energy and reactive oxygen species production and resistance to apoptosis and to chemotherapeutic agents (Barros et al. 2021). On the other hand, depletion or masking of PI, specifically the PI(4, 5)P2, was also related with mitochondrial fragmentation and possible autophagy activation in mouse fibroblasts (NIH 3T3), human breast cancer cells (MCF-7) and liver hepatocellular carcinoma cells (HepG2) (Rosivatz and Woscholski 2011). These observations demonstrated that phospholipid homeostasis is essential for maintaining optimal physical and biochemical properties of membranes that in turn support cell functioning and survival. Mitochondria perform lipid biosynthesis, but that activity also depends on phospholipid trafficking from the endoplasmic reticulum and the Golgi apparatus (Mejia and Hatch 2016).

Other significantly relevant metabolic marker found was the methylhexanoyl-CoA, a medium-chain acyl-CoA participating in the synthesis and oxidation of fatty acids. β-oxidation of the 2-methylhexanoyl-CoA originates acetyl-CoA, an important coenzyme oxidizing pyruvate in the citric acid cycle that takes place in the mitochondrial matrix (HMDB 2009) (Figure 3). Alterations in these coenzymes affect the synthesis of substrates required for the subsequent steps of cellular respiration. In that sense, bioenergetic analysis of hepatic mitochondria exposed to diuron showed reduction in the ATP content, characteristic phenomenon of oxidative phosphorylation impairment (Simões et al. 2017). Other studies evaluating the toxicity of diuron found adverse effects indicative of mitochondrial injury; a significant increase in the production of RONS was observed in two human cancer cell lines

(breast adenocarcinoma: MCF-7; placental choriocarcinoma: BeWo) at 200 µM (Huovinen et al. 2015), and a decrease in the cellular ATP content was seen using isolated perfused rat liver as experimental model (Simões et al. 2017). Increased RONS production and accumulation possibly reflect the inability of the antioxidants to deal with these reactive species, which is in accordance with the alteration herein found in the molecule related to the synthesis of ascorbic acid, an important antioxidant. In the present study, dehydro-L-gulonate was considered a differential marker only in the comparison between negative control and diuron, especially in diuron 100 µM. Via uronic acid cycle, conversion of L-gulonate and NAD^+ into dehydro-L-gulonate and NADH is catalyzed by the oxidoreductase enzyme L-gulonate 3-dehydrogenase. This cycle is an alternative pathway for glucose metabolism and plays essential role in the biosynthesis of ascorbic acid and glucuronic acid, and is also linked to the pentose phosphate cycle, another alternative pathway to glycolysis, since has pentoses as a bioproduct (Horecker 1976; Agrawala et al. 2018). Due the ability of ascorbic acid to donate electrons, it acts as a reactive oxygen species scavenger and aid to reduce higher oxidation states (Smirnoff 2018). It should be emphasized that some groups of animals, among which humans are included, have lost the ability to synthesize ascorbic acid during their evolution due to loss of function mutations in the gene for L-gulono-1,4-lactone oxidase (GLO) (Smirnoff 2018). Interestingly, the gene for human glutathione reductase is located at the same chromosomal sub-band than the GLO gene, which could explain its non-functionality (Nishikimi et al. 1994). Considering our findings, the hypothesis can be raised that alterations in the uronic acid pathway only occur in organisms exposed to high concentrations of pesticides, such as diuron. Furthermore, it has been demonstrated that conjugation with glucuronic acid is a major pathway in the biotransformation and elimination of xenobiotics and, therefore, an increase in dehydro-L-gulonate may indicate an attempt to improve detoxification (de Groot et al. 2007).

[Figure 3 near here]

[Figure 4 near here]

In summary, alterations herein observed may contribute to support the mechanistic framework recently proposed by our research group (Souza et al. 2020), which indicates mitochondrial dysfunction as the MIE of the AOP launched by diuron and its metabolites in the urothelium, leading to the urothelial cell damage observed in previous studies. Our results reinforce the importance of broader studies using metabolomics and to the best our knowledge, this is the first reported metabolomic experimental assessment of the effects of diuron on the urothelial mitochondria.

Acknowledgements

The authors are grateful to Paulo Roberto Cardoso and Paulo César Georgete for technical assistance.

Conflict of interest statement

This study is associated to the Botucatu Medical School, Unesp, SP, Brazil and after its completion, TRRL assumed job position in a private company. The authors have no conflicts of interest to declare.

Funding

This work was supported by the São Paulo Research Foundation (FAPESP) [Grant No. 2017/25402-5; and 2019/05718-3 for JD]; the National Council for Scientific and

Technological Development (CNPq) [Grant No. 167774/2018-2]; and by the Center for Evaluation of Environmental Impact on Human Health (TOXICAM), Unesp, Brazil.

References

Agrawala N, Hossainb S, Skelton AA, Muralidhar K, Kaushikc S. 2018. Unraveling the mechanism of L-gulonate-3-dehydrogenase inhibition by ascorbic acid: Insights from molecular modeling. Comput Biol Chem. 77:146-53.

APVMA. 2011. Review of the mammalian toxicology and metabolism/toxicokinetics of diuron. Australian Pesticides and Veterinary Medicines Authority.

Ball WB, Neff JK, Gohil VM. 2018. The role of nonbilayer phospholipids in mitochondrial structure and function. FEBS Lett. 1273-90.

Barros MBL, Pinheiro DdR, Borges BdN. 2021. Mitochondrial DNA Alterations in Glioblastoma (GBM). Int J Mol Sci. 22:5855.

Braga CP and Adamec, 2019. J. Metabolome Analysis. In: Shoba Ranganathan MG, Kenta Nakai, Christian Schönbach, editor. Encyclopedia of bioinformatics and computational biology: Academic Press, p. 463-75.

Burgos-Aceves MA, Cohen A, Paolella G, Lepretti M, Smith Y, Faggio C, et al. 2018. Modulation of mitochondrial functions by xenobiotic-induced microRNA: From environmental sentinel organisms to mammals. Sci Total Environ. 645:79-88.

Cardoso APF, Catalano SMI, Sanches M, Garcia M, Camargo JLVD, de Oliveira MLSC. 2013. Dose–response of diuron [3-(3,4-dichlorophenyl)-1,1-dimethylurea] in the urothelial mucosa of Wistar rats. Toxicology. 312:1-5.10.1016/j.tox.2013.07.007.

Chong J, Soufan O, Li C, Caraus I, Li S, Bourque G, et al. 2018. MetaboAnalyst 4.0: towards more transparent and integrative metabolomics analysis. Nucleic Acids Res. 46:W486–W94.

Cohen SM, Ohnishi T, Clark NM, He J, Arnold LL. 2007. Investigations of rodent urinary bladder carcinogens: Collection, processing, and evaluation of urine and bladders. Toxicol Pathol. 35(3):337–47.

da Rocha MS, Arnold LL, Dodmane PR, Pennington KL, Qiu F, de Camargo JLV, et al. 2013. Diuron metabolites and urothelial cytotoxicity: In vivo, in vitro and molecular approaches. Toxicology. 314:238-46.10.1016/j.tox.2013.10.005.

da Rocha MS, Arnold LL, Oliveira MLSC, Catalano SMI, Cardoso APF, et al. 2014. Diuron-induced rat urinary bladder carcinogenesis: Mode of action and human relevance evaluations using the International Programme on Chemical Safety framework. Crit Ver Toxicol. 1-14.10.3109/10408444.2013.877870.

da Rocha MS, Arnold LL, Pennington KL, Muirhead D, Dodmane PR, Anwar M, et al. 2012. Diuron-induced rat bladder epithelial cytotoxicity. Toxicol Sci. 130(2):281-8.10.1093/toxsci/kfs256.

da Rocha MS, Nascimento MG, Cardoso APF, Lima LAD, Zelandi EA, Camargo JLVD, de Oliveira MLS. 2010. Cytotoxicity and regenerative proliferation as the mode of action for Diuron-induced urothelial carcinogenesis in the rat. Toxicol Sci. 113(1):37-44.10.1093/toxsci/kfp241.

de Groot M, Lewis D, Modi S. 2007. Molecular modeling and quantitative structure–activity relationship of substrates and inhibitors of drug metabolism enzymes. Comprehensive Medicinal Chemistry II. 5: Elsevier.

Dreier DA, Mello DF, Meyer JN, Martyniuka CJ. 2019. Linking mitochondrial dysfunction to organismal and population health in the context of environmental pollutants: Progress and considerations for mitochondrial adverse outcome pathways. Crit Perspect. 38(8):1625–34.

Esterhuizen K, Van der Westhuizen FH, Louw R. 2017. Metabolomics of mitochondrial disease. Mitochondrion. 16S1567-7249:30145-3.

Fava RM, Ferragut APF, Sanches M, de Oliveira MLSC. 2015. Evaluation of early changes induced by diuron in the rat urinary bladder using different processing methods for scanning electron microscopy. Toxicology. 333:100-6.10.1016/j.tox.2015.04.006.

Ferrucio B, Franchi CAdS, Boldrin NF, de Oliveira MLCS, de Camargo JLV. 2010. Evaluation of Diuron (3- [3 , 4-dichlorophenyl] -1 , 1-dimethyl urea) in a two-stage mouse skin carcinogenesis assay. Toxicol Pathol. 38:756-64.10.1177/0192623310375452.

Frey B, Haupt R, Alms S, Holzmann G, König T, Kern H, et al. 2000. Increase in fragmented phosphatidylcholine in blood plasma by oxidative stress. J Lipid Res. 41:1145-53.

Giacomazzi S, Cochet N. 2004. Environmental impact of diuron transformation: a review. Chemosphere. 56(11):1021-32.

HMDB. 2009. 2-Methylhexanoyl-CoA; [accessed 2021 Jan 30]. https://hmdb.ca/metabolites/HMDB0011660.

Horecker B. 1976. The biochemistry of sugars. Int Z Vitam Ernahrungsforsch Beih. 15:1-21.

Houten SM, Chen J, Belpoggi F, Manservisi F, Sánchez-Guijo A, Wudy SA, et al. 2016. Changes in the metabolome in response to low-dose exposure to environmental chemicals used in personal care products during different windows of susceptibility. PLoS ONE. 11:e0159919.

Huovinen M, Loikkanen J, Naarala J, Vähäkangas K. 2015. Toxicity of diuron in human cancer cells. Toxicol In Vitro. 29:1577–86.

Ihlaseh SM, Bailey KA, Hester SD, Jones C, Ren H, Cardoso APF, et al. 2011. Transcriptional profile of Diuron-induced toxicity on the urinary bladder of male Wistar rats to inform mode of action. Toxicol Sci. 122(2):330-8.

Ihlaseh SM, Bailey KA, Paula A, Cardoso F, Ren H, Fry RC, et al. 2014. Dose and temporal effects on gene expression profiles of urothelial cells from rats exposed to diuron. Toxicology. 325:21-30.

Kubiatowski T, Jang T, Lachyankar MB, Salmonsen R, Nabi RR, Quesenberry PJ, et al. 2001. Association of increased phosphatidylinositol 3-kinase signaling with increased invasiveness and gelatinase activity in malignant gliomas. J Neurosurg. 95(3):480-8.

Mejia EM, Hatch GM. 2016. Mitochondrial phospholipids: role in mitochondrial function. J Bioenerg Biomembr. 48:99-112.

Melo CFOR, Delafiori J, de Oliveira DN, Guerreiro TM, Esteves CZ, Lima EdO, et al. 2017. Serum Metabolic Alterations upon Zika Infection. Front. Microbiol. 8(1954).

Meyer JN, Hartman JH, Mello DF. 2018. Mitochondrial toxicity. Toxicol Sci. 162(1):15–23.

Nascimento MG, Luiza M, Sartor C, Lima AS, Camargo VD. 2006. Effects of Diuron [3-(3,4-dichlorophenyl)-1,1-dimethylurea] on the urinary bladder of male Wistar rats. Toxicology. 224:66-73.

Nishikimi M, Fukuyaman R, Minoshiman S, Shimizux N, Yagis K. 1994. Cloning and chromosomal mappingo of the human nonfunctional gene for L-Gulono-y-lactone Oxidase, the enzyme for L-Ascorbic Acid biosynthesis missing in man. J Biol Chem. 269(18):13685-8.

Pascual F. 2021. Reframing the question: Does mitochondrial damage set the stage for future inflammation? Environ Health Perspect. 129(6).

Pedersen PL, Greenawalt JW, Reynafarje B, Hullihen J, Decker GL, Soper JW, et al. 2019. Preparation and characterization of mitochondria and submitochondrial particles of rat liver and liver-derived tissues. Methods Cell Biol. 78:411-81.

Rosivatz E, Woscholski R. 2011. Removal or masking of phosphatidylinositol(4,5)bisphosphate from the outer mitochondrial membrane causes mitochondrial fragmentation. Cell Sig. 23(2):478-86.

Roubicek DA, de Souza-Pinto NC. 2017. Mitochondria and mitochondrial DNA as relevant targets for environmental contaminants. Toxicology. 391:100-108.

Simões MdS, Bracht L, Parizotto AV, Comar JF, Peralta RM, Bracht A. 2017. The metabolic effects of diuron in the rat liver. Environ Toxicol Pharmacol. 54:53-61.

Smirnoff N. 2018. Ascorbic acid metabolism and functions: a comparison of plants and mammals. Free Radic Biol Med. 122:116–29.

Souza NP, Lima TRR, Pereira LC, de Camargo JLV. 2020. AOP for urothelial carcinogenesis due to chemical cytotoxicity by mitochondrial impairment; [accessed 2021 Jan 30]. https://aopwiki.org/aops/335.

Surowiec I, Noordam R, Bennett K, Beekman M, Slagboom PE, Lundstedt T, et al. 2019. Metabolomic and lipidomic assessment of the metabolic syndrome in Dutch middle-aged individuals reveals novel biological signatures separating health and disease. Metabolomics. 15:23.

Szlasa W, Zendran I, Zalesińska A, Tarek M, Kulbacka J. 2020. Lipid composition of the cancer cell membrane. J Bioenerg Biomembr. 52:321-42.

Tasseva G, Bai HD, Davidescu M, Haromy A, Michelakis E, Vance JE. 2013. Phosphatidylethanolamine deficiency in mammalian mitochondria impairs oxidative phosphorylation and alters mitochondrial morphology. J Biol Chem. 288(6):4158–73.

Van der Veen JN, Kennelly JP, Wan S, Vance JE, Vance DE, Jacobs RL. 2017. The critical role of phosphatidylcholine and phosphatidylethanolamine metabolism in health and disease. Biochem Biophys Acta Biomembr. (9 Pt B): 1558-72.

Vukajlović JM, Drakulić D, Pejić S, Ilić TV, Stefanović A, Petković M, et al. 2020. Increased plasma phosphatidylcholine/lysophosphatidylcholine ratios in patients with Parkinson's disease. Rapid Commun Mass Spectrom. 28(4),34:e8595.

Walker DI, Uppal K, Zhang L, Vermeulen R, Smith M, Hu W, et al. 2016. High-resolution metabolomics of occupational exposure to trichloroethylene. Int J Epidemiol. 45:1517–27.

Wishart DS. 2019. Metabolomics for investigating physiological and pathophysiological processes. Physiol Rev. 99:1819–75.

Table 1. Proposed metabolites from urothelial mitochondria exposed to diuron or its metabolites elected by PLS-DA VIP scores.

Molecule	MID[a]	Adduct	Experimental *m/z*	Molecular formula	MSMS[b]
PC 46:7	60196	$[M+Na]^+$	939	$C_{54}H_{94}NO_8P$	447, 924, 865, 515
PS P-38:6	78832	$[M+H]^+$	792	$C_{44}H_{74}NO_9P$	592, 724, 676, 674
PI 34:1	61168	$[M+Na]^+$	859	$C_{43}H_{81}O_{13}P$	773, 595, 507, 567, 623
Methylhexanoyl-CoA	62405	$[M+H]^+$	880	$C_{28}H_{48}N_7O_{17}P_3S$	806, 680, 679, 834
Dehydro-L-gulonate	58394	$[M+K]^+$	233	$C_6H_{10}O_7$	71, 172, 200, 151

Isomers with the same m/z and similar fragmentation profile are not distinguished. [a]METLIN ID; [b]In tandem mass spectrometry; PC-phosphatidylcholine; PI-phosphatidylinositol; PS-phosphatidylserine.

Figure 1.

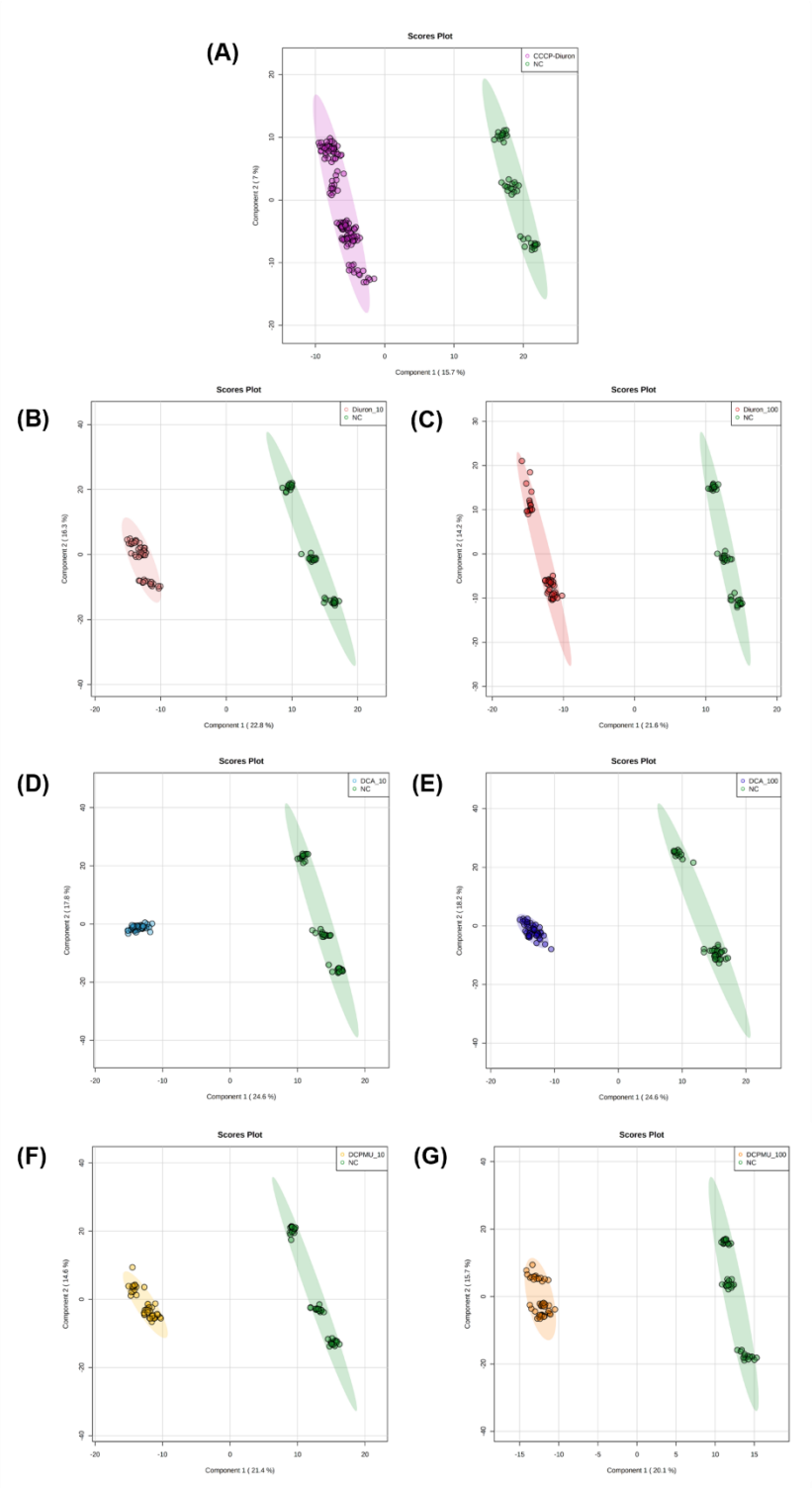
(A)
Scores Plot
CCCP-Diuron
NC
Component 2 (7 %)
Component 1 (15.7 %)
(B)
Scores Plot
Diuron_10
NC
Component 2 (16.3 %)
Component 1 (22.8 %)
(C)
Scores Plot
Diuron_100
NC
Component 2 (14.2 %)
Component 1 (21.6 %)
(D)
Scores Plot
DCA_10
NC
Component 2 (17.8 %)
Component 1 (24.6 %)
(E)
Scores Plot
DCA_100
NC
Component 2 (18.2 %)
Component 1 (24.6 %)
(F)
Scores Plot
DCPMU_10
NC
Component 2 (14.6 %)
Component 1 (21.4 %)
(G)
Scores Plot
DCPMU_100
NC
Component 2 (15.7 %)
Component 1 (20.1 %)

Figure 2.

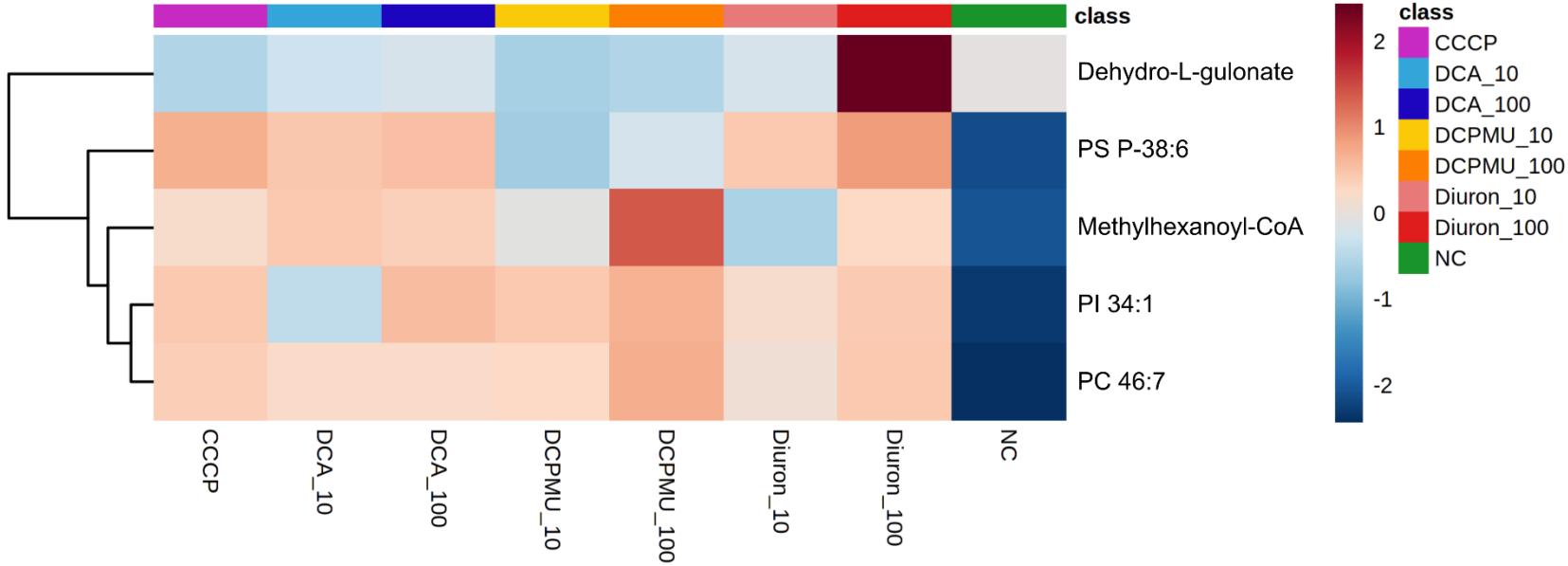
class
Dehydro-L-gulonate
PS P-38:6
Methylhexanoyl-CoA
PI 34:1
PC 46:7
CCCP
DCA_10
DCA_100
DCPMU_10
DCPMU_100
Diuron_10
Diuron_100
NC
2
1
0
-1
-2

Figure 3.

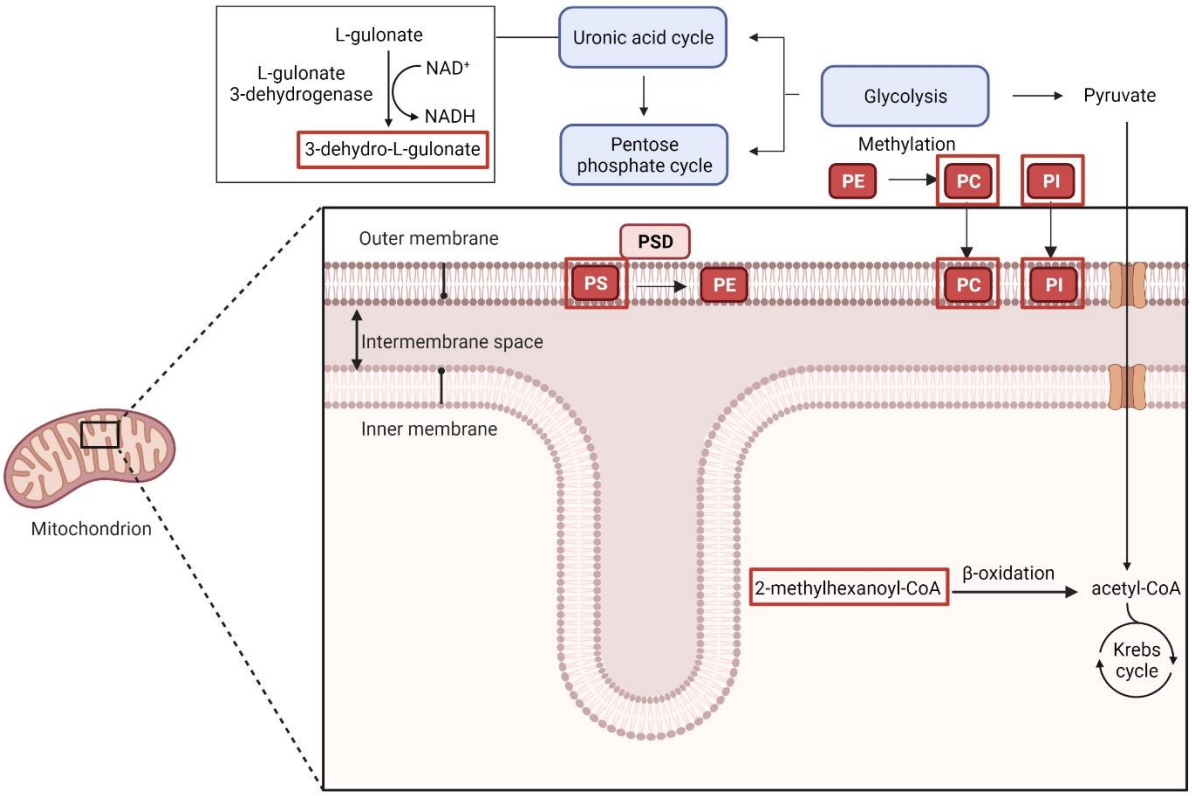
L-gulonate
L-gulonate 3-dehydrogenase
NAD+
NADH
3-dehydro-L-gulonate
Uronic acid cycle
Pentose phosphate cycle
Glycolysis
Pyruvate
Methylation
PE
PC
PI
Outer membrane
PSD
PS
PE
PC
PI
Intermembrane space
Inner membrane
Mitochondrion
2-methylhexanoyl-CoA
β-oxidation
acetyl-CoA
Krebs cycle

Figure 4.

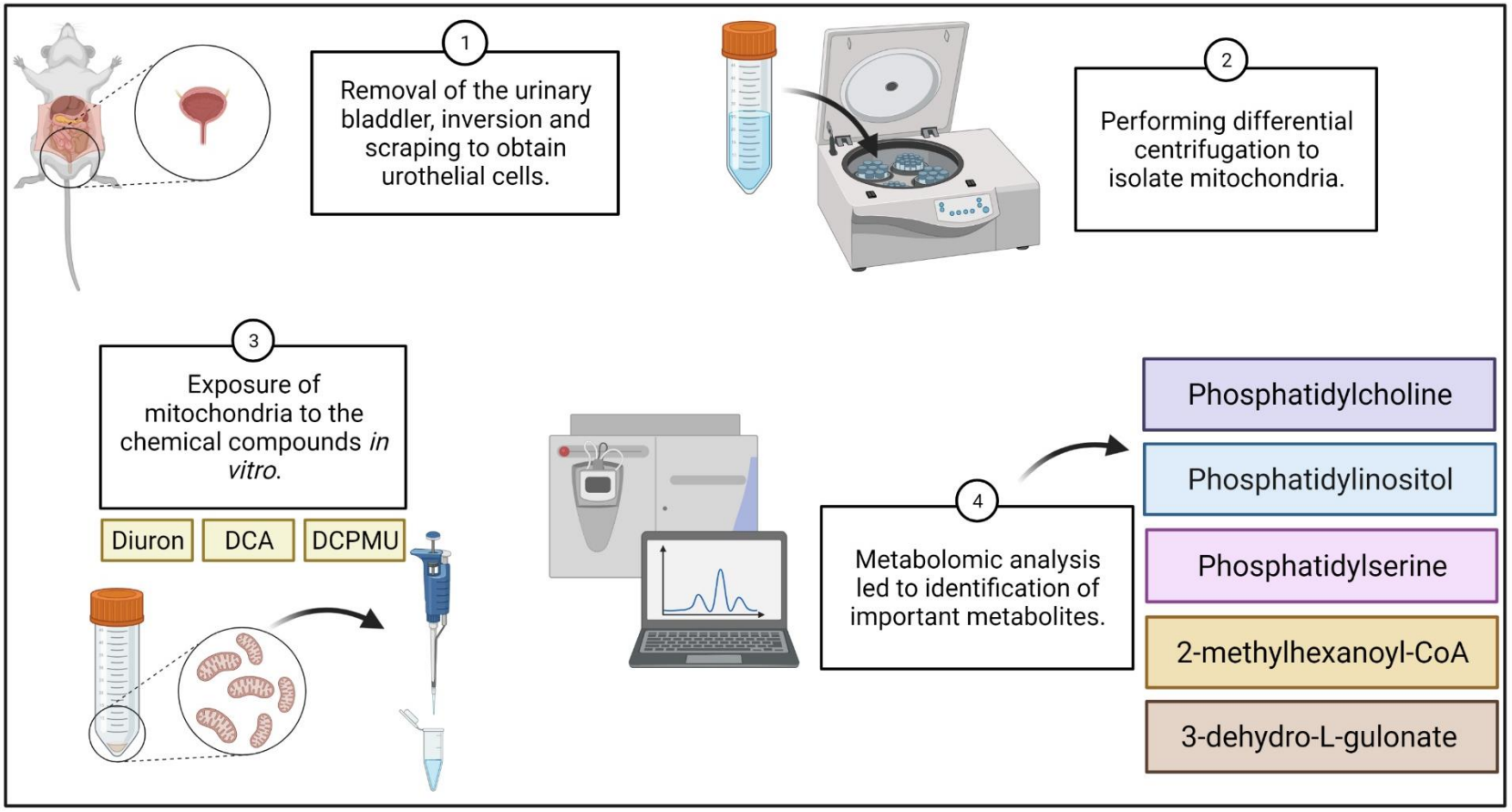
1
Removal of the urinary bladdler, inversion and scraping to obtain urothelial cells.
2
Performing differential centrifugation to isolate mitochondria.
3
Exposure of mitochondria to the chemical compounds *in vitro*.
Diuron
DCA
DCPMU
4
Metabolomic analysis led to identification of important metabolites.
Phosphatidylcholine
Phosphatidylinositol
Phosphatidylserine
2-methylhexanoyl-CoA
3-dehydro-L-gulonate

Figure captions

Figure 1. Partial Least Square-Discriminant Analysis (PLS-DA) score plot showing separation between negative control (NC) and chemical exposed groups in A- CCCP-Diuron, B-Diuron_10, C- Diuron_100, D- DCA_10, E- DCA_100, F- DCPMU_10 and G-DCPMU_100 clustering with data on positive ion mode.

Figure 2. Heatmap demonstrating the frequency averages of the markers per group. In general, chemically exposed groups have an increased abundance of annotated metabolites when compared to the negative control (NC). PC-phosphatidylcholine; PI-phosphatidylinositol; PS-phosphatidylserine

Figure 3. Detected molecules using metabolomic analysis and their relationship with mitochondria. PC-phosphatidylcholine; PI-phosphatidylinositol; PS-phosphatidylserine; PS decarboxylase-PSD. *Created with BioRender.com*.

Figure 4. Graphical abstract showing the main steps involved in the metabolomic analysis and the five important metabolites detected. *Created with BioRender.com*.

NumWords: 4507

Supplementary material

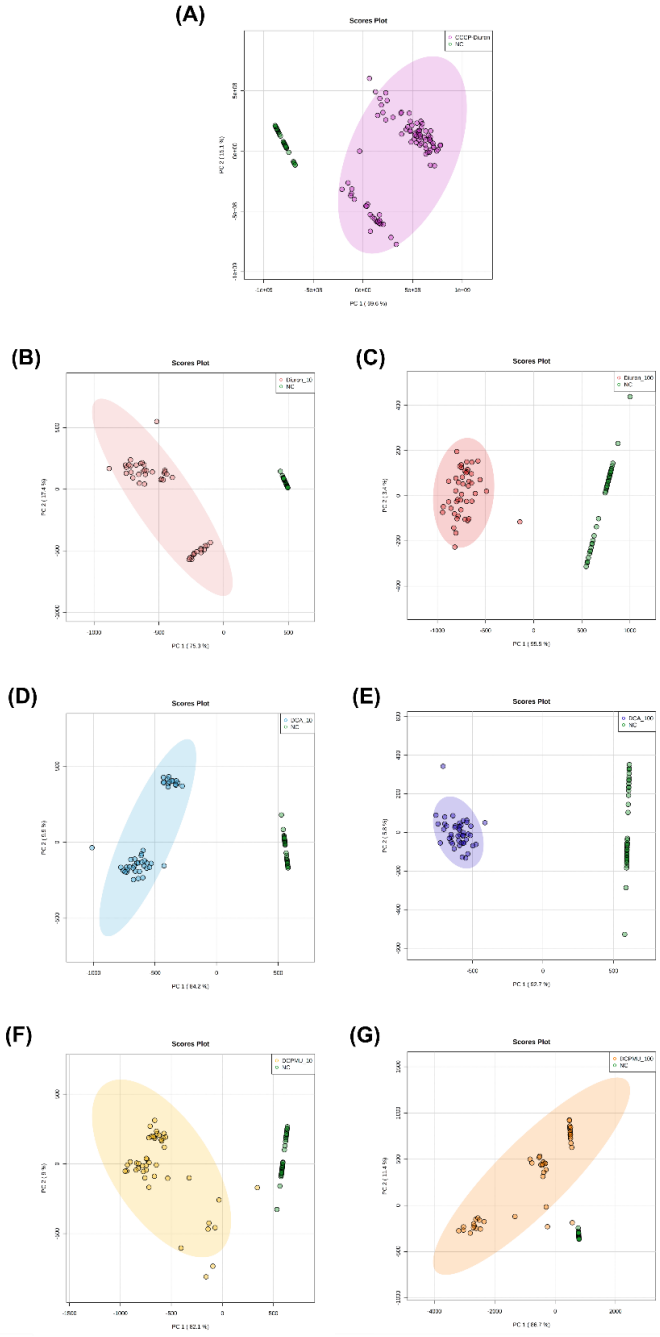

Figure S1. Principal Component Analysis (PCA) score plot validation with the selected markers showing separation between negative control (NC; green) and chemical exposed groups in A-CCCP-Diuron, B-Diuron_10, C- Diuron_100, D- DCA_10, E- DCA_100, F- DCPMU_10 and G-DCPMU_100.

Table S2. Significance of markers' intensities variation (Fold change - FC) between comparisons of each chemical exposed groups to negative controls (NC) were tested with t-test using FDR adjusted p-value.

Molecule	FC (p-value)						
	CCCP-Diuron/ NC	**Diuron_10/ NC**	**Diuron_100/ NC**	**DCA_10/ NC**	**DCA_100/ NC**	**DCPMU_10/ NC**	**DCPMU_100/ NC**
PC 46:7	582.94 (< 0.01)	6.05 (< 0.01)	6.80 (< 0.01)	5.79 (< 0.01)	5.94 (< 0.01)	20.171 (< 0.01)	31.029 (< 0.01)
PS P-38:6	509.29 (< 0.01)	6.84 (< 0.01)	6.39 (< 0.01)	6.05 (< 0.01)	6.10 (< 0.01)	9.01 (< 0.01)	4.20 (< 0.01)
PI 34:1	496.06 (< 0.01)	6.68 (<0.01)	8.63 (< 0.01)	4.54 (< 0.01)	6.19 (< 0.01)	21.78 (< 0.01)	24.09 (< 0.01)
Methylhexanoyl-CoA	370.35 (< 0.01)	4.55 (< 0.01)	10.92 (< 0.01)	6.04 (< 0.01)	6.18 (< 0.01)	25.93 (< 0.01)	33.49 (< 0.01)
Dehydro-L-gulonate	0.4928 (< 0.01)	0.92 (0.14)	2.24 (< 0.01)	0.87 (0.02)	0.92 (0.16)	0.72 (< 0.01)	0.75 (< 0.01)

PC-phosphatidylcholine; PI-phosphatidylinositol; PS-phosphatidylserine.

Conclusão

Nossos resultados permitiram caracterizar os danos induzidos pela exposição a diferentes concentrações entre 0,5 e 500 µmol/L do diuron e seus metabólitos em células uroteliais humanas 1T1, sendo os efeitos mais expressivos observados para os metabólitos e nas concentrações mais altas. Ainda, considerando os achados em mitocôndrias uroteliais isoladas de ratos Wistar, sugere-se a disfunção mitocondrial como evento inicial no desencadeamento de eventos envolvidos na citotoxicidade dos compostos testados. Este estudo investigou *endpoints* diversos decorrentes da exposição *in vitro* aos compostos químicos e fornece subsídios para a realização de ensaios adicionais, incluindo a avaliação da ativação de caspases com o objetivo de esclarecer o envolvimento da apoptose nesse mecanismo de ação tóxica. A compreensão global do mecanismo de ação subjacente é crucial para estabelecer estratégias de prevenção e terapêutica aos efeitos nocivos em cenários de intoxicação, além de auxiliar na tomada de decisão regulatória.

Anexos

TOXICOLOGY MECHANISMS AND METHODS
https://doi.org/10.1080/15376516.2022.2062271

Taylor & Francis
Taylor & Francis Group

RESEARCH ARTICLE

Molecular signatures associated with diuron exposure on rat urothelial mitochondria

Thania Rios Rossi Lima[a,b], Estela de Oliveira Lima[a], Jeany Delafiori[c], Rodrigo Ramos Catharino[c], João Lauro Viana de Camargo[a,b] and Lílian Cristina Pereira[a,b,d]

[a]Medical School, São Paulo State University (Unesp), Botucatu, Brazil; [b]Medical School, Center for Evaluation of Environmental Impact on Human Health (TOXICAM), Unesp, Botucatu, Brazil; [c]Innovare Biomarkers Laboratory, School of Pharmaceutical Sciences, University of Campinas (UNICAMP), Campinas, Brazil; [d]School of Agriculture, São Paulo State University (Unesp), Botucatu, Brazil

ABSTRACT

Diuron, 3-(3,4-dichlorophenyl)-1,1-dimethylurea, is a worldwide used herbicide whose biotransformation gives rise to the metabolites, 3-(3,4-dichlorophenyl)-1-methylurea (DCPMU) and 3,4-dichloroaniline (DCA). Previous studies indicate that diuron and/or its metabolites are toxic to the bladder urothelium of the Wistar rats where, under certain conditions of exposure, they may induce successively urothelial cell degeneration, necrosis, hyperplasia and eventually tumors. The hypothesis was raised that the molecular initiating event (MIE) of this Adverse Outcome Pathway is the mitochondrial toxicity of those compounds. Therefore, this study aimed to investigate *in vitro* the metabolic alterations resulting from urothelial mitochondria isolated from male Wistar rats exposure to diuron, DCPMU and DCA at 10 and 100 µM. A non-targeted metabolomic analysis using mass spectrometry showed discriminative clustering among groups and alterations in the intensity abundance of membrane-associated molecules phosphatidylcholine, phosphatidylinositol and phosphatidylserine, in addition to methylhexanoyl-CoA and, particularly for diuron 100µM, dehydro-L-gulonate, all of them involved in critical mitochondrial metabolism. Collectively, these data indicate the mitochondrial dysfunction as an MIE that triggers cellular damage and death observed in previous studies.

ARTICLE HISTORY
Received 8 November 2021
Revised 28 March 2022
Accepted 30 March 2022

KEYWORDS
Herbicide; DCA; DCPMU; mitochondrial dysfunction; diuron toxicity

Introduction

Numerous studies used metabolomics to assess damage caused by environmental stresses or to identify potential biomarkers to understand the mechanisms of disease development (Houten et al. 2016; Walker et al. 2016; Surowiec et al. 2019). Metabolomics is one of the most recent additions to the '-omics' family, characterized as a high-throughput analytical method for measuring and comparing a large number of low molecular mass (up to 1500 Daltons) metabolites (metabolome) present in biological samples (Braga and Adamec 2019; Wishart 2019). Since the metabolome is at the endpoint of all cellular activity, the implementation of its analysis may contribute to clarify subcellular alterations involved in the toxic effects caused by xenobiotics, including environmental contaminants such as pesticides (Braga and Adamec 2019; Wishart 2019). Considering that most of cellular metabolites are conserved in several animal species, research findings in experimental animals can be extrapolated to humans (Wishart 2019), in order to elucidate the mode of action (MoA) and mechanisms of action of toxic chemicals.

Diuron, 3-(3,4-dichlorophenyl) 1,1-dimethylurea, is a worldwide used herbicide whose biodegradation in the environment or metabolization in mammals results in the metabolites 3-(3,4-dichlorophenyl)-1-methylurea (DCPMU), 3,4-dichlorophenylurea (DCPU) and 3,4-dichloroaniline (DCA) (Giacomazzi and Cochet 2004; APVMA 2011). Since in mammals the excretion of these compounds occurs mainly through urine, the urothelial tissue which lines the urinary tract from the renal pelvis and ureters to the bladder, is one of the most affected by their potential toxicity. Previous studies with diuron demonstrated that its MoA on the urinary bladder of Wistar rats involves chemical metabolic activation leading to initial cytotoxicity followed by cell degeneration, exfoliation and necrosis, continuous regenerative hyperplasia and eventual tumors after a long-term exposure (Nascimento et al. 2006; da Rocha et al. 2010; Ferrucio et al. 2010; Ihlaseh-Catalano et al. 2011; da Rocha et al. 2012; Cardoso et al. 2013; da Rocha et al. 2013; da Rocha et al. 2014; Ihlaseh-Catalano et al. 2014; Fava et al. 2015). Recently, the hypothesis was put forward that this sequence of successive events induced by diuron and/or its metabolites could comprise an Adverse Outcome Pathway (AOP) in which the mitochondrial toxic damage represents the initiating molecular event (MIE) (Souza et al. 2020).

Recently, metabolomics has been increasingly applied in the mitochondrial-related disease research and diagnosis

CONTACT Thania Rios Rossi Lima thania.lima49@gmail.com Medical School, São Paulo State University (Unesp), TOXICAM, UNIPEX – Block 5, Botucatu, São Paulo 18618-970, Brazil

Supplemental data for this article can be accessed here.

UNIVERSIDADE ESTADUAL PAULISTA
CAMPUS DE BOTUCATU
FACULDADE DE MEDICINA

unesp

FMB

CEUA Ética

Comissão de Ética no Uso de Animais

Criada através da Portaria DFM nº 611 de 13/12/2012

CERTIFICADO-RETIFICADO

Certificamos que a proposta intitulada **"Avaliação dos mecanismos de citotoxidade do diuron em células uroteliais – possível papel de lesão mitocondrial."** conduzida pela Pesquisadora: **Thania Rios Rossi Lima**, Orientadora: Profa. Dra. Lilian Cristina Pereira, Coorientadores: Prof. Dr. João Lauro Viana de Camargo e Profa. Dra. Carla Adriene da Silva, registrada com o nº 1253/2017, que envolve a produção, manutenção ou utilização de animais pertencentes ao filo Chordata, subfilo Vertebrata (exceto humanos), para fins de pesquisa científica – encontra-se de acordo com os preceitos da Lei nº 11.794, de 8 de outubro de 2008, do Decreto n. 6.899, de 15 de julho de 2009, com as normas editadas pelo Conselho Nacional de Controle de Experimentação Animal (CONCEA), e foi APROVADO pela Comissão de Ética no Uso de Animais da Faculdade de Medicina de Botucatu/UNESP, em reunião ordinária de 29 de março de 2018.

Retificação: Mudança de orientador e Inclusão de Coorientadores.

Finalidade	( ) Ensino - (X) Pesquisa Científica
Vigência da autorização	28 de fevereiro de 2022
Espécie/Linhagem/Raça	Ratos Isogênicos/Wistar
Nº total de animais	35
Sexo	macho
Idade/Peso	04 semanas/180g
Origem	Biotério do CEMIB - UNICAMP

Graziela Nogueira Bertani
Secretária Responsável
Comissão de Ética no Uso de Animais – CEUA

Prof. Dr. Guilherme Antônio Moreira de Barros
Presidente
Comissão de Ética no Uso de Animais - CEUA

Distrito Rubião Junior, s/nº - Botucatu – S.P. CEP: 18.618-970 / Fone: (14) 3880.1608 – 3880.1609 / E-mail Secretaria: ceua@fmb.unesp.br